QUANTIFYING COASTLINE CHANGE FOR PLAYA GUIONES & PLAYA PELADA, COSTA RICA

QUANTIFYING COASTLINE CHANGE FOR
PLAYA GUIONES & PLAYA PELADA,
COSTA RICA

JASON MICHAEL LEWIS, Hons. B.A.

A Thesis
Submitted to the School of Graduate Studies
In partial fulfillment of the Requirements
For the Degree Masters of Masters of Science
McMaster University, Hamilton, Ontario

MASTER OF SCIENCE (2009) McMaster University

TITLE: Quantifying Coastline Change – Playa Guiones & Playa Pelada, Costa Rica Hamilton, Ontario

AUTHOR: Jason Michael Lewis, Hons. B.A.

SUPERVISORS: Susan Vajoczki

NUMBER OF PAGES: xii, 164

ABSTRACT

This study was conducted over two years (2005 and 2007) and consisted of data collected over one wet season and one dry season at two beaches, separated by a rocky headland, located along the Pacific coast of the Nicoya Peninsula, Costa Rica. Although the beaches are concurrent along a 7 km stretch of coastline, both are characterized by a unique combination of: beach slope, length and shape; sediment composition, size and mineralogy; and vegetation. These beaches have discrete land uses. Playa Guiones is a tourist beach that is experiencing rapid development and Playa Pelada is the only local beach that provides boat access for local fishermen. It was hypothesized that the active tectonism in the region combined with the distinct wet/dry seasons will result in dynamic beaches with distinct morphology.

The first objective is to quantify and explain changes in sediment accretion or deposition between the two distinct seasons. The second objective is to quantify longer term temporal coastline changes through analysis of air photos and satellite imagery from 1940 to 2005 for the region. It was hypothesized that this time series will provide evidence of the influence of tectonics on coastline position.

This analysis involves a comparison of Digital Elevation Models (DEMs) created from real-time kinematic GPS data collected in June 2005 and January/February 2007 with aerial photography and satellite imagery representing the period 1940-2005. Results show that from wet to dry season there is substantial net sediment accumulation for Playa Guiones and net sediment erosion for Playa Pelada. It should be noted that the seasons were particularly dry and particularly wet, thus, the results may indicate maximum levels of variation. The time series analyses of the digital imagery show little variation of coastline position during the period of record. The digital imagery was severely limited by the resolution and scale of the imagery. It appears that these beaches experience moderate to large amount of seasonal variation but are relatively stable over a longer time period.

ACKNOWLEDGEMENTS

Throughout this various stages of completing this thesis there are a number of people who have helped along the way and I am grateful for their support. First, I would like to thank my supervisor, Dr. Sue Vajoczki, who for the past three years has provided constant encouragement, advice and wisdom that allowed me to complete this thesis. From the initial planning of the project, to the great times collecting data in the field, to the analysis and write up of this work, Sue has always been there for me. The knowledge and skills that I take away from this work will benefit my future endeavours and for that I'm truly appreciative.

I would like to express my gratitude to Dr. Bill Morris, who in addition to providing the equipment necessary for this project, also provided on numerous occasions stimulating discussions on both the technical and theoretical aspects pertaining to this work. Hernan Ugalde was essential as the go to "Oasis" guru that could answer any software question related to processing data.

Aaron Bertram, a long standing friend and colleague who did the first master's thesis in this area was an asset to learn from during my undergrad thesis and during the initial stages of this project. The data could not have been collected without the backbone support (literally) of Nic Cowan and Jackie Ellis, who worked in extreme heat and long days to help collect the geospatial data. Their positive attitudes and good natured approach to the work helped make the long field seasons productive and enjoyable.

I would also like to thank friends and family who allowed me to miss numerous functions and provided on-going support and encouragement to complete this project. Without their encouragement this project would not have been completed.

TABLE OF CONTENTS

LIST OF FIGURES

LIST OF TABLES

CHAPTER ONE: INTRODUCTION

1.1 Overview

This research describes the geomorphology and evolution of two Costa Rican beaches: Playa Pelada and Playa Guiones (Figure 1.1 and Figure 1.2), on both a seasonal (wet versus dry season) and a longer term temporal time scale (1945-2007). This work is significant because: the two beaches are located in an active tectonic region that has experienced past seismic uplift of the coastline relative to sea level (Marshall and Anderson, 1995); the beaches form part of the protected Ostional Wildlife Refuge where marine turtles nest (Campbell, 1998); and, the region is experiencing a rapid increase in development in close proximity to the beach (Bertram, 2006).

1.2 Thesis Objectives

This research project builds on prior work by Bertram (2006). Through use of wet season geospatial data collected by Bertram (2006) and combining it with dry season data collected by the researcher in 2007 seasonal changes in beach morphology can be measured. The primary objective of this project is to qualitatively compare and quantify differences of geomorphologic features between the 2005 'wet' and 2007 'dry' season along the two beaches. The analysis of three-dimensional models created from geospatial data surveyed during these seasons allow geomorphologic features such as shoreline position, beach slope and accommodation space to be both identified and quantified. The

secondary objective is to use aerial and satellite imagery of the region from 1944 to 2005 for the purpose of describing and quantifying shoreline evolution.

Figure 1.1: A relief map indicating the location of Playa Pelada and Playa Guiones along the western coast of the Nicoya Peninsula, in Guanacaste Province, Costa Rica (Modified from Gaba, 2008).

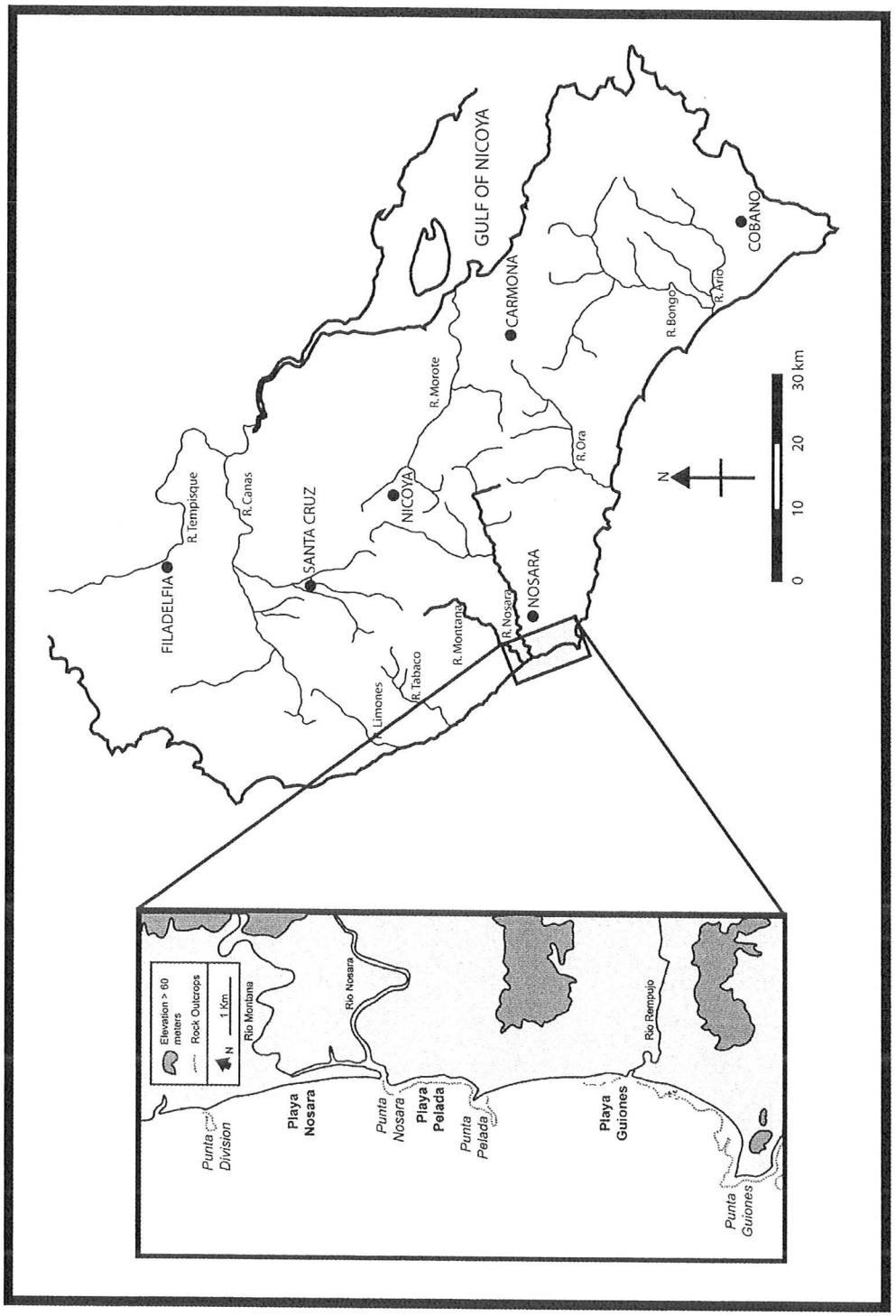

Figure 1.2: Detailed map of the Nicoya Peninsula, Costa Rica (Modified from Hare and Gardner, 1985). The enlarged inset map is the study area of Playa Pelada and Playa Guiones (Modified from Campbell, 1998).

1.3 Relevance

Some of the greatest challenges faced by countries that have an increasing amount of development near the coastline are creating policies, regulations and decisions that adequately protect the environment as well as man-made structures (Windevoxhel *et al,* 1999). Frequently, when these policies, regulations and decisions are made there is a lack of knowledge about the specific coastal situation resulting in poor decision making such as building coastal features to reduce the amount of erosion only to accelerate it (Windevoxhel *et al,* 1999).

The results presented in this study will provide two beneficial additions to the overall greater knowledge of this coastal area. This study will provide highly sampled geospatial data of the two beaches that were surveyed in February 2007 building the database of previous collected data from June 2005. Since limited to only one set of data for both the wet and dry season, we cannot assume that the beaches were in their typical state, however, we can begin to form conclusions on seasonal differences on these beaches. Monitoring the shoreline over a long temporal time frame with the remotely sensed imagery allows improved prediction about future coastal evolution. The increased knowledge about seasonal variations and the longer term temporal variations will permit more informed decision-making.

1.4 Organization of Thesis

Chapter One presents a generalized introduction of the research including the objectives and relevance of the work. Chapter Two describes the study area and provides

the background geology, climate and tectonics of the region. In addition a review of coastal geomorphology, shoreline definitions and indicators, and sources for acquiring shoreline positions are discussed. As well a variety of interpolation methods are reviewed. Chapter Three explains the methodology used for site selection, field seasons, field methods as well as the methods used for processing and analyzing the data. Chapter Four presents the results with a discussion on the analysis of each component. In Chapter Five, conclusions and recommendations are stated based on the results.

CHAPTER TWO: BACKGROUND AND PREVIOUS WORK

This chapter begins by providing background information on the region and describes the two study sites, Playa Guiones and Playa Pelada. The description includes a comparison of the observed weather to historical climate records, the regional tectonic activity and geology. An in depth review of coastal geomorphology is then presented. This is followed by a definition of a shoreline and a review of the various indicators that can be used to measure it. The final section in this chapter reviews three interpolation methods that can be used for estimating geospatial data.

2.1 Regional Setting

2.1.1 Playa Guiones and Playa Pelada, Guanacaste, Costa Rica

Playa Guiones and Playa Pelada are two concurrent beaches located on the western coast of the Nicoya Peninsula, located near the town of Nosara, Guanacaste Peninsula, Costa Rica. This region was largely undeveloped until large-scale livestock ranching began in the province in the 1950's and large tracks of trees were cut down (Campbell, 1998). An area of land (1110 hectares) between Nosara and the two study sites were purchased between 1969 and 1972 by Alan Hutchinson for the purpose of developing the area into vacation properties, forest preserves and parks (Nosara Civic Association, 2008). The Nosara Civic Association was established in 1975 to oversee the development of the area while "maintaining intact the natural beauty of our area" (Nosara Civic Association, 2008).

Playa Pelada and Playa Guiones, in addition to Playa Nosara and Playa Ostional together form the Ostional Wildlife Refuge which was established in 1983 for the purpose of protecting nesting marine turtles (Figure 2.1) (Campbell, 1998). Although most turtles nest on Playa Ostional and Playa Nosara and relatively few marine turtles nest on Playa Pelada and Playa Guiones, these beaches were included in the refuge to protect the region against the increasing pressure of development along the coast.

Playa Pelada is a narrow, calcareous sediment embayed beach, approximately 1.5 kilometers in length, and less than 100 m wide that is bounded by rocky headlands, Punta Nosara at the northern extent and Punta Pelada at the southern extent. Three low-lying rocky outcrops extend perpendicular from the shore of Playa Pelada that divide the beach into four sections. These outcrops vary in elevation and are partially obscured during high tide. A number of boats are beached along Southern Playa Pelada where local fishermen have taken advantage of the protection offered by the headlands from severe weather. Tourism is present on this beach in the form of fishing charters, occasional sunbathers and surfers and a number of vacation properties located further inland.

Playa Guiones, a much larger beach compared to Playa Pelada at 6 kilometers in length, and has the appearance of an embayed beach sharing Punta Pelada at the northern extent and Punta Guiones to the south. Within this headland bounded beach, there are five rivers of various size that discharge inland sediment into the ocean. These rivers are ephemeral, thus, depending on the amount of precipitation and size of drainage basin they typically only flow during the wet season. These rivers from north to south are: Queb Pelada, Quebrada Corea, Rio Rempujo, Estero Garcia, and Queb Guiones (Figure 2.2).

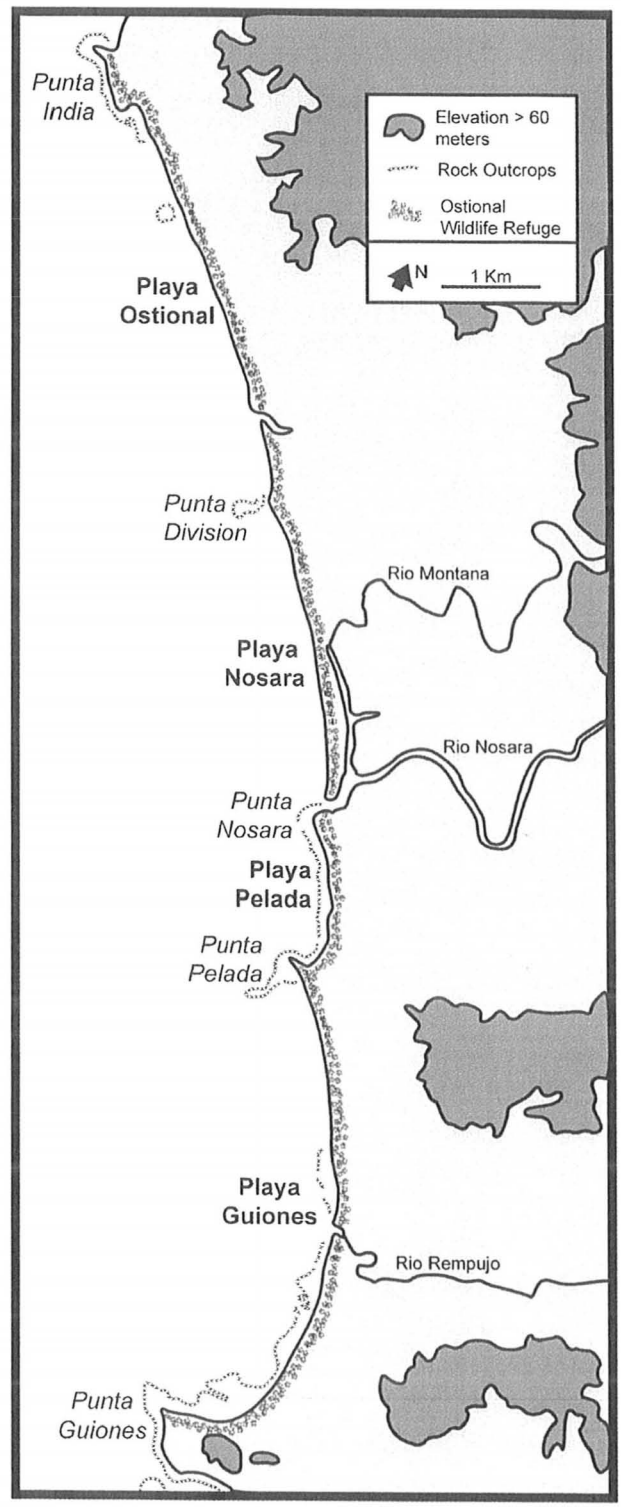

Figure 2.1: Map of Playa Pelada and Playa Guiones, in relation to the Ostional Wildlife Refuge (Adapted from Campbell, 1998).

The coastal geomorphology inventory completed by Bertram (2006) found that during the wet season, sediment is predominately fine grained carbonate shell material that is coarser towards the center of the beach at Rio Rempujo. The southern headland identified as part of the Samara group contained limestone, interbedded sandstone and siltonstone, whereas, the northern headland contained sandstone from the Punta Pelada Formation.

Tourism is the dominate land use for this beach, with the attraction of good surf conditions and a sandy beach. As a result of the tourism appeal of the beach there has been an increase in development of properties within the area. Bertram (2006) found the number of buildings within 1.25 km of the beach grew from 9 in 1977, to 39 in 1991, 43 in 1997 and 140 in 2004 which illustrates the increasing pressure of development in this region.

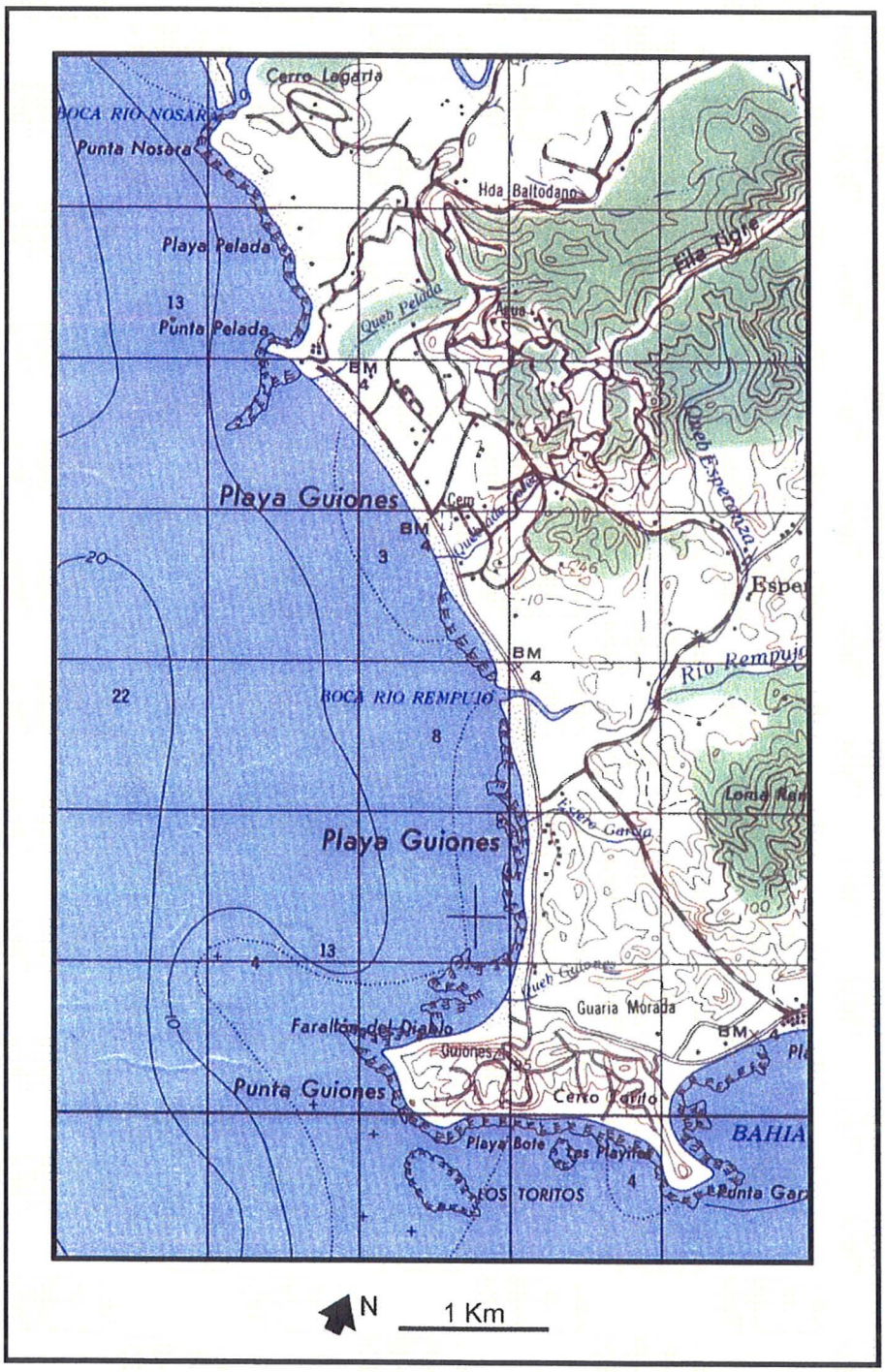

Figure 2.2: Topographic image Playa Guiones and Playa Pelada (IGN, 1983)

2.1.2 Climate

As indicated by the climograph for Liberia, Costa Rica in Figure 2.3, this region has a distinct climate where there is a defined wet season from May – November and a dry season from December – April. Liberia is the nearest weather station located 80 km NNW from Playa Guiones and is situated 20 km east of coast (Figure 1.1, pg 2). During the wet season, the average number of days with precipitation ranges from 12 to 28 days, whereas, during the dry season the average ranges from 0 to 4 days (IMN, 2006). The average maximum daily temperature is highest during the dry season in April at 36°C (winter), with a lower wet season average maximum daily temperature of 31-32°C (summer). The average minimum daily temperature has a similar trend with have a lower minimum temperature in the dry season when compared to the wet season.

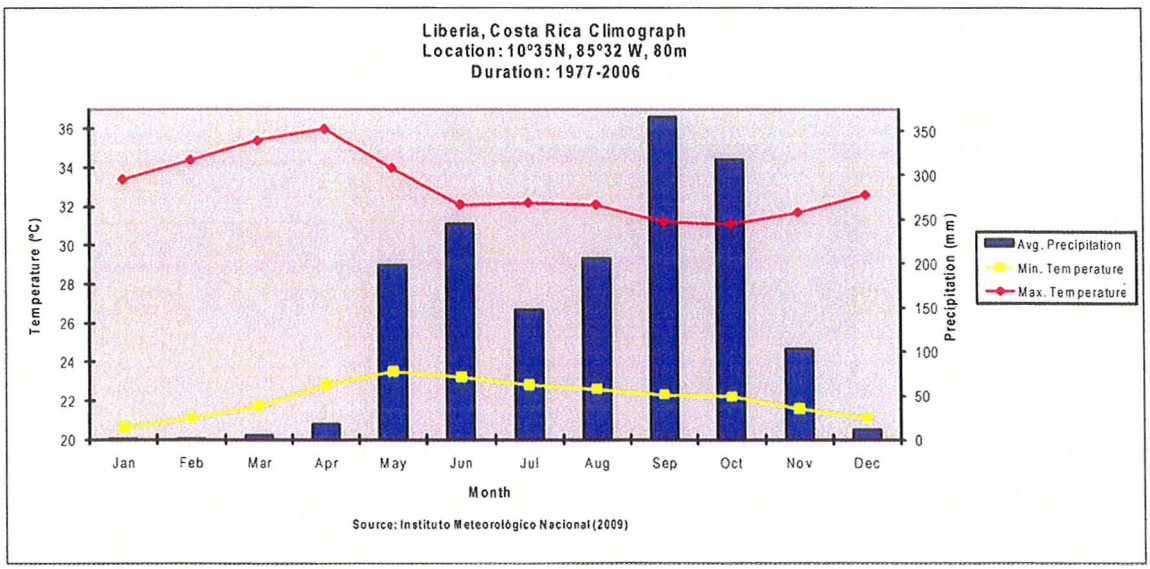

Figure 2.3: Climograph of Liberia, Costa Rica.

2.1.3 Observed Weather Vs Climate

As seen in Table 2.1, observed climate variables were compared to long term monthly averages for six months prior to and following the 2005 wet season study period at Liberia, Costa Rica. These variables consisted of minimum and maximum temperature, total amount of precipitation and number of days with precipitation. The observed averages and totals with the long term averages for the June/July 2005 field season are highlighted with light shading. It can be seen that both the observed and long term monthly averages for minimum and maximum temperature are similar throughout the table. However, the total amount of precipitation there is a large difference between what was observed during June, 2005 (463.5 mm) and long term monthly average (244.8 mm), indicated by the dark shading. The number of days with precipitation observed (22 days) are similar with the long term average of 23 days for this month. This shows that in June 2005 the region experienced 218.7 mm more rain than on average, with a similar number of days with precipitation. The additional precipitation amounts during the field season indicate that it was an uncharacteristically wet, wet season.

This increase in precipitation may have had significant effects on the beach system, thus, influencing the data. An increase in total precipitation would cause an increase both the velocity and volume of the river discharge. The increase would be proportional to drainage basin size with larger river basins receiving greater amount of precipitation. The increase velocity and volume would result in both greater size and total amount of sediment being transported downstream and potentially deposited into the beach system. Changes in volume and velocity would also affect the morphology of the

Table 2.1: Comparison of observed climate data to long term averages. Observed climate data were monthly averages or totals based on daily averages or totals (NCDC, 2009). These were compared to long term monthly averages from January 1, 1997 to December 21, 2006 for Liberia, Costa Rica (IMN, 2009). The light shaded area of the table indicated the 2005 wet field season. The dark shaded cell highlights that for June 2005 the total precipitation was over 200 mm when compared to the long term average.

Month/Year	Avg. Daily Min. Temp.		Avg. Daily Max. Temp.		Total Monthly Ppt. (mm)		Number Days with Ppt.	
	Observed	Long Term Avg.	Observed	Long Term Avg.	Observed	Long Term Avg.	Observed	Long Term Avg.
Jan 2005	20.4	20.6	33.9	33.9	0.0	1.2	0	1
Feb 2005	20.1	21.1	34.3	34.4	0.0	1.8	0	0
Mar 2005	22.3	21.7	36.6	35.7	13.7	5.2	4	0
Apr 2005	23.1	22.8	36.9	36.0	1.0	17.5	2	3
May2005	23.6	23.5	34.5	34.0	200.6	198.3	8	15
June2005	23.1	23.2	31.4	32.1	463.5	244.8	22	23
July 2005	23.1	22.8	32.4	32.2	98.0	147.2	12	18
Aug 2005	22.6	22.6	32.7	32.1	140.7	205.8	14	19
Sept 2005	22.7	22.3	31.6	31.2	249.1	366.1	10	28
Oct 2005	22.4	22.2	28.8	31.1	464.5	317.5	27	25
Nov 2005	21.5	21.6	31.2	32.1	59.1	103.1	14	12
Dec 2005	19.9	21.1	33.1	32.6	2.0	11.3	3	4

river mouth, whereby the spatial location could shift in both directions, parallel and perpendicular to the shore. An increase in the amount of turbulence created at the river-ocean boundary from additional discharge may influence both erosion and deposition of sediment and influence the energy and direction of currents and waves in the vicinity of the river mouth.

The observed weather variables were compared with long term monthly averages for six months prior and following 2007 dry season study period in Table 2.2 for Liberia, Costa Rica. The observed averages and totals compared with the long term averages for the January/February 2007 field season are highlighted with light shading. The observed and long term monthly average minimum and maximum temperature are similar throughout the table. However, prior to this study period, there are a number of months in which the observed amount of total precipitation was significantly less than the long term monthly average as indicated in Table 2.2 with the dark shading.

The months August, September and November experienced less observed precipitation when compared to the long term average and the difference for each of the months were 103.2 mm, 284.2 mm and 65.5 mm, respectively. When the observed number of days with precipitation were compared with the longer term averages for these months, both August and November had a similar number of days of precipitation. Whereas September, which had the greatest decrease in precipitation, observed only 15 days of precipitation compared to 28 days. Since the normal dry season for the region is from December to March, due to the decrease in observed total amount of precipitation when compared to the long term averages from August to November, the dry season

Table 2. 2: The light shaded row of the table indicates 2007 dry field season. The observed data was the daily weather averaged or totaled for each month and compared to the long term monthly averages from January 1, 1997 to December 21, 2006 for Liberia, Costa Rica (Data Source: NOAA).

Month/Year	Avg. Min. Temp.		Avg. Max. Temp.		Total Ppt. (mm)		Number Days with Ppt.	
	Observed	Long Term Avg.	Observed	Long Term Avg.	Observed	Long Term Avg.	Observed	Long Term Avg.
Aug 2006	71.6	72.7	90.3	89.8	102.6	205.8	14	19
Sept 2006	70.2	72.1	89.3	88.2	81.8	366.1	15	28
Oct 2006	71.0	72.0	88.5	88.0	307.8	317.5	15	25
Nov 2006	68.0	70.9	87.7	89.7	37.6	103.1	13	12
Dec 2006	69.0	70.0	90.0	90.7	19.6	11.3	5	4
Jan 2007	70.9	69.1	90.0	92.1	0	1.2	0	1
Feb 2007	69.4	70.0	91.9	93.9	0	1.8	0	0
Mar 2007	70.4	71.1	93.7	95.7	0	5.2	0	0
Apr 2007	72.5	73.0	93.9	96.8	58.2	17.5	2	3
May2007	74.1	74.3	91.4	93.2	261.1	198.3	16	15
June2007	74.3	73.8	89.4	89.8	138.7	244.8	15	23
July 2007	73.2	73.0	90.8	90.0	240.4	147.2	15	18

which is from December to March began with moisture conditions drier than usual.

The effects from drier conditions prior to the dry season could result in changes in the beach system and the data collected during this field season would represent an uncharacteristically dry season. Overall, there would be a decrease in the amount of water discharging into the ocean from rivers, with rivers draining smaller drainage basin having potentially zero discharge at the start of the dry season. The decrease or total reduction of velocity and volume could result in little or no sediment discharging into the ocean. This reduction will change the sediment balance and depending on the state of the beach could result in morphological changes. Ephemeral river channels during this dry period will change shape through aeolian and wave processes such that sediment from the beachface will be deposited in these channels without the discharging river water maintaining the river channel.

2.1.4 Tectonic Activity

Costa Rica experiences active tectonics along its western coast due to its location on a convergent margin with the Cocos plate subducting beneath the Caribbean plate (Figure 2.4). The two plates converge at the Middle America Trench where the Cocos plate has been estimated to be moving in the northeastern direction at rate between 83 to 100 mm/year (Gardner *et al,* 1987; DeShone *et al,* 2006). There are a large number of seamounts located on the converging boundary of the Cocos plate that cause resistance between the plates while subducting. Once the driving force overcomes the resistance created by the seamounts, the results are typically high magnitude earthquakes that cause

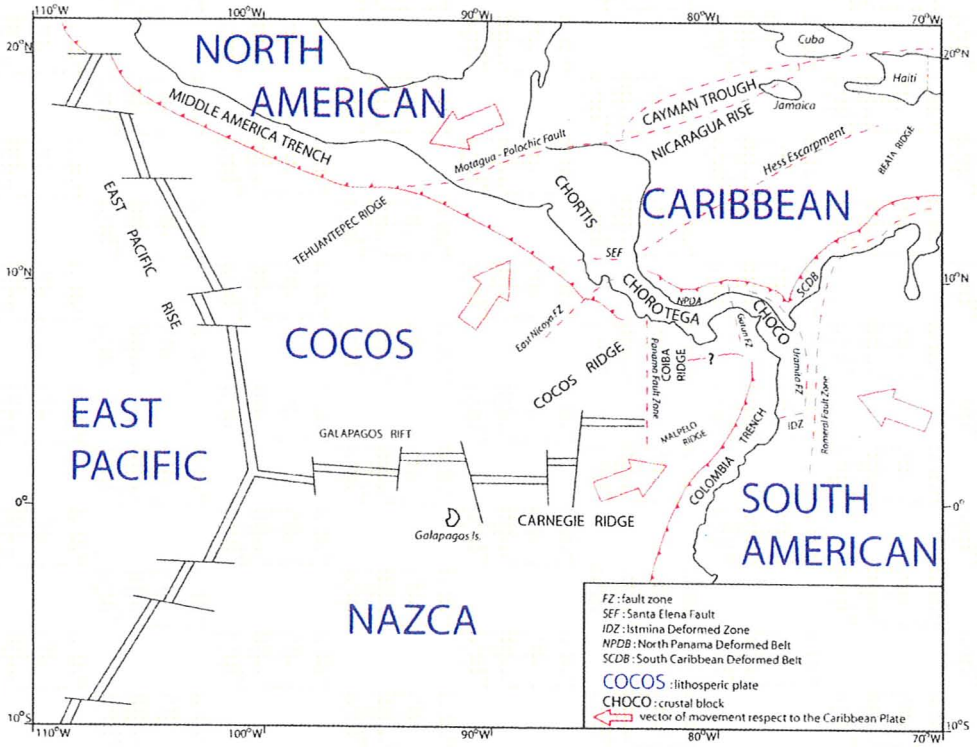

Figure 2.4: Plate tectonic map illustrating the location of the Cocos plate subducting under the Caribbean plate at the Middle American Trench (Bertram, 2006).

considerable amount of damage, as well as, vertical uplift of the western portion of the Caribbean plate (Gardner *et al*, 1987; Marshall and Anderson, 1995; De Shon *et al*, 2006). This uplift, depending on the tilt and the direction can only been seen on perpendicular features. If the tilt occurred parallel along the shore, features such as headlands that are perpendicular to the shoreline would have an increase in elevation that is equivalent to the distance and angle of the tilt.

Marshall and Anderson (1995) interviewed locals concerning the relative vertical uplift of the Nicoya Peninsula caused by the 1950 earthquake that measured 7.7 Mw. It was found that the locals were in agreement with the evidence presented in the study that

there was at least a 1 meter relative uplift of the region that was determined by changes in various geoindicators (Marshall and Anderson, 1995). Since that earthquake, the area has experience gradual subsidence causing a relative decrease in elevation of the affected area, however since 1950 there have been three additional recorded earthquakes (August 23, 1978 – 6.9 Mw, March 25, 1990 – 7.0 Mw and August 20, 1999 – 6.9 Mw) that may have affected relative sea level of the region (Gardner *et al,* 2001; De Shonetal *et al*, 2006).

2.1.5 Geology

Based on stratigraphic and structural features identified by early investigators the southern portion of Central America was defined into two separate geological provinces. The northern province consists of Guatemala, Honduras and northern Nicaragua with the southern province consisting of southern Nicaragua, Costa Rica and Panama (Escalante, 1990). The northern province has since been renamed as the Chortis block and the southern province has been divided at the narrowest point of central Panama with the northern area termed Chorotega block and the southern area as the Chocó block (Escalante, 1990).

Costa Rica can be divided into three structural units that are termed the forearc region, the magmatic arc and the backarc region that have a direction trend of northwest to southeast and divide the country with the magmatic arc in the central region of the country with the forearc and backarc forming the Pacific and Caribbean coast respectively (Escalante, 1990).

The basement complex of Costa Rica is "composed of mafic igneous flows of oceanic origin that occupies a tectonic belt along the Pacific Side" and has been described as the Nicoya Complex (Escalante, 1990). The Nicoya Complex has been studied in detail and is thought to be an ophiolite sequence that has contains early Jurassic radiolarites, late and early Cretaceous radiolarites, to early and late Cretaceous fauna (Escalante, 1990). Occurances of cretaceous deposits of both carbonate and clastic marine sequences have been mapped on the western coast of Costa Rica (Escalante, 1990).

2.2 Coastal Geomorphology

Various processes continuously evolve, reshape and alter the morphology of coastlines around the world. The field of study which analyzes these processes and the resulting coastline is known as coastal geomorphology. There is significant merit in advancing the knowledge of the discipline since it has been estimated that nearly 3 billion people live within 60 km of the shoreline (Woodruff, 2002).

2.2.1 Types of Coasts

Throughout the world there are various types of coasts that can be classified as rocky shores, sandy beaches, salt marshes, mangroves, estuaries, lagoons, deltas, barriers and muddy beaches. Short (1993) has categorized these coasts into two main categories, convergent and passive margin coasts, due to their location relative to the plate boundary. Convergent coasts form along a plate margin that has at least two plates converging

together which result in a mountainous region with high cliffs along the coastline (Short, 1999). Embayed beaches are typically located along a convergent coast, are enclosed at either end by rocky headlands, and consist of gravel to finer sediment or various size combination of sediment (Short, 1999).

Passive coasts are found along the lee side of a convergent plate margin, that developed over time and can be categorized into three smaller subsets based on the stage of their development: Amero are well developed passive coasts, Afro are moderately developed passive coasts and Neo are developing passive coasts. The width of the continental shelf in addition to the development of the coastal plains and deltas will determine the classification given to passive coasts (i.e. a well developed passive coast, an Amero coast, has a wide continental shelf and a well developed coastal plain and delta). Although passive and convergent coasts are very different from one another, both coasts can be divided up into multiple zones based on wave processes interacting with morphology.

2.2.2 Zones of a Coast

The majority of textbooks on this subject have classified the coast into four unique zones based on wave processes and morphology, however, within the literature these names have been misused and interchanged creating some confusion on this topic. For this reason, the zone classification provided by Short (1999) will be used to define and explain these zones for this research. The morphologic (wave process) defined zones starting at the shore and moving towards the sea are: subaerial beach (swash zone), surf

(wave breaking zone), nearshore (wave shoaling zone) and the inner continental shelf as illustrated in Figure 2.5.

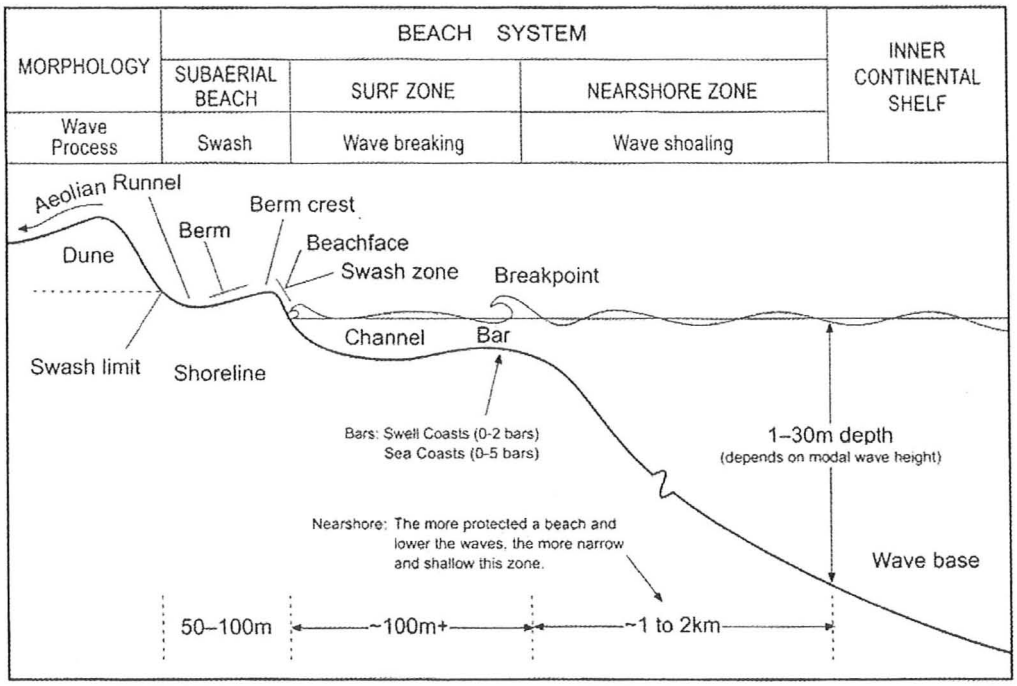

Figure 2.5: The beach system is divided into four zones based upon morphology and wave process. Boundaries between these zones can be identified by geomorphic features (Short, 1999).

The swash zone is a narrow section of beach that has a dynamic boundary that changes with the tide but can be defined as the point of collapse of a wave or where the wave bore reaches the dry beachface and extends to the upper limit of the swash action (Short, 1999). The incoming wave travels up the beachface to the upper limit while at the same time percolating into the sediment until gravity causes the remaining water to recede (Short, 1999). These processes affecting the beachface are influenced by many factors such as wave type, wave height, tide range/stage, beach morphology, shape/width and sediment sorting/size/permeability (Short, 1999). The furthest landward position of

the water level is called the shoreline and its position rises and falls with the tidal cycle, which is different from the term coastline which is the land/water margin at high tide (Bird, 2000).

The surf zone extends from the swash zone out towards the sea to where waves first begin to break (Short, 1999). This width of this zone is the most dynamic of all four zones and can range from a few centimeters as observed in laboratory studies to hundreds of meters on a beach (Short, 1999). Morphologic characteristics of the surf zone such as bars, troughs and channels are dynamic, as they are continuously changing in shape, size and location due to the process of breaking waves and wave-current transformation (Short, 1999). These processes are highly influenced by the tidal range since a change in water depth will change how and the amount of energy that will affect evolution of these features (Short, 1999).

The nearshore zone extends seaward beyond the surf zone, where wave shoaling occurs, until it reaches the offshore zone. This boundary has been defined as the point in which the modal wave base ceases to interact with the seafloor in a manner that moves sediment towards the shore (Short, 1999). Since the wave base depth is determined by the height and period of waves, when these variables are increased it results in an increase in depth of wave base which increases the lateral distance of the zone seaward (Short, 1999). The offshore zone, also referred to as the inner continental shelf is defined as the region where wave processes have no effect on seafloor morphology (Short, 1999). Since all four zones were defined in part by wave processes, it is important to understand wave terminology and wave energy sources which are discussed in the following section.

2.2.3 Wave Terminology

The main process that changes the morphology of a beach is wave energy. To properly understand how wave energy affects beach morphology, a basic understanding of wave terminology is necessary (Figure 2.6). Wave height is the vertical distance from the top of the wave crest to the bottom of the trough, and wavelength is the horizontal distance between the top of two successive crests or troughs (Open University, 2005). The amount of time it takes for two successive crests or troughs (i.e., one wavelength) to pass through a single point is called the period; whereas, the number of peaks or troughs that pass through the point in a second is called the frequency (Open University, 2005). Different types of waves will affect beach morphology, and can be produced from a variety of energy sources such as, wind, gravity, mass movement and tectonic activity.

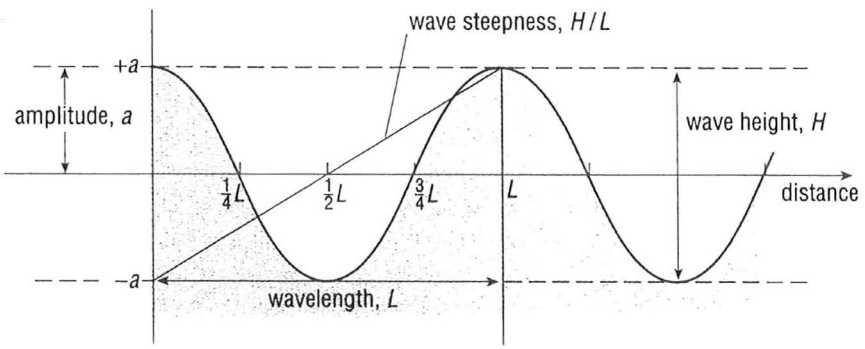

Figure 2.6: Diagram explaining the various terms used to describe a wave such as, wave height, wavelength, wave steepness, and amplitude. (Open University, 2005).

2.2.4 Energy Sources of Waves

Wind - Wind energy can produce a number of different waves that consist of varying wavelengths that affect the beach differently depending on the distance from the origin to the beach. The longest traveled waves to reach a shore are called ocean swells

and are produced by large storms and hurricanes. These waves have long wavelengths that permit quick travel and a low wave height decreases resistance which allows them to travel thousands of miles from the origin of the storm (Open University, 2005). Waves produced by storms near the coastline result in waves of larger height and shorter wavelength, thus, slower travel speed (Open University, 2005). When these storms produce strong onshore winds for a number of days, it can raise the sea level up to 6 meters creating what is known as storm surge (Bird, 2000). This surge can increase in height during periods of high spring tide resulting in devastating effects such as massive amounts of erosion and coastal flooding (Bird, 2000). These increases in wave energy result in an increase in seafloor interaction that can drastically change the morphology of the beach. Waves produced during non-storm activities are called nearshore waves that are much smaller then storm waves and cause less change to the beach morphology. Due to the increased amount of energy within ocean swells and storm waves, these affect the beach much more then nearshore waves.

Gravity - Gravity produced waves, also known as tides, cause a raise in sea level known as a flood and a decrease in sea level known as an ebb due to the gravitational pull of the moon and sun. The tide has a long period and wavelength that changes the height of sea level, yet the total amount of rise and fall various throughout the globe varies depending on factors such as the total gravitation pull of the sun and moon due to the location of the water body on the earths surface and the morphology that can intensify the tidal range such as bays that can trap the wave (Open University, 2005).

Tidal range is influenced in three ways due to the interaction of gravity between the sun, moon and the earth. The first influence is the gravitational pull on water from the moon, while the moon orbits the earth as the earth rotates on its axis (Open University, 2005). The greatest gravitation pull would be at the earth's surface closest to the moons center of gravity, while the opposite side of the globe would have the least (Open University, 2005). It takes 24 hours and 50 minutes for the earth to complete one rotation, during this time there will be two periods of high tide and two periods of low tide thus, the time difference between high and low tide is 6 hours and 12.5 minutes (Open University, 2005).

The second influence, called lunar tides, involve the moons declination as it orbits the earth and ranges from 0 degrees to 28.5 degrees over a 27.3 day period (Open University, 2005). During this time period there are two sets of 2 tides known as a tropic tide or an equatorial tide (Open University, 2005). A tropic tide occurs when the declination of the moon is above the Tropics which have the greatest influence on the diurnal tidal range (Open University, 2005). This is in contrast to an equatorial tide which will have no diurnal inequalities in the tidal range (Open University, 2005).

The third influence is the relative position of the sun and moon to the earth, which will dictate if their gravity influences will be cumulative or subtractive on the tidal range (Open University, 2005). If the sun and moon are located on the same side of the earth, their gravitational pull is cumulative increasing the tidal range to its maximum resulting in the highest and lowest tides, which are called spring tides (Open University, 2005). When the sun and moon are on opposite sides of the earth, their gravitational forces work

against one another reducing the total amount of gravitational pull on the tides resulting in the minimum tidal range which are called neap tides (Open University, 2005).

Mass Movement and Tectonic Activity - A mass movement (e.g., landslides) or the tectonic activity of an earthquake or volcanic eruption can result in the displacement of water that can produce multiple sets of long waves that are called tsunamis (Bird, 2000). Tsunamis have very long wavelengths that allow them to travel great distances, very rapidly. When these waves approach the coast, the decrease in water depth, causes the wave to build in height. In coastal areas, specifically with embayed shorelines, there is a funneling effect due to the narrow channel resulting in waves that can build to heights up to 40 meters tall (Bird, 2000). Due to this wave energy, tsunamis can cause coastal flooding and massive erosion of the beach. As shown in this section, waves can be produced from a variety of different energy sources. These processes can be combined with tidal processes which will have a greater influence on the morphology of the coast as will be discussed in the following section.

2.2.5 Tide Processes

The amount of influence tide processes have on the morphology of coastal areas can be grouped into three categories based on their tidal range: micro-tidal less than two meters; meso-tidal between two and four meters; and, macro-tidal greater than four meters (Short, 1999). In general, meso-tidal beaches have a combined influence of wave and tide processes, whereas, micro-tidal beaches are more influenced with wave processes and macro-tidal are more influenced with tidal processes (Short, 1999).

However, the beach gradient must be taken into consideration when combined with tidal range, since a low gradient beach will have a greater beachface exposed during low tide when compared to a steeper beach. Short (1993, pg. 205) states that these tidal beaches are where "aeolian, swash, surfzone and shoaling wave processes shift both vertically and horizontally with the rise and fall of the tide" unlike tide-less beaches such as most lakes. This shift in position can impact the beach morphodynamics through variation inwave height, location of wave breaking and development of rip currents.

Wave height is decreased during low tide because of a wider shoreface that allows the "wave energy to dissipate due to bed friction" (Short, 1999, pg. 207). Beach morphodynamics can change dramatically due to a steeper gradient during high tide compared to a lower gradient during low tide. An example of these changes is that during high tide the surf zone could be "reflective or intermediate with plunging/surging breakers in a narrow zone, whereas, dissipative conditions during low tide resulting in spilling breakers" (Short, 1999, pg. 208). The location of breaking waves can change during low/high tide due to variation in the number of sand bars which wave energy interacts. During low tide, the wave energy could interact with a couple of bars that would decrease the amount of energy reaching the shore, whereas, during high tide some of these bars would have less influence allowing stronger waves to reach the shore (Short, 1999). The amount of bar interaction also affects rip currents in a similar fashion. High tide allows for a greater area for offshore flow of water; whereas, bars limit the area during low tide of the receding flow resulting in the concentration of offshore flow in channels producing stronger rip currents during low tide (Short, 1999).

Due to the changes that occur on a tidal beach, a new morphodynamic classification scheme was created to reflect these changes taking into consideration the relative tide range (RTR) and the dimensionless fall velocity (Short, 1999). These two parameters quantify the following four physical constraints: modal breaking wave height; modal breaking wave period; sediment characteristics of the upper beachface; and, mean spring tide range (Short, 1999). The classes in the new scheme can be seen in Figure 2.7 and Table 2.3 (Short, 1999) which has the previous classification of wave dominated, mixed wave-tide and tide dominate beaches divided into seven categories that are reflective, barred, dissipative, low tide terrace, low tide bar/rip, ultra-dissipative and transitional. Three of these classifications (low tide terrace, low tide bar/rip and ultra-dissipative) will be explained in detail since it was anticipated that the Playa Guiones and Playa Pelada would be influenced by a mixture of wave and tide processes.

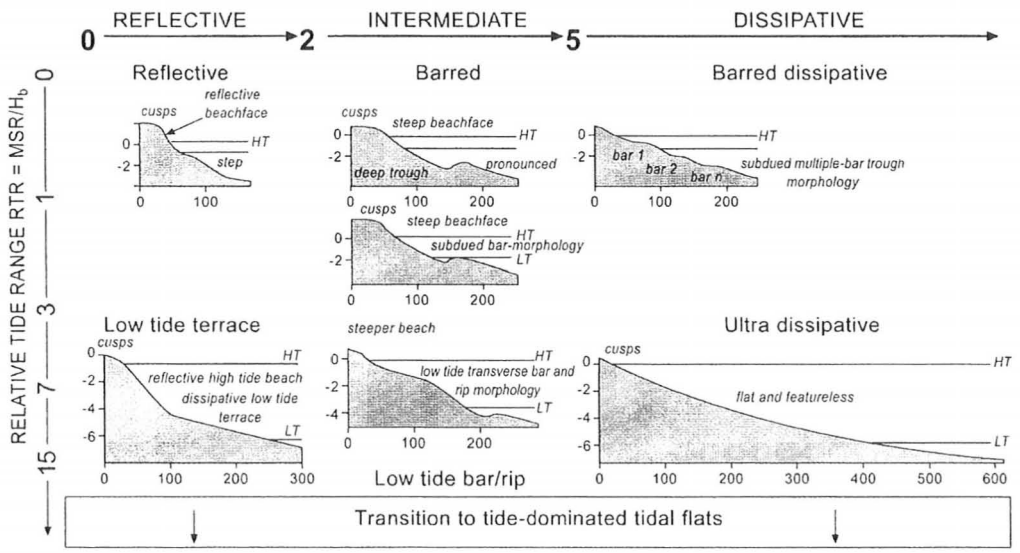

Figure 2.7: Reclassification of beach type using reflective, intermediate and dissipative characteristics with the addition of relative tide range in meters (Short, 1999).

Table 2.3: Summary of figure 2.6 that includes the specific values of relative tidal range in meters and includes the process most dominate for each beach type (Short, 1999)

Relative tide range	Group	Beach type
$RTR < 3$	Wave-dominated	1. Reflective
		2. Barred
		3. Dissipative
$3 < RTR < 15$	Mixed wave–tide	4. Low tide terrace
$3\ RTR < 7$		5. Low tide bar/rip
$3\ RTR < 15$		6. Ultra-dissipative
$RTR > 15$	Tide-dominated	7. Transitional (beach to tidal flat)

Low tide terrace beaches have a steep upper slope that contains coarse sediment with grain size greater then 0.3 mm and have a gradual low tide terrace that is composed of finer sediments (Short, 1999). Surging/plunging waves on the beachface are typical for high tide, whereas, spilling breakers in a dissipative surfzone during low tide (Short, 1999).

Low tide bar/rip beaches have intertidal swash bar morphology and transverse bar/rip morphology at low tide levels (Short, 1999). During high tide, plunging waves break along the upper beach, whereas, when the tide is falling the waves break increasingly on the bar and reform in the trough increasing the rip currents due to the topography (Shore, 1999). Ultra-dissipative beaches are very flat and featureless with a low gradient that creates a very wide beachface with spilling breakers throughout the tidal cycle (Short, 1999). Due to the lack of features, these beaches are considered very stable even to large storms (Short, 1999). Depending on the wave and tide processes affecting the type of beach, there are a variety of coastal beach features that will be created as discussed in the following section.

2.2.6 Coastal Beach Features

Bar Morphology - Beaches are classified as barred or unbarred depending upon the formation of bar(s) in the nearshore. The formation of bars is a result of sediment converging, whereas, troughs form as a result of sediment divergence (Short, 1999). Climate has been associated with bar formation and the terminology for this cycle variation is "winter" or "summer" and corresponds to wave energy rather then season. The difference in beach profile for each season is very distinct due to the wave energy the changes the shape of the profile as seen in Figure 2.8. "Winter" or high energy environments cause the removal of sediment from the berm and create breakpoint bars (Short, 1999). "Summer" or low energy environments cause a landward migration of the bars which eventually results in beach accretion (Short, 1999). In a given year, a beach may experience multiple cycles of "winter and summer" depending on the on the climate (Short, 1999).

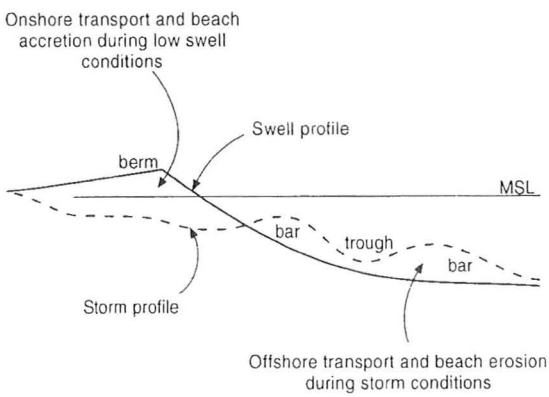

Figure 2.8: Beach profile comparison between a "summer" low energy environment (solid line) and a "winter" high energy environment (dashed line). "Summer" and "Winter" refer to the amount of energy and not a particular season. A high energy environment will erode sediment from the berm and deposit sediment in bars, whereas, low energy environment will move these bars back towards shore and deposit a new bearm (Short, 1999).

The number and shape of nearshore bars can range dramatically from one beach to the next but the formation is a result of wave energy and beach slope. Short (1999) found that the number of bars will increase as beach slope decreases and the spacing between bars will increase exponentially offshore. Transverse bars are typical of low energy environments, crescentic bars are found in intermediate energy environments and linear bars form in higher energy environments (Short, 1999). Bar formation occurs in the surf zone as a result of plunging breakers that remove sediment leaving a bar behind the breakpoint (Short, 1999).

Berms - Formed along the shoreline on the beachface, berms are created from accreting sediment that is deposited by wave uprush. The shape and size of the berm is a function of the wave energy with the maximum height of berm formation being as high as the swash. There are three ways berms can develop. First, during neap tides when there is significant longshore transport, sediment accumulates on the beachface at high tide, with subsequent tides redistributing the sand and building the berm (Short, 1999). Second, is the slow onshore migration of swash bars. The third way they occur is when the onshore migration of swash bars is so rapid they form a wide berm ridge (Short, 1999).

Berms can be eroded in three different manners depending on the type of beach. First, on steep reflective beaches, moderate swell conditions will enhance the run-up and over-topping which results in eroding the berm caused by resonance of subharmonic water level fluctuations in the surf zone (Short, 1999). Second, on less steep dissipative beaches, erosion will cause a berm cut due to significantly higher incident storm energy

(Short, 1999). On intermediate beaches the previous two erosion process can occur in addition to scour of the berm caused by rips (Short, 1999).

Beach Step - This morphological feature is located at the base of the beachface where the gradient of the slope is greatest and can range in height from a few centimeters to over a meter (Short, 1999). Often the sediment found in the beach step is coarser then the sediment found on either side and is formed from swash zone processes. There are three sections that compose a beach step: the step face, the step crest that separates the step from the beachface and the horizontal step that extends from the face to away from shore (Short, 1999). Reflective and intermediate beaches commonly have beach steps and this feature can sometimes form on dissipative beaches (Short, 1999). The beach step is created from the backwash of a wave creating a vortex as seen in Figure 2.9. The vortex circulates the water towards the beach cutting into the beachface and then back out to the sea on the surface (Short, 1999). The size of the beach step is positively related to the wave height and period as well as larger sediment that result is higher steps forming.

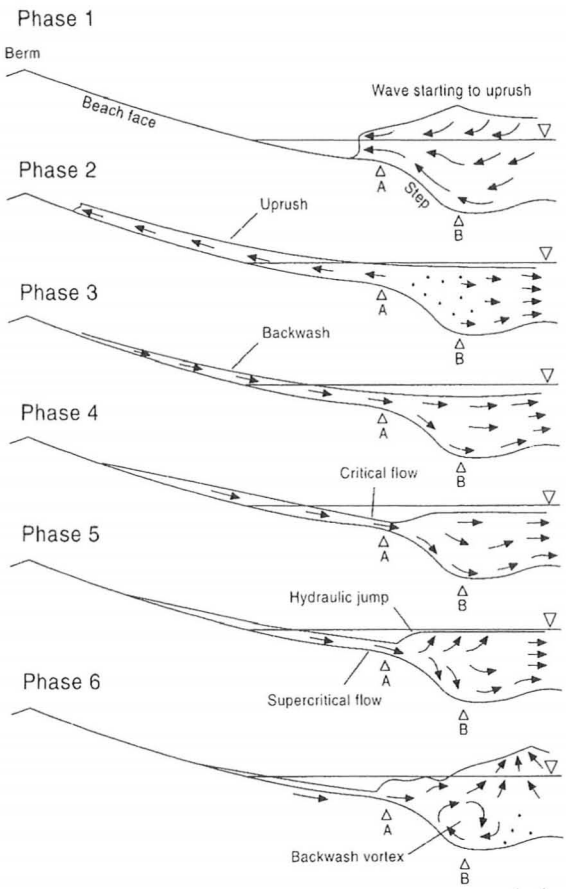

Figure 2.9: Formation of a beach steep created due to the backwash vortex that erodes the sediment and transports the sediment on the surface out to sea. Arrows indicate the flow direction (Short, 1999).

Swash Cusps – An interesting coastal feature whose formation processes have intrigued scientists are crescentric, concave-seaward features, usually consisting of coarser sediment then the beach, that are formed at regularly spaced intervals along the shoreline (Short, 1999). The sediment that is deposited during cusp formation is well sorted by grain size, which allows greater water permeability in coarser sediment, encouraging cusp development. A classification scheme was developed by Dolan and Ferm (1968) that organizes the cusps into three groups based on spacing between cups: typical beach cups (8-25m), storm cusps (70-120m) and giant cusps (70-1500m). This

classification scheme has since been replaced by differentiating between swash cusps that are spaced up to tens of meters and rhythmic topography that has cusp spacing greater then fifty meters (Short, 1999).

There are two opposing theories that attempt to explain how swash cusps are formed. The first theory involving standing edge waves, was introduced in 1937 and is the one most widely accepted. This theory states that cusps are formed from standing waves that have the same period as incoming waves. When the two waves mix there are two possible outcomes: either the incoming wave is enhanced and greater erosion occurs, or if the standing wave crest combines with the incoming wave trough deposition will occur (Short, 1999). The question remaining to be answered from this theory involves the uncertainty of how the regular spacing of the cusps occurs. The other theory involves self-organization. It attempts to combine swash flow with beachface morphology to explain cusp formation. This theory states that depressions on the beachface accelerates the flow of water resulting in an increase in erosion that creates cusp swales (Short, 1999). Recent experiments have not shown conclusive evidence that either theory has the ability to predict when cusps were removed, if there would be reformation of cusps or at regular spacing (Short, 1999).

2.2.7 Backshore Beach Features

The backshore zone is the area from the swash limit that extends landward where backshore features are formed from sediment transported through swash and aeolian processes (Short, 1999). Many features can form on the backshore, such as, beach ridges

and a variety of dunes that include foredunes, blowouts, parabolic and transgressive dunefields (Short, 1999). The profile and features formed on the backshore are related to the extent of the backshore and is dependent on the beach type (reflective, dissipative or intermediate), modal beach width, dynamic beach state (stable, eroding or accreting) and sediment supply (Short, 1999).

Beach Ridges - These features can be formed during fair-weather and storm related swash and overwash processes in which sediment is deposited linearly along shore the closely resembles a berm (Short, 1999). The distinction between a berm and a beach ridge it that berms are created in microtidal processes and beach ridges form in all tidal stages (Short, 1999)

Foredunes - Created on the top of the backshore by sediment that accumulates in the vegetation that has been transported from the beachface by aeolian processes (Short, 1999). These features are "shore-parallel, convex, symmetric to asymmetric dune ridges" that can be classified into two categories, incipient and established (Short, 1999). The creation of incipient foredunes is dependent on the density, height and type of vegetation, sediment supply and wind velocity (Short, 1999). The introduction of vegetation along the backshore allows wind-transported sediment to be trapped and deposited by the new vegetation (Short, 1999). As the sand accumulates, the vegetation also increases allowing for further dune development. These dunes can be scarped or removed by storm surges after which the dune building process begins again once vegetation is introduced into the backshore (Short, 1999). The vegetation species that inhabit an incipient foredunes tend to be small plants such as grasses or vines. As the foredune continues to

grow into an established foredune, the species present will also change to larger, woody plants increasing how stable the dune will be under storm surges.

Established foredunes can range in height from small, 1 -2 m to large, 30-35 m dunes depending on the amount of sediment supply and wind velocity (Short, 1999). Foredunes typically found on dissipative beaches are larger then dunes that occur on reflective beaches due to the surf zone processes. Figure 2.10 is a diagram that depicts various types of foredunes in a life cycle that includes both eroding and accreting processes (Short, 1999). The amount vegetation species richness and succession on the foredune can be highly influenced by the amount of seasalt aerosols (Short, 1999). Reflective beaches found outside the tropics have higher species richness with a defined zonation due to lower levels of salt because of lower waves and a narrower surf zone in this region (Short, 1999). This is in contrast to dissipative beaches, common in the tropics, which have higher salt concentrations and a wider surf zone due to higher waves (Short, 1999).

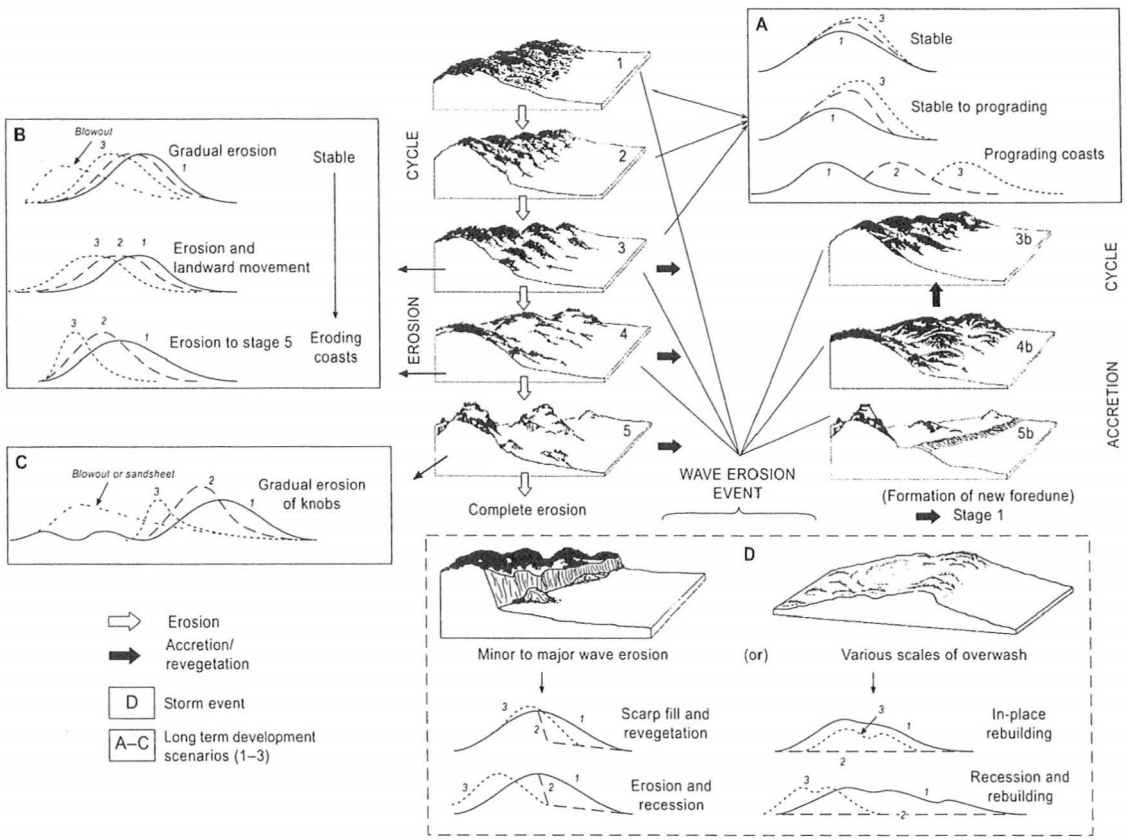

Figure 2.10: Evolution of a foredune including the erosion and accreting cycle (Short, 1999).

Foredune Plains - Occasionally a new foredune will form on the seaward side of an existing foredune causing the original to become a relic foredune (Short, 1999). A foredune plain is created from a group of relic foredunes that forms over thousands of years and depending on the number of relic foredunes included in the plain, the width can vary from tens of meters to thousands.

Blowouts - These features are created though aeolian erosion on existing dune formations along the backshore and are divided into two categories based on the shape of the depression. Saucer blowouts are circular in shape, whereas, trough blowouts are more elongated in shape (Short, 1999). The sediment removed from the depression

forms a depositional lobe as seen in Figure 2.11. The initial creation or further development of a blowout has many variables such as size of original dune, the type and density of dune vegetation, wind velocity, amount of human activity and the amount of wave erosion and overwash at the backshore (Short, 1999).

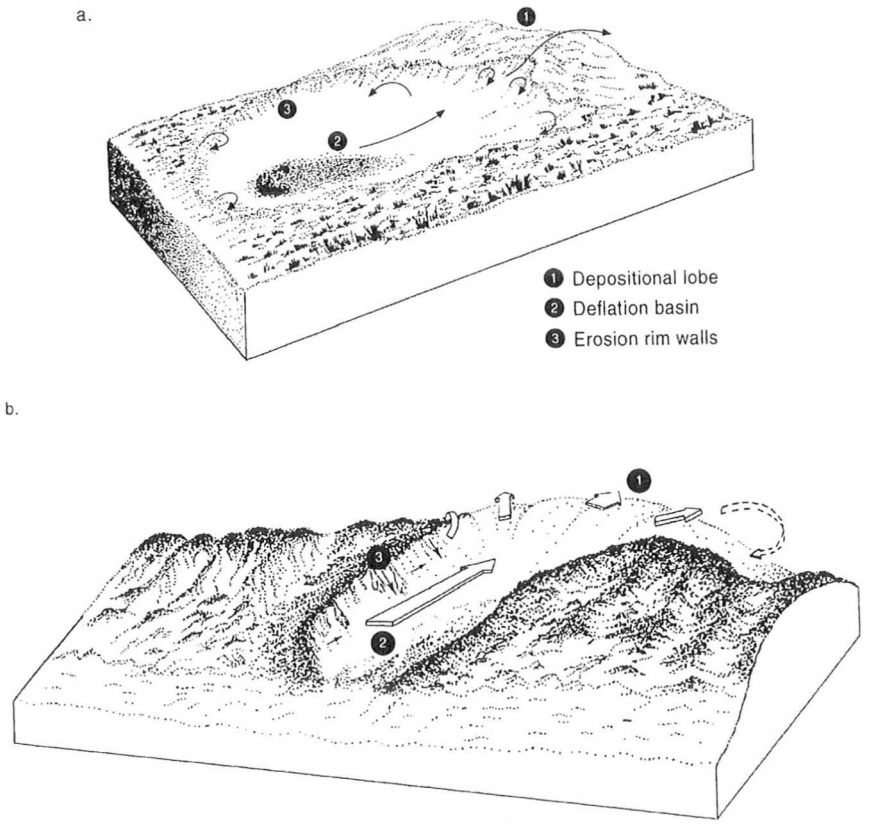

Figure 2.11: Illustration of a saucer blowout dune (a) and a trough blowout dune (b) highlighting areas of erosion (deflation basin) and deposition (depositional lobe)(Short, 1999).

2.2.8 Embayed Beaches

Embayed beaches are typically bounded by rocky headlands or structures that control the beach planform, morphodynamics and beach rotation (Short, 1999). The pre-existing bedrock topography is the control factor that dictates the length of the beach and

the location of the headlands. These were formed in mountainous regions along the coast during the Holocene sea level transgression when areas where partially flooded creating valleys that eventually turned into headlands (Short, 1999). Due to the refraction pattern created by the headlands, prevailing waves arrive along the entire length of the embayed beach shore normal resulting in no longshore transport if hydrodynamic conditions are in equilibrium (Short, 1999). Weak currents will exist flowing in the direction of high wave energy towards low wave energy, with rip currents exiting at the furthest ends of the embayment (Short, 1999). As seen is Figure 2.12, the shape of the embayed beach is asymmetric, having a "strongly curved shadow zone, mildly curved center of the embayment and a relatively straight downcoast end" (Short, 1999).

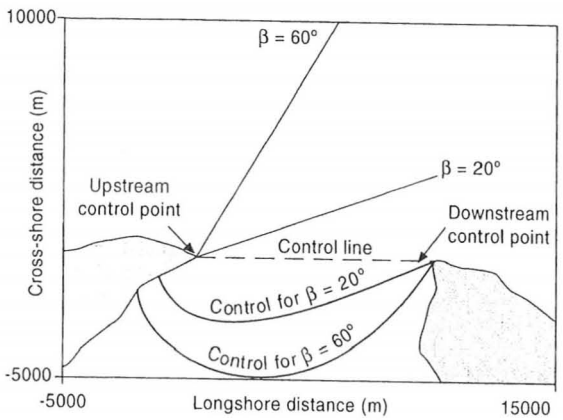

Figure 2.12: Illustration of an embayed beach with control points, control line and the angle of the incoming incident wave that is used to determine the distance of indentation of the embayment (Short, 1999).

The overall shape of an embayed beach and the amount of distance inland that the strong curved shadow will reach has been formulated by Hsu *et al.* (1987) as seen in Figure 2.12. This calculation involves the distance between two control points (R_0) that

represents the control line (Short, 1999). The first control point is the upcoast headland where incident waves first diffract towards the embayment and the second control point is the downcoast headland or straight section of coastline where incident waves are parallel to the shore (Short, 1999). Wave obliquity (β), is the angle of the incident waves in comparison to the control line (Short, 1999). To determine the position of the shoreline, a straight line is drawn from the point of diffraction on the first control point towards the shore and the angle is measured (θ) to the incident waves (Short, 1999). These values are used in the formula:

$$R/R_0 = C_0 + C_1(\beta/\theta) + C_2(\beta/\theta)^2$$

The rocky headlands impact the wave dynamics such that normal surf zone circulation is affected due to wave reflection. When headlands are spaced far apart and wave height is increased, the surf zone circulation is affected only near the headlands with normal circulation between them (Short, 1999). Headlands that are spaced close to each other, or wave height is increased further, the entire surf zone circulation can be affected resulting in increased rip systems. These embayed beaches are common on convergent coastal margins where at some point of time the sea level was above the current level (Short, 1999). This assisted in the formation of embayed beaches, but has created emerged and submerged coastlines due to the rise and fall of mean sea level in the past as will be discussed in the following section.

2.2.9 Emerged and Submerged Coastlines

Emerged Coastlines – The relative sea level can rise or fall for a variety of reasons that are explained in Section 2.3.2-Causes of Sea Level Rise/Fall, however, an increase in sea leave will result in the creation of a new coastline and beaches. These beaches will eventually become emerged beaches when relative sea level drops below the newly formed beaches (Bird, 2000). Emerged beaches are distinguishable due to features created such as terraces or beds composed of deposited marine sediment or marine organisms (Bird, 2000). These features are best persevered when formed in permeable rocks, such as, sandstone, limestone or gravelly formations unlike impermeable rocks that resist and deny the formation of the terraces (Bird, 2002). These formations can be difficult to locate along the coastline, due to the amount of erosion or deposition of mountainous sediment that has occurred and the dense vegetation that is commonly present along the coastline.

Submerged Coastlines - A submerged coastline is similar to an emerged coastline, but with the opposite evolutionary history in the creation of the features such as terraces and beds (Bird, 2000). These coastlines form after there has been a drop in relative sea level and the terraces being to form on the new coastline (Bird, 2000). These features can be more difficult to identify and even less preserved due to the wave processes that affect the seafloor during the rise in sea level (Bird, 2000). During this time, wave processes continue to erode the terraces, depositing sediment that can hide the features until the water depth is great enough that the effective wave base has no affect the no seafloor (Bird, 2000). Although these features can be more difficult to locate, they

have been found throughout the world, for example along the US and Japan coast (Bird, 2000).

2.3 Shoreline

2.3.1 Definition

There is a large abundance of literature pertaining to the monitoring of coastlines around the world due to: the importance of identifying hazard zones, creation of policies to regulate coastline development, the design/construction/assessment of components used for coastal protection, and the provision of additional information on coastal processes because of an increase in numerical modeling research (Boak and Turner, 2005). Monitoring the shoreline can be a useful indicator to how a coast in changing throughout time, but before a shoreline can be measured it must be clearly defined due to the many possible ways it can be identified.

The shoreline is defined as the physical land-water boundary that is under constant rise/fall due to a variety natural processes and anthropogenic effects (Camfield and Morang, 1996; Boak and Tuner, 2005). These influences can cause the shoreline to change position within a wide time that ranges from instantaneously, to daily, to seasonally, and can be as long as decades or at the geological time scale (Camfield and Morang, 1996; Boak and Turner, 2005). A common error in many studies is assuming that the shoreline position being measured is "normal or average", since many natural phenomena can change what would be the average (Boak and Turner, 2005). It could be hypothesized that there is no average position and that the shore is always in transition.

2.3.2 Causes of Sea Level Rise/Fall

There are many reasons why the water level can rise or fall along a coast over a given time frame. Such processes can be include changes in climate (e.g., amount of precipitation/evaporation), ocean processes (cross-shore and alongshore sediment transport, waves, tides, storm surge, run up), tectonics (tsunamis, uplift, subsidence, liquefaction of sediments), climate change, anthropogenic influence (withdrawal of groundwater/oil, beach nourishment), isostatic adjustment of earths crust and events (e.g., El Ninõ, Southern Oscillation) (Morton *et al,* 1993; Camfield and Morang, 1996; Boak and Turner, 2005). The magnitude of change caused by these things can vary as well as the timeframe required for the change as seen in Table 2.4.

Table 2.4: Various reasons for sea level change, both long and short term, with the associated timescale or range of effect and vertical effect associated with each cause. (Adapted from Camfield and Morang, 1996)

Sea Level Changes Along The Coastal Zone		
Short-Term (periodic) causes	**Time Scale (P=period)**	**Vertical effect**
Periodic Sea Level Changes		
Astronomical Tides	6-12 h P	0.2 – 10 + m
Meteorological and oceanographic fluctuations		
Winds (storm surges)	1-5 days	Up to 5 m
Evaporation and precipitation	Days to weeks	
Ocean surface topography (changes in water density and currents)	Days to weeks	Up to 1 m
El Nino/Southern Oscillation	6 months every 5-10 years	Up to 60 cm
Seasonal variations		
River runoff/floods	2 months	1 m
Seasonal water density changes (temperature and salinity)	6 months	0.2m
Seiches	Minutes - Hours	Up to 2 m
Earthquakes		
Tsunamis	Hours	Up to 10 m
Abrupt change in land level	Minutes	Up to 10 m
Long-Term Causes	**Range of Effect**	**Vertical effect**
Change in volume of ocean basins		
Plate tectonics and seafloor spreading and change in seafloor elevation	Eustatic	0.01 mm/year
Marine sedimentaion	Eustatic	<0.01 mm/year
Change in mass of ocean water		
Melting or accumulation of continental ice	Eustatic	10 mm/year
Release of water from earth's interior	Eustatic	
Release or accumulation of continental hydrologic reservoirs	Eustatic	
Tectonic uplift/subsidence		
Vertical and horizontal motions of crust(in response to fault motions)	Local	1-3 mm/year
Sediment compaction		
Sediment compression into denser matrix	Local	
Loss of interstitial fluids (withdrawal of oil or groundwater)	Local	
Earthquake-induced vibration	Local	

2.3.3 Shoreline Indicators

There are a variety of indicators that are used to monitor the position of the shoreline. Boak and Tuner (2005) conducted a review of existing literature and found that these indicators can be classified into three classifications. The first classification grouped visually discernible coastal features such as: top/base of a cliff; vegetation line, storm/debris line, wet/dry line, etc (Boak and Tuner, 2005). The second classification is based on the tidal datum of a coast, where the shoreline is defined by the intersection of the profile with a vertical elevation corresponding to the tide such as mean sea level (Boak and Tuner, 2005). The third classification is a relatively new classification that is based on identifying the shoreline indicator with image processing software on digital coastal images in which the indicator is not visually discernable by the human eye (Boak and Tuner, 2005). Figure 2.13 shows a comparison of the different shoreline indicators from the first two classifications that are used in various studies.

Boak and Tuner (2005) found that after analyzing literature about identifying visually discernable shoreline indicators that they can be grouped into three categories: man-made structures (e.g., landward edge of a revetment structure); morphological features (e.g., erosion scarp), and position of the waterline (e.g., high-tide high water level (HWL)). The HWL has been widely used in past studies to identify the shoreline since it "is most appropriate reference because its position on the upper foreshore represents the landward limit of influence by average waves and water level" (Camfield and Morang, 1996). However, there is some controversy over the accuracy when using this indictor to map the shoreline since it "may not appear as a distinct line" or could be

misidentified if it actually was a "debris line, heavy mineral lag deposits, vehicle tracks or erosion scraps" (Boak and Tuner, 2005).

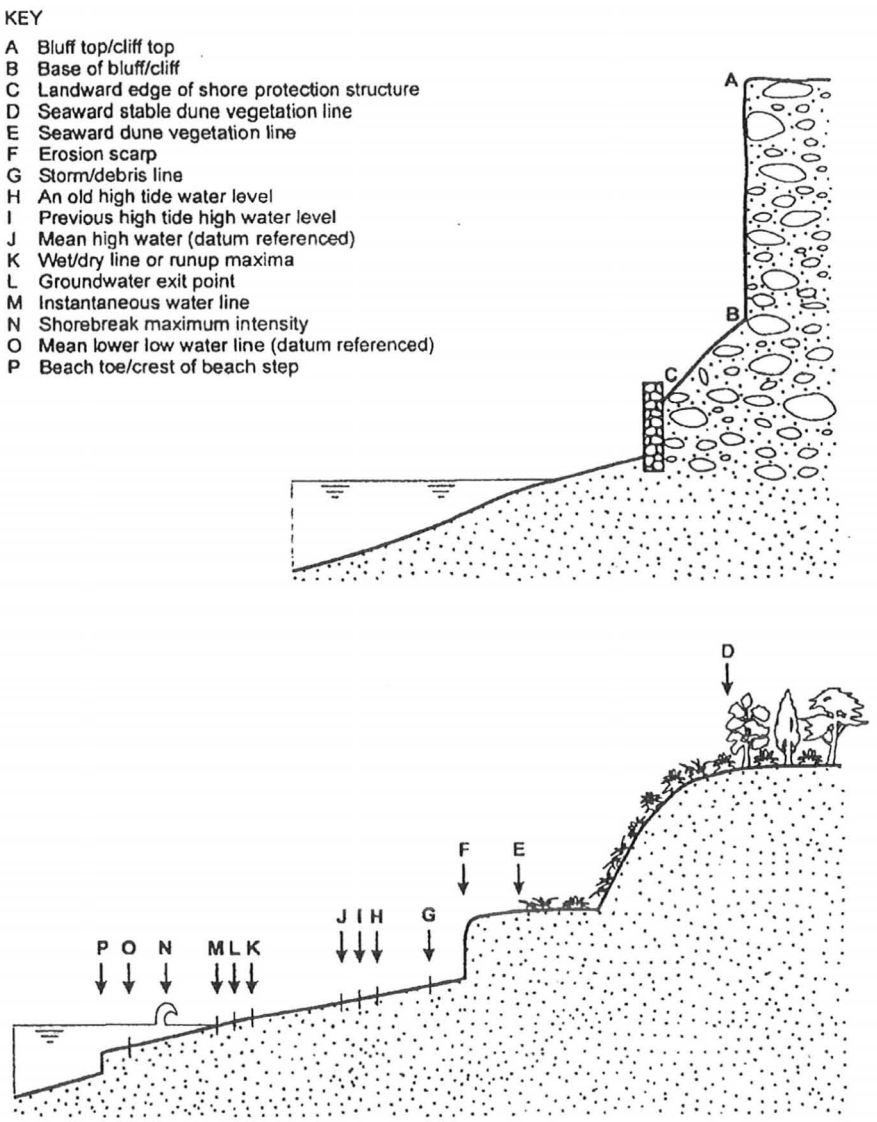

Figure 2.13: A variety of indicators that can be used to identify the shoreline. If measuring the shoreline to compare to previous measurements, this demonstrates the importance of using the same indicator due to the spatial difference between indicators chosen (Boak and Tuner, 2005).

2.3.4 Sources to Attain Shoreline Indicator

Coastal Maps and Charts - Many early coastal maps and charts were created using a variety of shoreline indicators that can have inaccuracies within them. If the surveyor was estimating the HWL by "noting the vegetation, driftwood, discoloration of rocks, or other visible signs of high tides" and then used as the mean high water (MHW), the charts are estimated to be inaccurate up to the order of 10 meters (Boak and Turner, 2005). Other potential errors of using historical map and charts "include errors of scale; datum changes; distortions from uneven shrinkage, stretching, creases, tears and folds; different surveying standards; different publications standards; projection errors and partial revision" (Boak and Tuner, 2005).

Aerial Photography – Collection of coastline images around the world began in the early 1920's, however, it was not until the 1930s before quality stereo aerial images were available (Boak and Tuner, 2005). These photographs have been used to create maps of the coastline and used in studies to observe how the coast has changed over a period of time. However, due to the cost of capturing this imagery the spatial and temporal coverage of can vary from one site to the next. The frequency of the images can also be biased towards post storm shorelines that are captured to analyze the damage and changes to the coast (Boak and Tuner, 2005). Due to the distortions that are inherent in the images caused by the camera lens, in flight movement and orientation of the aircraft the images need to be corrected before any analysis can be completed.

The distortions within the images are caused by radial lens distortion, tilt and pitch of the aircraft, variable scale and relief displacement (Camfield and Morang, 1996;

Lillesand *et al,* 2004; Boak and Tuner, 2005). Radial lens distortion, although minimized with newer lenses, still occurs and is the distortion created as a function of the distance from the photo iso-center (Camfield and Morang, 1996). It is also common that most aerial photographs are taken at a tilt between 1 and 3 degrees due to aircraft movement (Camfield and Morang, 1996; Lillesand *et al,* 2004). Since it is near impossible to fly at a constant altitude, there is variable scale between each image captured (Camfield and Morang, 1996). Relief displacement is created most often in images of uneven terrain with large differences in elevation (Camfield and Morang, 1996). With modern software these images can be digitalized, distortions can be corrected and a geo-rectified orthophoto can be produced so that a quantitative analysis can occur. The time of capture is also important to know so that it can be compared to the tide level. Even with the tidal information, correcting for this is difficult since knowing the slope of the beach would be necessary in calculating the horizontal offset (Camfield and Morang, 1996).

For geo-rectifying the images, there should be 60 percent overlap between each successive image as to limit the amount of distortion present in each image (Lillesand *et al,* 2004). Ground control points are required to correct for the distortions which can either be selected prior to the images being captured, however, the majority of older aerial photographs do not contain these predefined ground control points. The predefined ground control points are selected preflight in which reflectors deployed at known locations. The reflectors will appear as bright spots on the images and the latitude/longitude and elevation are known. For images without the predefined ground

control points, secondary points can be obtained by matching prominent features such as the corner of buildings or road intersections with their point in the field (Camfield and Morang, 1996).

When using aerial photographs as the source for selection the shoreline indicator, the greatest source of error is delineating the HWL. Another source of error are in images of a remote region where there are a lack of control points to register sequential photos due to lack of buildings/development or in heavily vegetated regions (Camfield and Morang, 1996). It has been estimated that errors associated with this type of identification can be as great as 10 meters (Camfield and Morang, 1996).

Beach Surveys – A technique that has been used for a long time to monitor shorelines is beach surveys which provide accurate sources of information but are limited both spatially and temporally due to the amount of time required to perform each transact (Morton *et al,* 1993; Boak and Turner, 2005). The equipment used to survey a beach can consist of: a simple graduated rods and chains; standard stadia rod and level; or a geodimeter and a reflecting prism (Morton *et al,* 1993). A typical beach will have multiple shore normal transacts that are tied into datum benchmarks that allowing for repeat surveys providing long term monitoring (Morton *et al,* 1993; Boak and Turner, 2005). A profile of the transact is created that can illustrate features such as "the shoreline, berm, dunes, vegetation line or a datum intercept" (Morton *et al,* 1993). These transects can be interpolated with each other to identify the shoreline and to provide three dimensional models so that sediment volume can be calculated (Morton *et al,* 1993; Boak and Turner, 2005). Problems associated with this technique can include lost/eroded

benchmarks or the surveyors straying off the transact (Morton *et al,* 1993). Due to the limited number of transacts additional limitations are associated such as: the transacts could be placed on dynamic morphological features such as beach cusps that are continuously changing; the distance between the transacts can be quite large so there is an assumption that the shoreline does not vary between these two transacts also putting uncertainty in volume calculations (Morton *et al,* 1993; Boak and Turner, 2005).

GPS Shorelines - A more efficient technique for completing beach surveys is through the use of kinematic global positioning system (GPS) units that can be mounted on four wheel drive vehicles or attached to backpacks worn by the surveyors (Morton *et al,* 1993; Boak and Turner, 2005). The kinematic GPS units can be used either in real-time or stop-and-go surveys that can provide a higher resolution of a beach survey then previously attainable with the classic beach profile surveys.

The GPS unit works by receiving three types of information from GPS satellites: the broadcast ephemeris; the pseudorange; and the carrier phase. The broadcast ephemeris provides the satellite position information. The pseudorange is the distance between the satellite and receiver which is calculated by the amount of time for the signal to travel from satellite to receiver, but error is introduced by the receiver clock bias (Morton *et al,* 1993). The carrier phase is "the difference between the incoming carrier wave and the phase of the reference signal generated by the GPS receiver" (Morton *et al,* 1993).

When four or more satellites are present, the receiver can solve the three-dimensional position and the clock bias. Differential GPS is when two receives work in

unison tracking the same group of satellite and solving the position. One receiver is stationary at a fixed known reference point while the other receiver is used to perform the survey (Morton *et al,* 1993). Since both receivers are tracking the same satellites and there is a reference point with the one unit, the errors that are introduced can be corrected and the measurements are very accurate (Morton *et al,* 1993).

The stop-and- go kinematic GPS survey is similar to a beach survey, in which the surveyor follows a set profile and uses the receiver to measure and record points at fixed locations. For a real-time kinematic GPS survey, the receivers are continuously receiving, calculating and recording points as the surveyor completes the intended survey at whatever predetermined time interval. Since the real-time kinematic survey can collect a far greater number of points then in a typical beach survey, it is possible for the surveyor to complete many more transacts that are spaced more tightly. The results can produce three-dimensional models of the beach that are much more accurate without the limitations associated with beach surveys.

Multispectral/Hyperspectral Imaging - As more satellites are deployed with better technology and electronics the capabilities for greater resolution has allowed for a near continuous monitoring of the worlds coastline that was previously unattainable. The main limitation for this technology is the pixel resolution which is determined by the electronics equipped on the satellite capturing the image. There are many satellites now used for imaging, each having a different number of spectral bands and widths and with different spatial resolution as seen in Table 2.5. The advantages of this technology is that it can: capture a great deal of information for a large area; provide the ability to aid in

coastal management with greater resolution; and, with multiple spectral bands it can provide data about the coastline that are not discernible or present in aerial photographs.

Table 2.5: Comparison of the spatial resolution, spectral bands, swath width, altitude and how many days in between to revisit of an area for four satellites that are available to the public to purchase images (Lillesand *et al*, 2004).

Satellite	Launch Date	Spatial Resolution (m)	Spectral Bands (μm)	Swath Width (m)	Altitude (km)	Revisit (day)
Landsat-7 ETM+	Apr. 15, 1999	30 30 30 30 30 60 30 15	1: 0.450-0.515 2: 0.525-0.605 3: 0.630-0.690 4: 0.750-0.900 5: 1.550-1.750 6: 10.40-12.50 7: 2.090-2.350 Pan: 0.520-0.900	185	705	16
IKONOS	Sept. 24, 1999	1 4	Pan:0.45-0.90 1: 0.45-0.90 2: 0.52-0.60 3: 0.63-0.69 4: 0.76-0.90	11	681	<11
EROS-A	Dec. 5, 2000	1.8	Pan: 0.50-0.90	13.5	480	10.5
QuickBird	Oct. 18, 2001	0.61 2.40	Pan: 0.45-0.90 1: 0.45-0.90 2: 0.52-0.60 3: 0.63-0.69 4: 0.76-0.90	16.5	450	1-3.5

Orthometric Vs Geodetic Data -There is a difference between orthometric and geodetic data that is related to the data collected. GPS data collected is referenced to a geocentric ellipsoid that is a mathematical representation of the earth and the elevation data is the distance above this ellipsoid. However, the earth is not perfectly ellipsoid and there are many undulations due to landmass and water which changes the amount of gravity at a particular location. This representation of the earth is known as the geoid and

mean sea level has the reference point of 0 meters. The difference in elevation above the geoid and ellipsoid varies between -106 m and +85 m around the earth. The GPS data collected was referenced to the ellipsoid but if the geoid reference is known at this location, an orthometric correction can be applied.

2.4 Interpolation Methods

When creating a DEM from topographic data, there are a variety of different interpolation methods that can be used such as tinning, minimum curvature and kriging. Frequently, the topographic data that are used to create DEMs are not in a grid pattern, but rather irregularly spaced over the sample area. All three interpolation methods have the ability to interpolate spatially irregular data with the final product being a regular grid of estimated points. When using tinning, the ability to create an irregular grid of estimated points also exists. Although all three methods achieve the same goal of using local estimation, they each use a different technique for calculating these points.

2.4.1 Global vs. Local Estimation

When estimating a value, samples that are used in the calculation can either be global or local. Global estimation uses either the total area, or a large portion of it, thus, including a large number of samples in the calculation of the estimate, whereas, local estimation considers a smaller number of samples within a much smaller area (Isaaks and Srivastava, 1989). Global estimation is commonly used to first view the overall pattern created before local estimation is applied. Global estimation works great for a data set

where samples are evenly distributed or random, but if clustering occurs then additional work is necessary to ensure the clusters do not affect the overall estimation of other points. Local estimation takes into account the distance away from the sample is from the estimation and can correct when there is a clustering of samples of similar value.

2.4.2 Tinning

Tinning is a type of interpolation process that uses sample points from the data set to create a grid of triangles that form a Triangular Irregular Network (TIN). This type of interpolation works well with irregularly sampled data points and creates a surface with irregular or regularly spaced grid nodes. Since there are an infinite number of possibilities that sample points can be connected to one another to form triangles, criteria can be used in the decision process that preserves the local variation implicit in the data (Jones and Nelson, 1992). This type of criteria avoids the creation of long, thin triangles (Jones and Nelson, 1992). Greedy triangulation and Delauney triangulation are two methods developed for triangle selection that incorporate different criteria in the selection.

Criteria - Greedy triangulation uses the criteria when creating the triangles "that no candidate edge is included if there is a shorter candidate edge that would intersect it" (Jones and Nelson, 1992). As illustrated in Figure 2.14, this would mean that for two triangles (triangle 1 and 2) that share a common edge (from point A to D) would be considered a quadrilateral. The quadrilateral has two diagonal lines (point A-D and point

B-C) that form two pairs of possible triangles, and the pair of triangles selected would be the one with the shortest diagonal line (triangles 3 and 4) (Jones and Nelson, 1992).

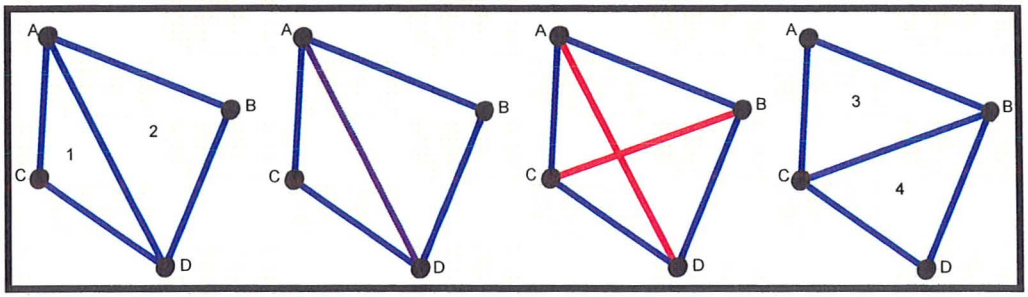

Figure 2.14: Greedy triangular selection of two pairs of triangles.

Delauney triangulation is most commonly used in algorithms that have the criteria of deciding what sample points to use in forming the triangles so that the circumference of each triangle cannot contain any other sample point as seen in Figure 2.15 (Jones and Nelson, 1992). This process creates triangles in which the minimum angle has been maximized, thus, minimizing the maximum angle (Jones and Nelson, 1992). Once a Delauney TIN is created from a dataset, Thiessen polygons also called Voronoi cells can be formed by taking the perpendicular bisector of each line from the triangle as shown with the dashed lines in Figure 2.16). Any point within a Thiessen polygon is closer to the sample point, then any other sample point (Jones and Nelson, 1992).

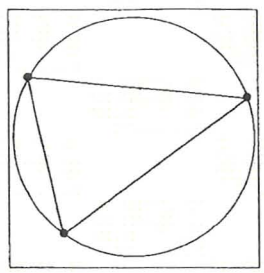

Figure 2.15: The circum-circle of a triangle (Jones and Nelson, 1992).

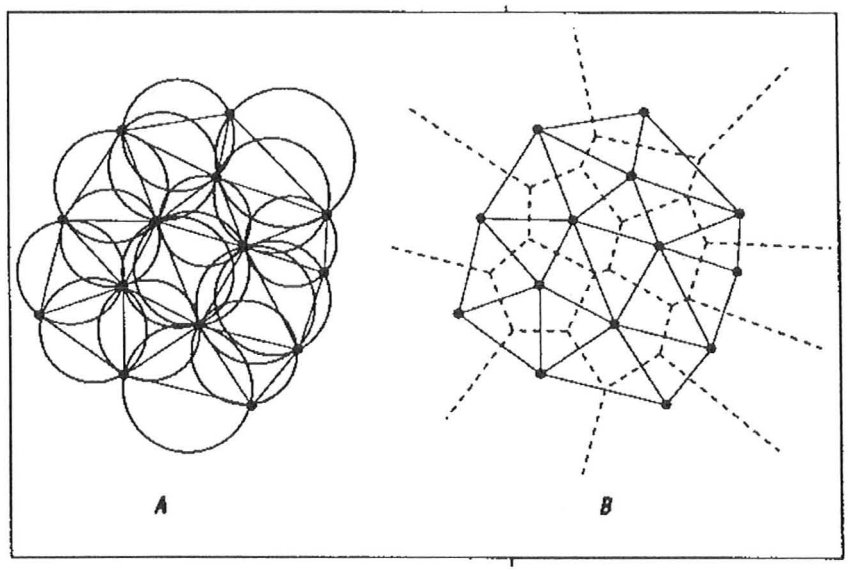

Figure 2.16: (a) Delauney TIN with the circumcircle showing that no other sample points lie within the circumcircle, (b) is the Thiessen polygons (Voronoi cells) that are created once a TIN is formed (Jones and Nelson, 1992).

Algorithms -There are two approaches that algorithms can use when applying the above criteria for creating a DEM. They can either be a "divide and conquer algorithm, which recursively subdivides the region of the data set" or incremental in which it starts at one location and adds points until it is complete (Jones and Nelson, 1992). The approach can either be iterative, in which the TIN is created and then modified until the criteria is satisfied, or it can be done in one-step where the first TIN produce would satisfy the criteria (Jones and Nelson, 1992). Since each of the algorithms approach and calculate TINs different, they also have varying processing time. Selection of an appropriate algorithm can save a great deal of time, when there is a large data set.

Convex Vs. Non-Convex Hull - The TIN created by various algorithms can produce either a convex or a non-convex hull (Figure 2.17). A convex hull is produced when the outer sample points are joined to each other creating a parameter convex in

shape. The convex hull has been described as "that shape that would be formed by a rubber band that was stretched around the outside of a set of nails representing the data points" (Jones and Nelson, 1992). Whereas, a non-convex hull would have a section of the outside parameter abruptly curve inwards to the center of the area.

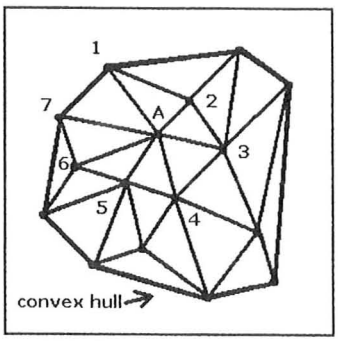

Figure 2.17: TIN with a convex hull (Sambridge *et al,* 1995).

How Points are Estimated - There are two types of interpolation that can be used to estimate a grid node that lies within a triangle; linear point estimation and natural neighbour.

Linear Point Estimation - The following describes how linear point estimation for a gird node is calculated within a triangle, whereby a plane is fitted to the three nodes of the triangle using the general expression (example from Isaaks and Srivastava, 1989):

$$ax + by + c = z \qquad \text{(Equation 2.1)}$$

The x and y are the location value for the point and z is the value of the point Using the following system of equations for the three points, the a, b and c coefficients can be solved:

$ax_1 + by_1 + c = z_1$
$ax_2 + by_2 + c = z_2$
$ax_3 + by_3 + c = z_3$

$63a + 140b + c = 696$
$64a + 129b + c = 227$
$71a + 140b + c = 606$

$a = -11.250$

$b = 41.614$
$c = -4421.159$

To estimate any point within the triangle, the x, y location can be plugged into Equation 2.2:

$$v = -11.250x + 41.614y - 4421.159 \qquad \text{(Equation 2.2)}$$

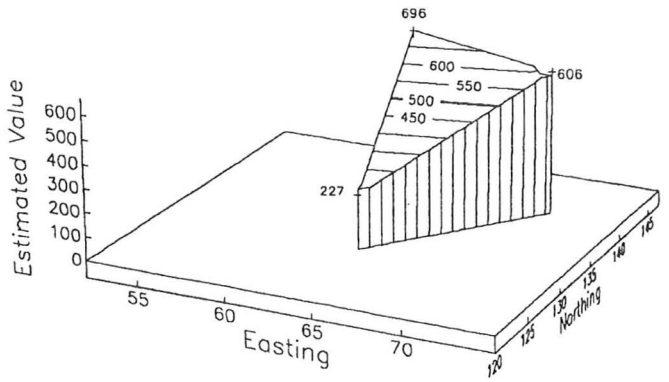

Figure 2.18: Linear point estimation within a triangle (Isaaks and Srivastava, 1989).

However linear interpolation's limitation is that it produces discontinuities in the first derivatives of the function across the bounds of the triangles and second derivatives are zero inside the triangles (Sambridge et al, 1995)

Natural Neighbour - Instead of using the TIN structure and estimating a grid point by the nodes on the TIN, this type of interpolation uses the Voronoi cells that were created as the by product from the Delauney triangulation. As seen in Figure 2.19, point x is located within the point 3 Voronoi polygon. A new Voronoi polygon is created around this point, which includes the natural neighbors that surround this point, which will result in a second order interpolation. Equation 2.3 is used to calculate this process.

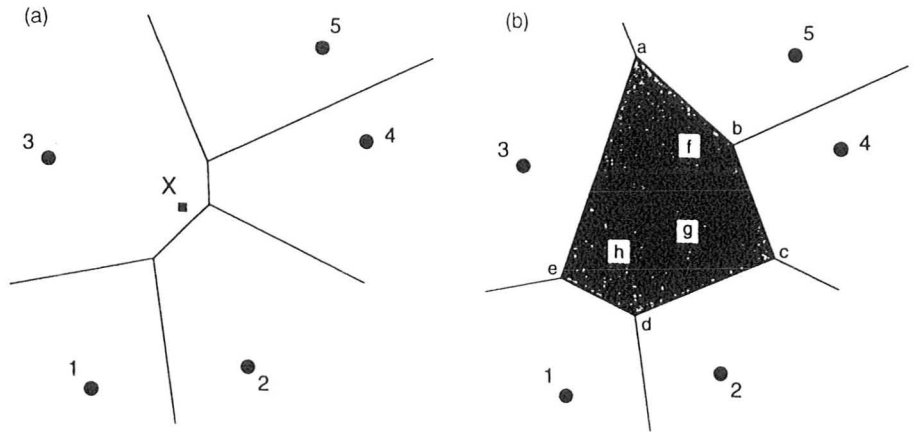

Figure 2.19: (a) Voronoi cells for 5 sample points and point x to be estimated, (b) the second order voromi cell created around point x (Sambridge *et al,* 1995).

$$f(x,y) = \sum_{i=1}^{n} Ø_i(x,y)f_i \qquad \text{(Equation 2.3)}$$

Since this interpolation is second order, it results in a smoother image then a linear first order interpolation method.

Advantages

- Can interpolate irregular and regular data into either an irregular (TIN) or regular grid either with linear or nearest neighbour interpolation
- Contours of similar values can be constructed directly from the triangles as opposed to grid
- Estimated points are honored to the original sample data value
- Ability to use breaklines that define linear features (fault, ridge, river) as opposed to grids
- Ability to use either local or global interpolation depending on desired results

Disadvantages

- Lengthy processing time for large databases

2.4.3 Minimum Curvature

Minimum curvature is based on the inverse distance average estimation but through multiple iterations to refit the grid to the data, and re-gridding the grid to a smaller and smaller cell size, it is possible to achieve a minimum curvature surface that attempts to honor the true value of the sample point (Geosoft, Unknown). The methodology of this interpolation process is described in detail by Briggs (1974), whereby the point is estimated by "solving the differential equation equivalent to a third-ordered spline" (Briggs, 1974).

The interpolation process begins with a coarse grid (typically 8 times the final grid) overlaid upon the data in which an estimate is calculated with a set of parameters for each grid node. The estimated grid is then shifted with multiple iterations to best fit the sample data (Geosoft, Unknown). Once the number of iterations is complete, the best fit is selected and the process is repeated with a finer grid that is half the size of the coarse grid until the final grid cell size is reached.

The estimated grid will be shifted to produce a minimum surface until it reaches one of two requirements. The first requirement is that the grid estimates are within a predetermined tolerance of the sample data and that a certain percentage of the grid cells fall within this tolerance. Or the number of iterations can be set to reduce the amount of time required since there are an infinite number of iterations that are possible. The results of this method of interpolation is that it provides the smoothest surface, however the surface does not honor all the samples points in which tinning and kriging both accomplish.

Advantages:

- Provides the smoothest surface of all interpolation methods
- Can interpolate irregular and regular data into a regular grid
- Ability to use either local or global interpolation determined by the size of the blanking distance

Disadvantages:

- The surface does not honor all sample points since it has been curved for smoothest fit

2.4.4 Ordinary Kriging

Ordinary Kriging is a weighted linear point estimation method that uses a statistical analysis of the sample data to estimate the values at each grid point based on maximum probability that is unbiased and minimizes the variance of the errors (Isaaks and Srivastava, 1989; Geosoft, Unknown). This type of interpolation is best suited for irregular data that are statistical in nature such as geochemical or geological sampling (Geosoft, Unknown). The typical process for Kriging a data set would be to create an observed variogram in which the distance between every pair of points is measured and graphed. This observed variogram is then compared to a number of model variograms. Out of the group of model variograms, one that is most similar to the observed variogram would be selected and that function used to estimate the grid points using a weighted linear equation.

Observed Variogram – This is the graphical representation of the statistical relationship of the sample data as a function of distance (Geosoft, Unknown). To produce an observed variogram, the distance between every pair of sample points in the dataset is measured and then calculated with Equation 2.4.

$$\gamma(h) = \frac{\Sigma[Z(x+h) - Z(x)]^2}{2} \qquad \text{(Equation 2.4)}$$

These points are then plotted on the graph (variogram), with distance (h) on the x-axis and the result of $\gamma(h)$ on the y-axis. As illustrated on Figure 2.20 there are three features of the variogram that are used to evaluate the data; the nugget, range and sill. The nugget is the point where the line intersects the y-axis (distance (h) = 0). The range is the distance (h) along the x axis, from the origin (distance = 0) of the graph until it reaches the point in which the line remains constant. At this point, the line has reached the sill, where the $\gamma(h)$ values remain fairly constant but can also continue to increase or decrease but after this point it is not statistically correlated.

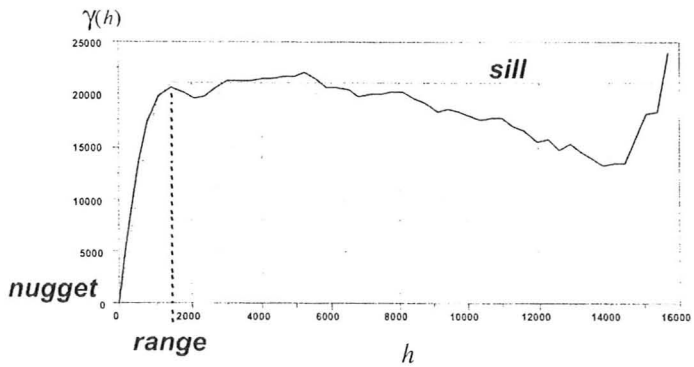

Figure 2.20: Variogram illustrating the nugget, range and sill (Geosoft, Unknown).

How grid points are estimated - The following describes the whole process of Kriging using the example from Isaaks and Srivastava (1989):

First, a table of the distance (h) between each pair of sample points (Table 2.6) and table of the sample point value (Table 2.7) are created.

Table 2.6: Table with distance (h) between each pair of sample points.

Location	0	1	2	3
0	0.00	4.47	3.61	8.06
1	4.47	0.00	2.24	10.44
2	3.61	2.24	0.00	11.05
3	8.06	10.04	11.05	0.00

Table 2.7: Table with distance (h) between each pair of sample point

Point	Value
0	?
1	477
2	696
3	227

Second, an observation variogram is then created. The sill, nugget and range are identified.

Example: Nugget = 0, Sill = 10, Range = 10

Third, the observational variogram is compared to a number of modeled variograms and the model that is most similar is selected. For this example, the exponential model was used with Equation 2.5.

$$\gamma(h) = \text{nugget} + (\text{sill} - \text{nugget})\,(1 - \exp(-3(h) / \text{range}) \qquad \text{(Equation 2.5)}$$

Fourth, the nugget, sill and range identified in the observation variogram are substituted into the modeled function with the distance between each pair of sample points and this produces a C matrix, which is the statistical distance between each pair of points.

$$C = \begin{vmatrix} \hat{C}_{11} & \hat{C}_{12} & \hat{C}_{13} & 1 \\ \hat{C}_{21} & \hat{C}_{22} & \hat{C}_{23} & 1 \\ \hat{C}_{31} & \hat{C}_{32} & \hat{C}_{33} & 1 \\ 1 & 1 & 1 & 1 \end{vmatrix} \qquad C = \begin{vmatrix} 10.00 & 5.11 & 0.44 & 1 \\ 5.11 & 10.00 & 0.36 & 1 \\ 0.44 & 0.36 & 10.00 & 1 \\ 1.00 & 1.00 & 1.00 & 1 \end{vmatrix}$$

Fifth, the nugget, sill and range identified in the observation variogram are substituted into the modeled variogram function with the distance between the sample point and the unknown grid point to produce a D matrix.

$$D = \begin{vmatrix} \hat{C}_{10} \\ \hat{C}_{20} \\ \hat{C}_{30} \\ 1 \end{vmatrix} \qquad D = \begin{vmatrix} 2.61 \\ 3.39 \\ 0.89 \\ 1.00 \end{vmatrix}$$

Sixth, to determine the weight (W matrix) of each sample point for the grid pint, it can be calculated with Equation 2.6.

C matrix * W matrix = D matrix

Or (Equation 2.6)

Inverse C matrix * D matrix = W matrix

$$\text{Inverse C} \begin{vmatrix} 0.127 & -0.077 & -0.013 & 0.136 \\ -0.077 & 0.129 & -0.010 & 0.121 \\ -0.013 & -0.010 & 0.098 & 0.156 \\ 0.136 & 0.121 & 0.156 & -2.180 \end{vmatrix} * D \begin{vmatrix} 2.61 \\ 3.39 \\ 0.89 \\ 1.00 \end{vmatrix} = W \begin{vmatrix} w_1 \\ w_2 \\ w_3 \\ \mu \end{vmatrix} \begin{vmatrix} 0.173 \\ 0.318 \\ 0.129 \\ 0.907 \end{vmatrix}$$

Seventh, the value of each sample point is multiplied by its corresponding weight and all weighted values of sample points are summed for the grid point estimate.

Grid Point Estimate = (0.173)(477) + (0.318)(696) + (0.129)(227)
= 333.13

Model Variograms

There are a variety of model variograms that have been created to model the phenomena of the observed data, such as the Power model, Spherical model, Exponential modal and the Gaussian model (Figure 2.21). Since the function is different for each of

these model variograms, the weights associated to every sample point are also different which results in different grid point estimates.

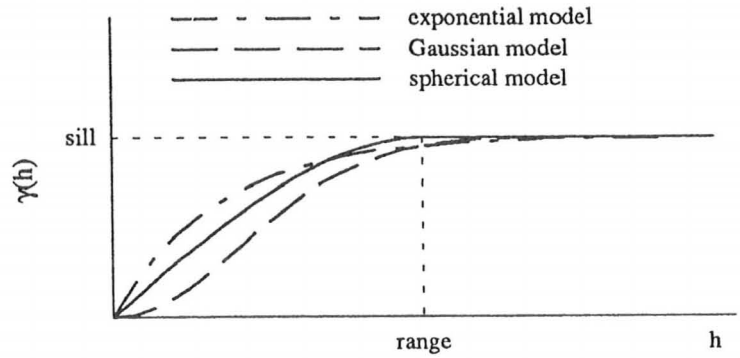

Figure 2.21: Model variogram comparing the spherical, exponential and Gaussian model (Isaacs and Srivastava, 1989).

Power Model - The simplistic model available is the power model that is most commonly used in mining geological applications (Geosoft, Unknown). Although it cannot model data that does not contain a sill, it can model linear behavior accurately (Geosoft, Unknown). The linear model (power = 1) is works well when the nominal sample interval is less then the range (Geosoft, Unknown). The function for the model is Equation 2.7.

$$\gamma(h) = \text{nugget} + (\text{slope})h^n \qquad \text{(Equation 2.7)}$$

Where n is the power chosen

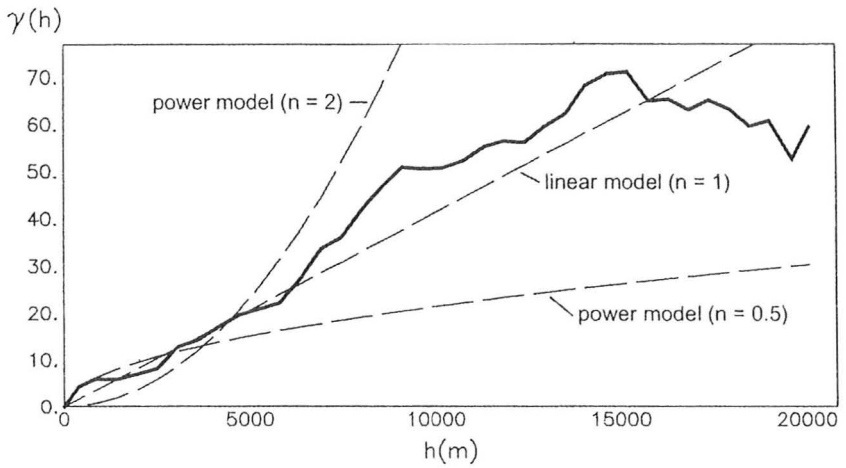

Figure 2.22: Power model variogram (Geosoft, Unknown).

Spherical Model - This function can model linear behavior near the origin while it reaches the sill at greater distances and is commonly used for geological data (Isaaks and Srivastava, 1989; Geosoft, Unknown) When comparing this model to the observation covariogram, "the tangent at the origin reaches the sill is at about two thirds the range" (Isaaks and Srivastava, 1989). The function for this model is Equation 2.8.

$$\gamma(h), (h < \text{range}) = \text{nugget} + \frac{1.5h\,(\text{sill} - \text{nugget})}{\text{range} - 0.5\,[h / \text{range}]^3} \quad \text{(Equation 2.8)}$$

$$\gamma(h), (h <= \text{range}) = \text{sill}$$

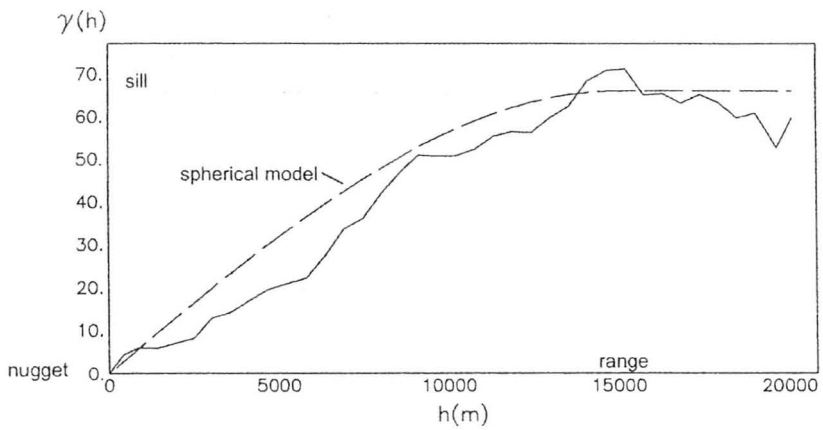

Figure 2.23: Spherical model variogram (Geosoft, Unknown).

Exponential Model - This model is similar to the spherical model in that in can model linear behavior near the origin but increases at a greater rate before the rate is reduced and gradually reaches the sill (Isaaks and Srivastava, 1989). When comparing this model to the observation covariogram, "the tangent at the origin reaches the sill at about one fifth the range" (Isaaks and Srivastava, 1989). The function for the model is Equation 2.9.

$$\gamma(h) = \text{nugget} + (\text{sill} - \text{nugget})\ (1 - \exp(-3(h) / \text{range}) \qquad \text{(Equation 2.9)}$$

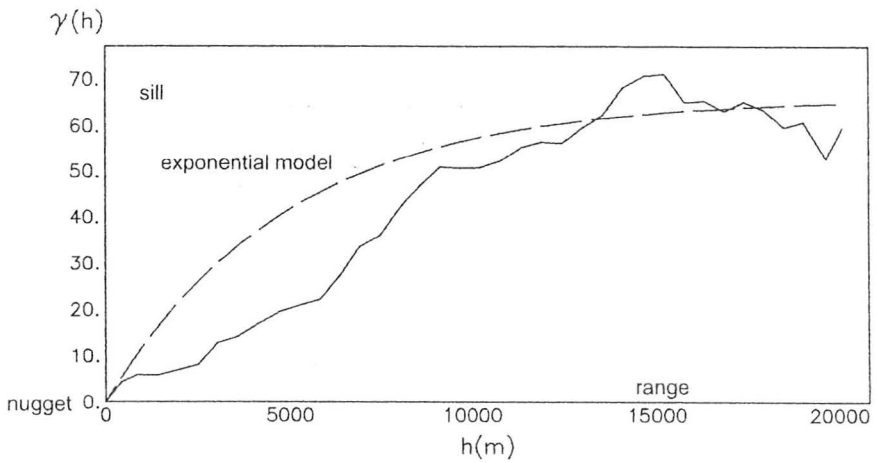

Figure 2.24: Exponential model variogram (Geosoft, Unknown).

Gaussian Model - This function has the ability to model parabolic behavior that is typically not found in geological data but often an extremely continuous phenomena (Geosoft, Unknown) Isaaks and Srivastava, 1989; Geosoft, Unknown). The function for the model is Equation 2.10):

$$\gamma(h) = 1 - \exp(-r^2 / \text{range}^2) \qquad \text{(Equation 2.10)}$$

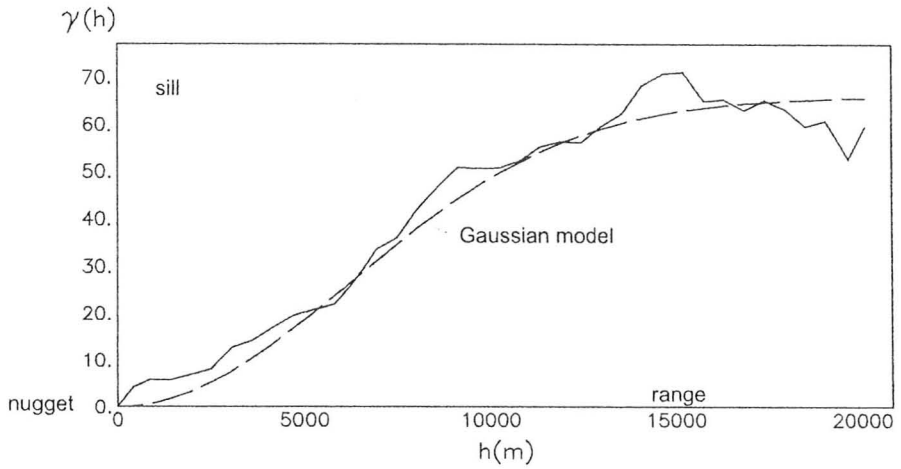

Figure 2.25: Gaussian model variogram (Geosoft, Unknown).

Advantages

- Can interpolate irregular and regular data into a regular grid using a variety of models that best imitate the sample data
- Estimated points are honored to the original sample data value
- Ability to show trends within the data
- Ability to use either local or global interpolation
- Ability to interpolate cluster data without creating sharp highs and lows on the resulting grid

2.4.5 Summary of Interpolation Methods

As discussed in the previous sections, it can be seen that each type of interpolation method has a different approach for point estimate which results in differences in the grids that they produce. The three methods can estimate points both with local or global sample points and is decided by the creator of the grid by the type and spatial distribution of the points. All the methods also have the ability to take either regular or irregular sample points, and create a regular grid of estimate points with the triangulation method having the extra ability to produce an estimated irregular grid.

Triangulation is the method with the least amount of creator control when estimating points since it uses predefined formulas, however it has the ability to interpolate both first and second order. The creator has more influence with minimum curvature method since adjustments can be made to both the parameters and the criteria for the number of iterations. This allows the creator to manually adjust for the type of topography being sampled. The kriging method has the greatest amount of creator control since the observational variogram is compared to model variograms for selecting the best one to represent the sample data. Also, the nugget, range and sill need to be identified by the creator for use in the function for estimating the various points.

Since each method has a different approach, the deciding factor of which interpolation process to use lies within the type of sample data. For topographic data, things that are of important consideration are the rate of elevation change and the spatial distribution of the points. If the topography of the sample area is very rugged, then selecting either tinning or kriging is optimal for a couple of reasons. First, both methods honor the sample points meaning that the estimated grid values at the sample points would have the same value. Also, depending on the model for kriging, both methods would put more weight for the estimation on closer values and in a rugged area the elevation can change dramatically. If the topography of the sample area is flat, or has a gentle relief, minimum curvature would be the best estimation method since it attempts to bend a plane over all the sample points within the estimated grid cell. Although the sample values are not honored as in the other two methods, it produces the smoothest surface of all three estimation methods.

CHAPTER THREE: METHODOLOGY

This chapter begins by explaining the methodology involved in the site selection followed by a section stating the dates for field work and what was accomplished. The third section explains the field methods utilized in gathering the aerial photographs and satellite imagery; establishing ground control points; completing detailed GPS beach of the study area. The final section discusses the methods used for processing and analyzing the data.

3.1 Site Selection

This research project involved the collection of topographic data, remotely sensed imagery and sediment that would allow a temporal and spatial comparison of current conditions (2007) and previous work completed by Bertram (2006) and Lewis (2006) for Playa Guiones and Playa Pelada, Guanacaste Province, Costa Rica. To originally select the sites, topographic and geologic maps of Costa Rica were reviewed to identify beaches that were:

- located within a reasonable distance of each other with vehicle access to allow transportation of equipment;
- composed of soft sediment and had sand grain sized (0.063 – 2 mm) particles; and,
- located in a tectonically active region.

After a reconnaissance trip to the region in February, 2005 to explore potential sites, two concurrent beaches (Playa Guiones and Playa Pelada) were chosen as the field sites for the original research project by Bertram (2006).

3.2 Field Dates

In order to ensure sufficient data to measure temporal changes in this research project a total of four field seasons were conducted over a two year period from February 2005 to February 2007. This region experiences heavy precipitation from May until November (wet season) with the following months (dry season) receiving little or no rainfall in any given year. The variability of low to high magnitude and intensity of precipitation and other climate variables will result in differences in the fluvial sediment supply to the coast, direction of longshore drift and wave refraction-diffraction patterns (Benavente, J *et al,* 2002). The dates of each field season were selected to coincide with this precipitation pattern so that data collected represent both the wet and the dry seasons.

The first field season, February 16-26, 2005 was a reconnaissance trip to the region to select the study sites. During this trip, detailed field observations of the beach were collected. In addition, this trip provided the opportunity to develop local contacts for assistance with both logistical and general knowledge of the area. Aerial photographs of the region were also obtained at this time.

The second field season, June 8 - July 7, 2005 involved collecting wet season data. Detailed kinematic GPS beach surveys were conducted, in addition to, sediment, vegetation and *in situ* rock samples that were collected and recorded within detailed sketch maps. Multiple ground control points (GCP's) were located throughout the region with the elevation and position recorded.

During the third field season, June 27 – July 6, 2006 sediment and vegetation identification and sampling occurred. Detailed sketch maps were completed, in order to

compare the two wet seasons (i.e., sediment and vegetation patterns). Additional remotely sensed images were obtained to expand the previously sets of acquired imagery.

The forth and final field season, January 12 - February 25, 2007 involved collection of dry season data. Detailed kinematic GPS beach surveys were conducted. Sediment and vegetation samples were collected and recorded within detailed sketch maps. Thirty additional GCP's were located throughout the region.

3.3 Field Methods

3.3.1 Detailed GPS Survey

Detailed GPS beach surveys were conducted using the Trimble RTK-GPS unit to collect topographic information of the beach and swash areas that were used to produce 3 dimensional models for both sites. Playa Pelada was surveyed from June 26 to July 1, 2005 for the wet season data collection and from January 30 to February 3, 2007 for dry season data collection. Playa Guiones was surveyed from June 13 to 26, 2005 for the wet season and from February 3 – 13, 2007 for the dry season.

The Trimble RTK-GPS unit consists of a rover and base receiver units, two radio antennas, battery packs and a handheld computer unit. Each day, the system is setup approximately in the center of the beach section being surveyed as seen in Figure 3.1. The base unit is secured to the top of a tripod that has the initialization bar between the tripod and base unit. The base unit is connected to a battery pack and radio antenna which is extended approximately 4 meters above ground. The rover unit is connected to the second radio

antenna and battery pack housed inside the backpack unit which is worn by the surveyor. During initialization of the system, the rover unit is attached to the initialization bar. Upon

Figure 3.1: Typical deployment of Trimble RTK-GPS system in the center of the beachface at Playa Guiones, Costa Rica. The enlarged image shows the position of GPS receivers for initialization at the base station.

initialization the rover unit is removed from the bar, attached to the top of backpack unit and the survey begins.

The initialization and operation of the system followed the same procedure for each day of the survey. First, the rover unit is attached to the tripod pointing due north of the base unit. Once the units received contact from a minimum of four satellites, the system initializes and the two units transmit their position to the handheld controller for real-time processing. A new file for each day was created to record the data points, with each data point having a

prefix that identified the date, the surveyor and what beach was being surveyed. The system was programmed to record data points at a one second time interval that included the geospatial coordinates and elevation using the WGS84 datum projected to UTM16N. Data points that had a horizontal error of less than 5 cm and a vertical error less than 5 cm were recorded.

The surveyor would begin the survey at the base unit located at the center of the section of beach and would walk to the first transact. The surveyor would then walk from the vegetation line, perpendicular to the shore towards the ocean until the water level reached the surveyors knees. At this point, the surveyor would walk shore parallel 3-5 meters before beginning the next transact towards the vegetation line. The spacing between transacts were kept within 5 meters for the wet season and 3 meters for the dry season. When the survey was completed for the day, the surveyor would close the survey by returning to the base unit before powering down the system. Once the first survey was completed on a beach, it was important that subsequent surveys overlap the previous day's since there was a necessary elevation correction that was applied to the data when processing caused by satellite positions. Due to the limited range of the radio antenna that was less than 500 m radius, it was not possible to complete a total survey along the beach that could tie all the data together to one benchmark. Figure 3.2 illustrates a typical survey grid for multiple days along a section of beach. At the end of each day, the data is downloaded from the handheld controller to a computer; converted from a .ds to .csv file using the Trimble Office program; and backed up.

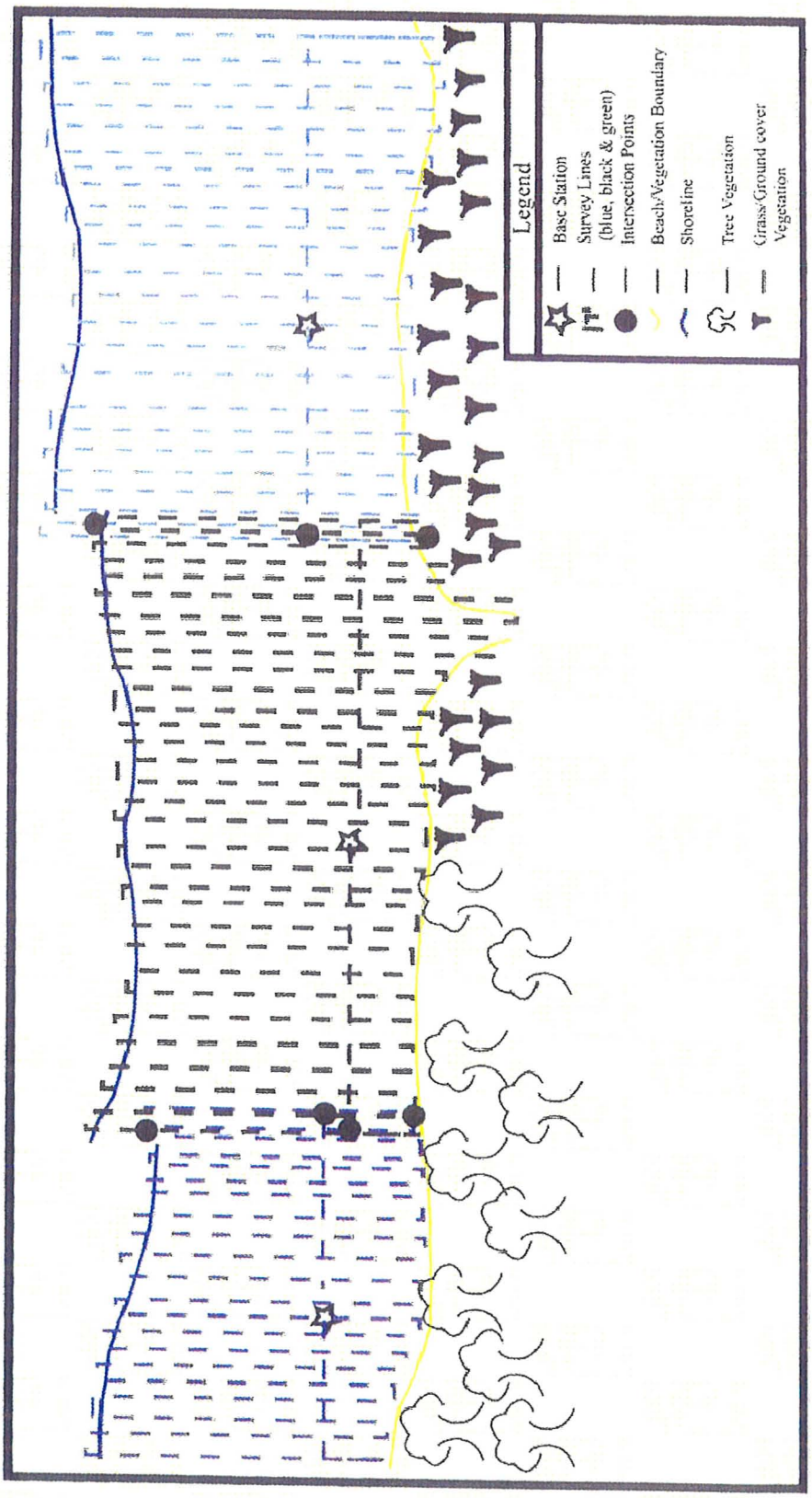

Figure 3.2: Illustration showing the overlap between surveys completed on different days. The base station is represented with a star, located near the center of the beachface and survey. The beach was surveyed from the vegetation line seaward until the water level was at the surveyor's knees (Bertram, 2006).

3.3.2 Aerial Photography and Satellite Imagery

Acquisition of Imagery - During the first field season, the Instituto Geographico Nacional located in San Jose, Costa Rica was visited to obtain aerial photographs of the study region. Multiple sets of imagery from various years and scales were examined to ensure total coverage of the study area and that the images were in good condition. Four sets of original aerial photographs were obtained by Bertram, 2006 as follows: 1945(1:40,000), 1975(1:10,000), 1991(1:10,000) and 1997(1:40,000).

The agency was visited a second time during the third field season to obtain additional photographs and to obtain specific details about the cameras used in flight. Additional photos were obtained to increase the overlap between successive images in order to enhance geo-rectification. An additional set of photographs from 1971(1:20,000) were also obtained.

DigitalGlobe provided a Quickbird image of the region that was captured on February 3, 2004. The image was georectified to the World Geodetic System 1984 (WGS84) and projected to the Northern Universal Transverse Mercator Zone 17 (UTM17N). The resolution of the Quickbird image was 0.6 cm panchromatic and 2.4 m multispectral.

Ground Control Points - During the second and fourth field season Ground Control Points (GCPs) were identified, located and recorded. These were used to rectify the aerial photographs in conjunction with the satellite image. To obtain a quality GCP, it was necessary that a specific location in the field could be precisely located in the aerial photograph. Many of the GCPs that were identified were features such as buildings, road

intersections or physical features. At each GCP, the geospatial coordinates were measured with the Trimble RTK-GPS (real-time kinematic global positioning system) unit. This unit consisted of a Trimble 4600LS Surveyor used in conjunction with the Trimble Handheld Computer TSC1. The exact location of the equipment at the GCP was photographed for future reference when rectifying the images (Figure 3.3). The coordinates, photograph numbers and comments were recorded in a field notebook and the location was accurately plotted on the aerial photographs.

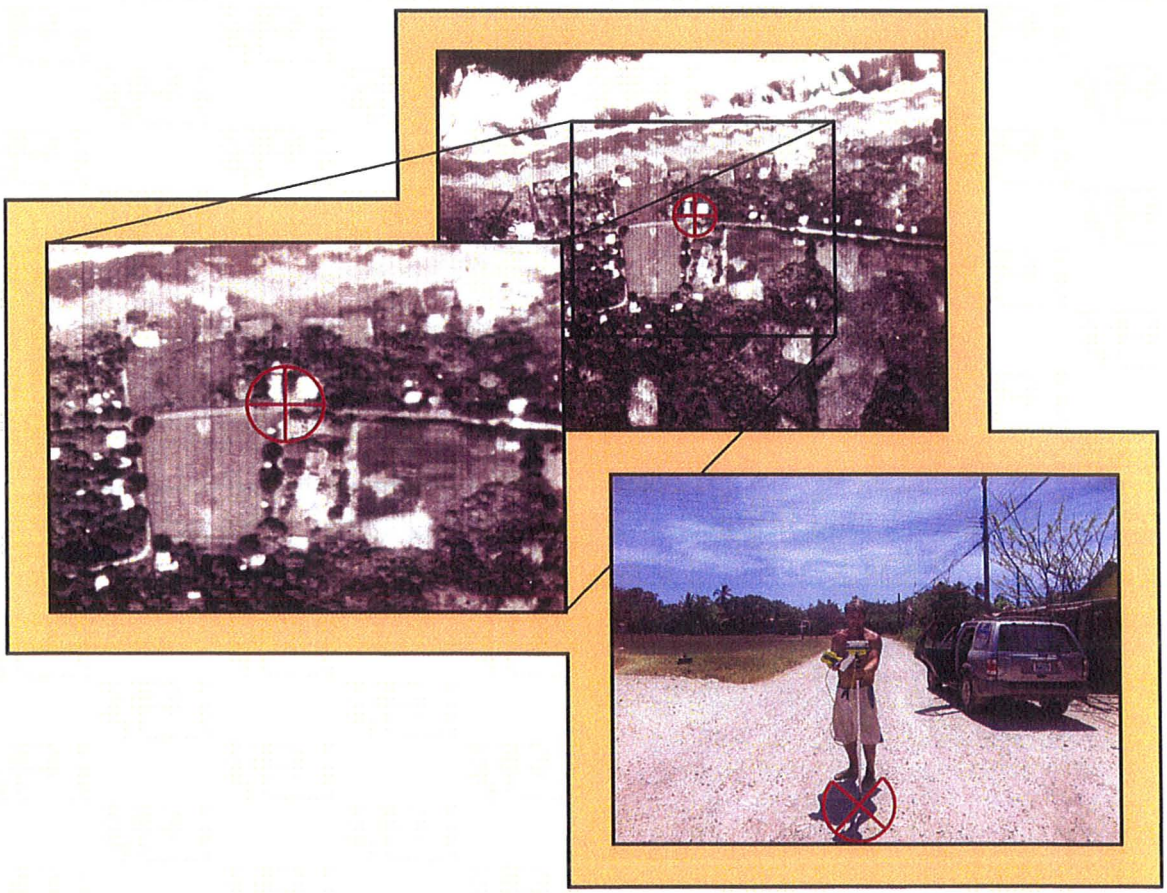

Figure 3.3: Ground control points were located on aerial images that corresponded to exact locations in which the geospatial coordinates were acquired with the Trimble GPS unit.

3.4 Data Processing and Laboratory Analysis

3.4.1 Digital GPS Survey Data

Creation of Digital Elevation Models

The final product that was created from the data collected during the detailed kinematic GPS beach surveys were Digital Elevation Models (DEM's) of each beach for the wet and dry seasons. The data were processed using the same technique for both beaches and seasons within Oasis Montaj. The following describes the steps taken after the file is imported into a new database from the original .csv files.

1) The data were separated into separate lines within the database for each day and were further split into sub-lines for each individual that wore the backpack unit during the survey.

2) For each line, the data were analyzed to identify erroneous data points that should be removed. Reasons for removal were: repetitive points at the same location that could be caused by the individual standing still for an extended period of time; and a large elevation change at the same location that was identified as the lifting or lowering of the backpack unit on to the surveyor occurring near the base station at the beginning or end of a survey.

3) A low-pass filter was applied to the whole database to remove high frequency noise caused by the surveyor walking on unconsolidated material.

4) Due to the height difference between surveyors, an elevation correction was applied to adjust for differences amongst the different surveyors. The process followed these steps:

i. Each line was gridded separately with a minimum curvature interpolation using the following parameters: grid cell size of 1 meters; blanking distance of 4 cells; and, extended the cells to beyond data by 0 cells.

ii. The grids produced from step (i) were subtracted from one another, resulting in a grid that represented the elevation difference between the two surveyors. Using the Grid Statistics function, a histogram was evaluated to determine if the median difference was an accurate value that would be used to correct for the elevation difference between the surveyors. If the histogram showed a skewness, then the grids were further analyzed to find and correct the underlying cause of the skewness. The grids were then re-gridded until a satisfactory histogram was produced.

iii. The median difference was then applied to the elevation data to correct the height difference amongst surveyors.

iv. The line containing a full day of data collection was then gridded with a minimum curvature interpolation using the following parameters: grid cell size 2 meters; blanket distance of 8 cells; and, extended by 2 cells. The DEM produced though this step had sun shading applied to the grid at an inclination of 45 degrees and declination of 45 degrees that would illuminate the any remaining erroneous data on the DEM. When erroneous data were identified, the data was further analyzed to identify the cause of the error and corrected. The result of this produced a final DEM, for a portion of the beach, representing each day of data collection.

5) Due to the initialization of the survey equipment, there were differences in the base

elevation height provided by the satellites for each day of data collection that needed to be corrected. The process to "level" the elevation between each day was identical to the process described in step 4 for correcting the height difference between surveyors with the exception of the gridding parameters due to a larger data size. The parameters used in step 4i were: cell size of 2 meters; blanking distance of 8 cells; and, extended by 4 cells and step 4iii were: cell size of 2 meters; blanking distance of 8; and, extended by 0 cells.

The result of these steps produced a DEM of the beach from data that had: all erroneous data removed; low-pass filtered applied; difference in height between surveyors corrected; and, base elevation leveled between each day.

Comparison of Digital Elevation Models

Since digital elevation models were created for both seasons on each beach, comparison DEMs were produced that would illustrate changes to the beach topology between the two seasons. The 2005 wet DEM was subtracted from the 2007 dry DEM, which create a DEM representing the changes that occurred in beach topography between successive wet and dry seasons. Before a DEM was subtracted from the other, the two grids required the same base elevation. This leveling is required when using elevation measurements that are of a dynamic nature such as a sand surface that is continuously changing over time. Typically, these types of surveys use permanent benchmarks which are plaques mounted on concrete markers or bedrock that provide elevation and the geospatial coordinates which are used to level the data to a known elevation. As seen in Figure 3.4, the

positions of the concrete benchmarks placed along these beaches were not in condition to be used due environmental weathering.

Figure 3.4: Example of the concrete markers located along the backshore of the beach that could not be used as a benchmark. The square 4"x4" post should be buried in the ground with the circular dish at ground level.

To resolve the issue of having no benchmarks incorporated into the surveys, it was decided that exposed rock located at the northern headland for Playa Guiones and the second rocky outcrop for Playa Pelada would be an adequate benchmarks between the two seasons. It is highly unlikely that there was any significant change in the elevation of the rock between the successive years. The elevation difference was applied to the dataset and new grids were created. These elevation corrected final grids were subtracted from one another to create the DEM that represented the change in elevation between the two seasons. The change in elevation data within this grid was extracted using a volumetric function that calculated the total amount of sediment either accumulated or eroded. This total was then divided up by the

total grid area to give a representation if spread evenly the amount of elevation change. This would provide insight to the sediment budget and sand supply for each beach.

A series of beach profiles along the beachface were extracted using Oasis Montaj. Within this program, the exact location coordinates for the start and end of the profiles in addition to the same sampling distance were used to extract the data from the DEMs. These profiles were plotted for visual analysis that allowed further insight to the changes observed on the beachface and through the whole beach.

3.4.2 Remotely Sensed Imagery

The remotely sensed imagery used for this study included one orthorectified satellite image and five sets of original aerial photographs. The satellite image projection was corrected from NUTM17 from NUTM16 using the Geocoding Wizard function within ER Mapper 7.1.

Each set of aerial photographs were geo-rectified and mosaiced together in an attempt to determine and quantify the amount of shoreline change during these periods. The following describes the process used to rectify the 1991 set of photographs since it was recent and had the greatest resolution. After a set was complete, it was used in conjunction with the satellite image for determining GCPs on the next set of images. This process was beneficial since it can be difficult to find the same feature located on an older aerial photograph and then on the recent satellite image.

1) Each image of the set was loaded into ER Mapper individually for geo-rectification

using the Geocoding Wizard function. The geocoding type chosen for rectification was the quadratic polynominal order which provides a smoother fit then a linear order, and also requires 6 ground control points as opposed to 4 ground control points. This method of rectification was used instead of orthorectification, which is typically used for aerial photographs, due to the specific information required (camera used, camera orientation such as pitch, role and yaw) that were unattainable for the historic photographs, however, could have been possible with the collected GPS information from the beach survey. The satellite image, having been corrected to the proper map projection, was used as the reference for selecting ground control points between the two images.

2) When selecting GCP points, the ideal features indentified in the aerial photographs and satellite image were permanent structures, distinct topography or geological landmarks, in which there were confidence no movement or alteration to the feature had occurred during the time period. Six ground control points were selected as the minimum and these points were spaced evenly thoughout the image.

3) While selecting the GCPs for each image, the RMS errors were monitored and when one or more points had greater than 10 RMS, the GCP was reexamined and another possible GCP was selected until the RMS errors were below 10.

4) The image was then rectified, imported along with the satellite image into Oasis Montaj and compared to one another. To monitor shoreline change it is essential to remove or minimize the amount of distortion along coastline for the rectified image. The two images were overlaid upon each other and multiple landmarks were compared in both images to determine the amount of distortion in the rectified image. If there were distortions in

landmarks situated near the coastline, the GCP's used to rectify the image were examined and changed if necessary until the landmarks in the final rectification showed the least amount of distortion.

5) Once a full set of aerial photographs were completely rectified, the images were cropped in ER Mapper to remove the overlap between successive images. These images were then mosaic together using the Mosaic function within ER Mapper to produce the final image of the study area.

These final images were imported into Oasis Montaj and the historical shorelines were delineated from the seaward extent of the vegetation line. The historical shorelines were compared amongst one another to identify any changes in shoreline position. Changes in land-use for this area were also observed using these mosaic images.

CHAPTER FOUR: RESULTS AND DISCUSSION

This chapter is divided up into four sections. The first section presents the results of the digital elevation model analysis along with the sediment distribution for both Playa Guiones and Playa Pelada for both the wet(2005) and dry season (2007). A discussion of the results follows the presentation of results for each beach. Limitations that pertain to both beaches are then discussed. The final section presents the results of the aerial photography analysis, followed by a discussion and the limitations associated with the project. The 2005 data was collected as part of Aaron Bertram's thesis (2006). All of the data was reworked as part of this thesis in order to ensure similarity in the methodology for the 2005 and 2007 data.

4.1 Playa Guiones

4.1.1 DEMs and Profiles

2005 Wet Season DEM

Figure 4.1 is the digital elevation model of Playa Guiones with data collected during the 2005 wet season. It is overlain on the satellite image (2004) of the area. This DEM was gridded with a cell size of 3 meters, a blanking distance of 7.5 meters and extended by 1 cell past the data. As seen Figure 4.1, the DEM coverage of Playa Guiones is approximately 3 kilometers in length running approximately north-south. The remaining 2 km of the beach is not represented in the DEM because no data was collected. No data was collected for the southern extent of Playa Guiones for a number

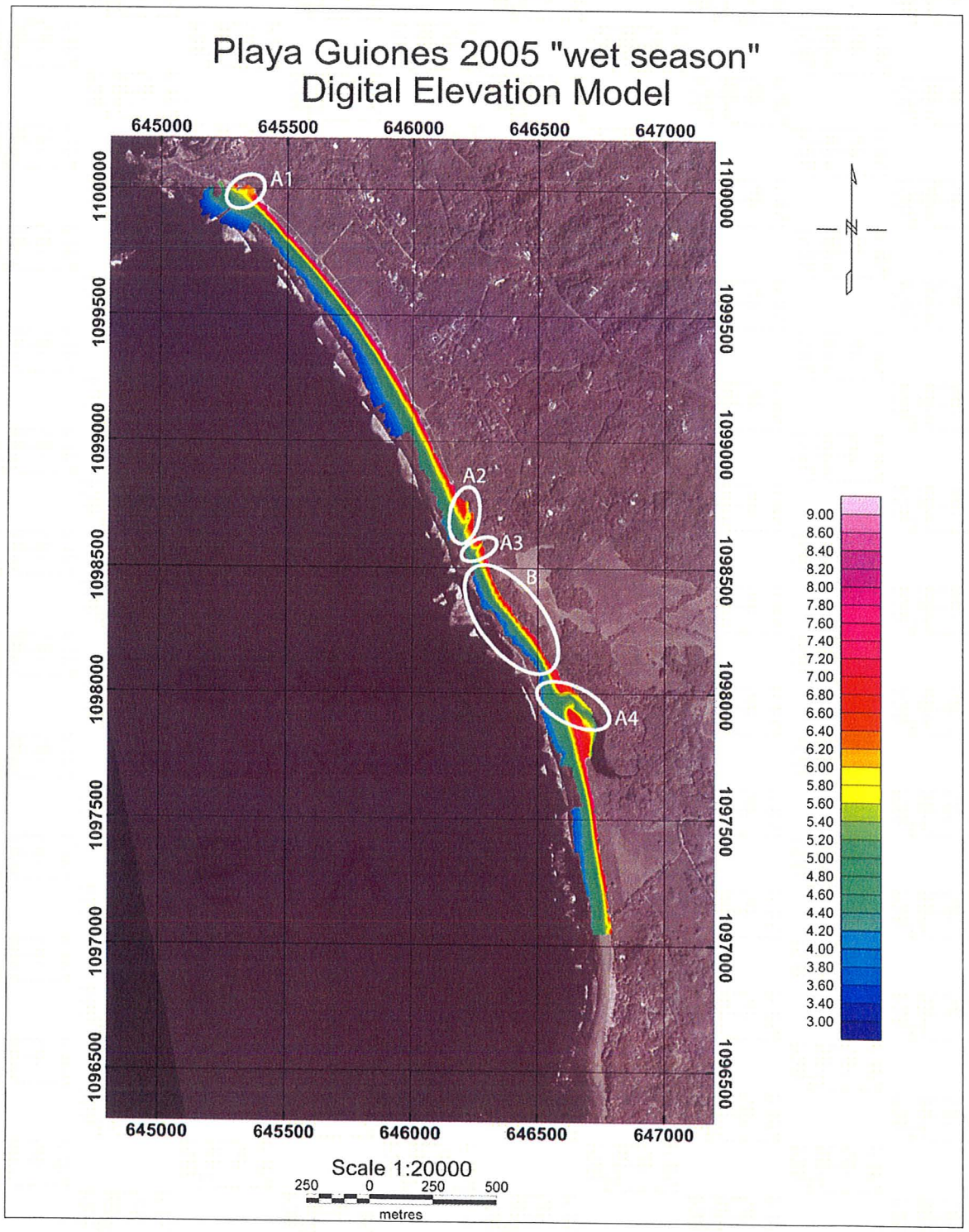

Figure 4.1: DEM of Playa Guiones created from data collected during 2005 wet season. Location A1, A2, A3, and A4 appear to be similar features of elongated depressions not parallel to the shore. Location B appears to be a group of elevated crescent shaped features.

of reasons. First, the majority of this area is exposed rock with only a small area that had sand accumulation and this project is primarily interested in short-term changes in beach morphology. Short-term changes would only be evident in the sand portion of the beach. Second, the vegetation along this section of the shoreline was extremely dense and the overhanging tree canopy blocked the transmission of satellite signals to the receiver making it impossible to collect reliable data.

The 2005 DEM allowed a visual display of the beach topography for the collected area. The northern portion of Playa Guiones has a greater elevation at the vegetation line when compared to the southern portion. Throughout the DEM, the beach slope appears to be the steepest at the beachface and a more gradual slope is evident in the surf zone. For the majority of the DEM, the elevation contoured parallel to the shape of the shoreline except at locations A1, A2, A3 and A4. At these four locations, the shore parallel elevation contours change pattern and an elongated depression not parallel to the shore is observed. These features coincide with previously identified rivers that discharge into the Pacific Ocean during the wet season (Figure 2.2). Feature A1, was a shallow, wide river channel, whereas, features A2 and A3 were deep, narrow river channels with steep banks. Feature A4, identified as Rio Rempujo, was the widest and deepest river with well established riverbanks.

At location B, a group of elevated crescent-shaped features are observed along the beachface. These features were observed during data collection as cusps that consisted of coarse calcareous sediment with decreasing grain size with increasing distance seaward from the center.

2007 Dry Season DEM

Figure 4.2 is the digital elevation model that represents Playa Guiones during 2007 dry season. The 2007 DEM was gridded with a cell size of 2 meters, blanking distance of 5 meters and extended 1 cell past the data. Due to similar reasons described for the 2005 DEM, the southern 1.5 km of Playa Guiones was not surveyed due to the large amount of exposed rock and dense vegetation limiting satellite reception.

Similar to the 2005 DEM, the 2007 DEM showed that the elevation at the vegetation line was greater in the northern portion when compared to the southern portion. Also, the beach slope was steepest at the beachface, with a more gradual slope within the surf zone. The gradual slope observed in the surf zone, appears to be consistent along the length of the beach from the northern extent southwards, until it reaches location A in Figure 4.2. Location A has the most gentle slope of the entire beach. The slope then increases in steepness in a southward direction. The elongated depression at location A, was previously identified as Rio Rempujo, the same feature as A4 in Figure 4.1. Similar to the 2005 DEM, the parallel to shore elevation contours change direction indicating presence of river channel, however, the shape, size and depth of the channel are different than the 2005 DEM. During the 2007 data collection period, Rio Rempujo was a standing river with a landlocked river mouth no longer discharging into the ocean with remnants of previous riverbanks on either side.

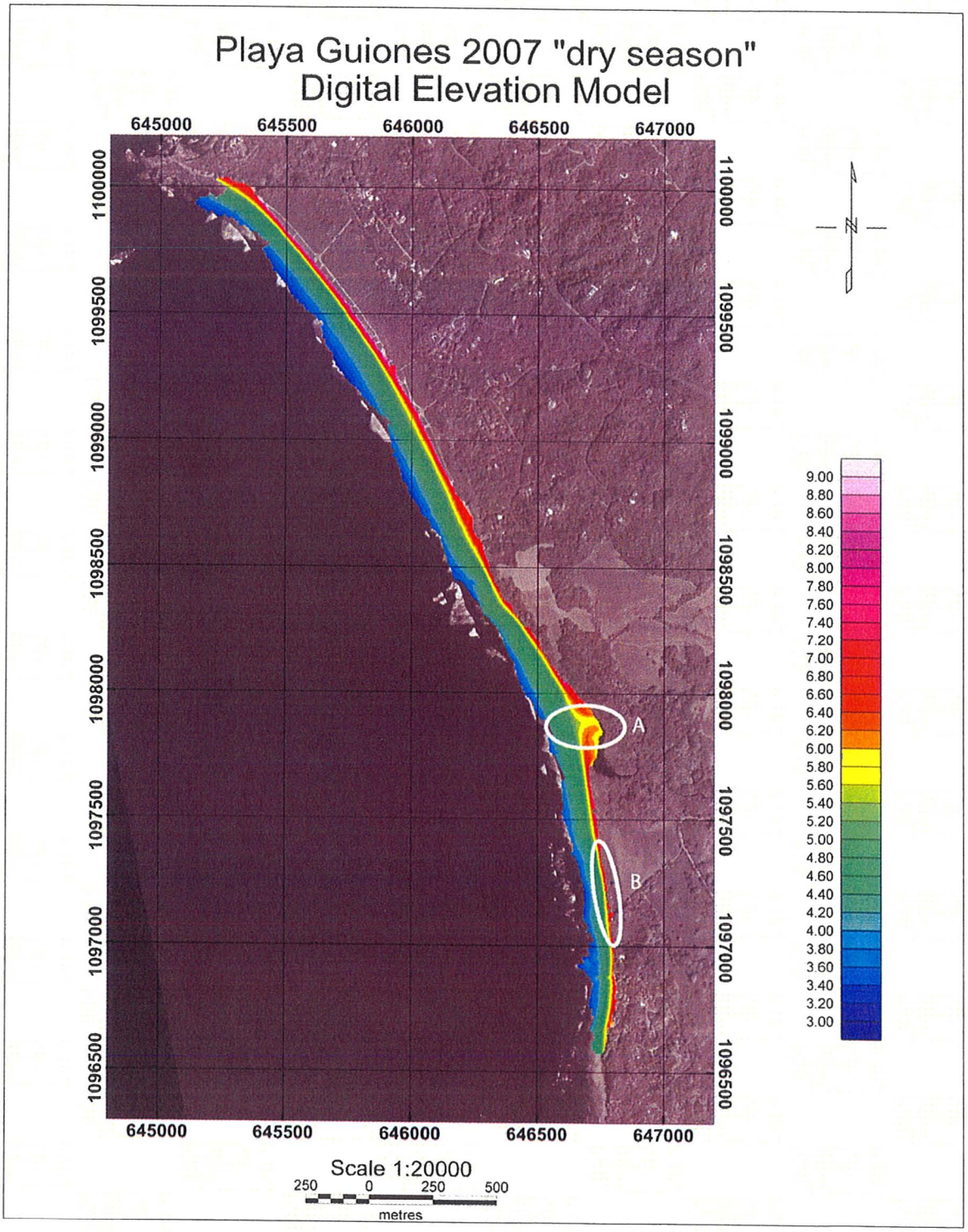

Figure 4.2: DEM of Playa Guiones created from data collected during 2007 dry season. Location A, was a feature previously identified on the 2005 DEM as an elongated depression not parallel to the shore.

2007 Wet Season – 2005 Dry Season DEM

Figure 4.3 is a DEM that represents the change in elevation by subtracting the 2005 DEM from the 2007 DEM. The DEM was divided into three sections (northern Playa Guiones, central Playa Guiones and southern Playa Guiones), enlarged, and profiles were extracted. Initial observations were formed from the overall DEM in Figure 4.3. The upper half of the DEM has a uniform distribution of elevation change within a smaller range whereas, the lower half that has a greater range in elevation change and the elevation change is sporadically distributed.

For the majority of the northern portion of the DEM, it appears that there were elevation increases on both the beachface and the surf zone (i.e., a net accumulation of sediment), with only a small number of areas that experienced a decrease (i.e., a net loss of sediment). Sediment change within this section ranged from an accumulation of nearly 1.2 m to a loss of 1.5m. The distribution of sediment change across the beach were different in the southern portion of the DEM was different than in the northern portion. In the southern portion of the DEM the beachface experienced a loss of sediment and in the surf zone there was an accumulation of sediment. The surf zone had a greater range of net accumulation and net loss. There was an approximant loss of 1.95 m and an approximant gain of 1.65 m in this region.

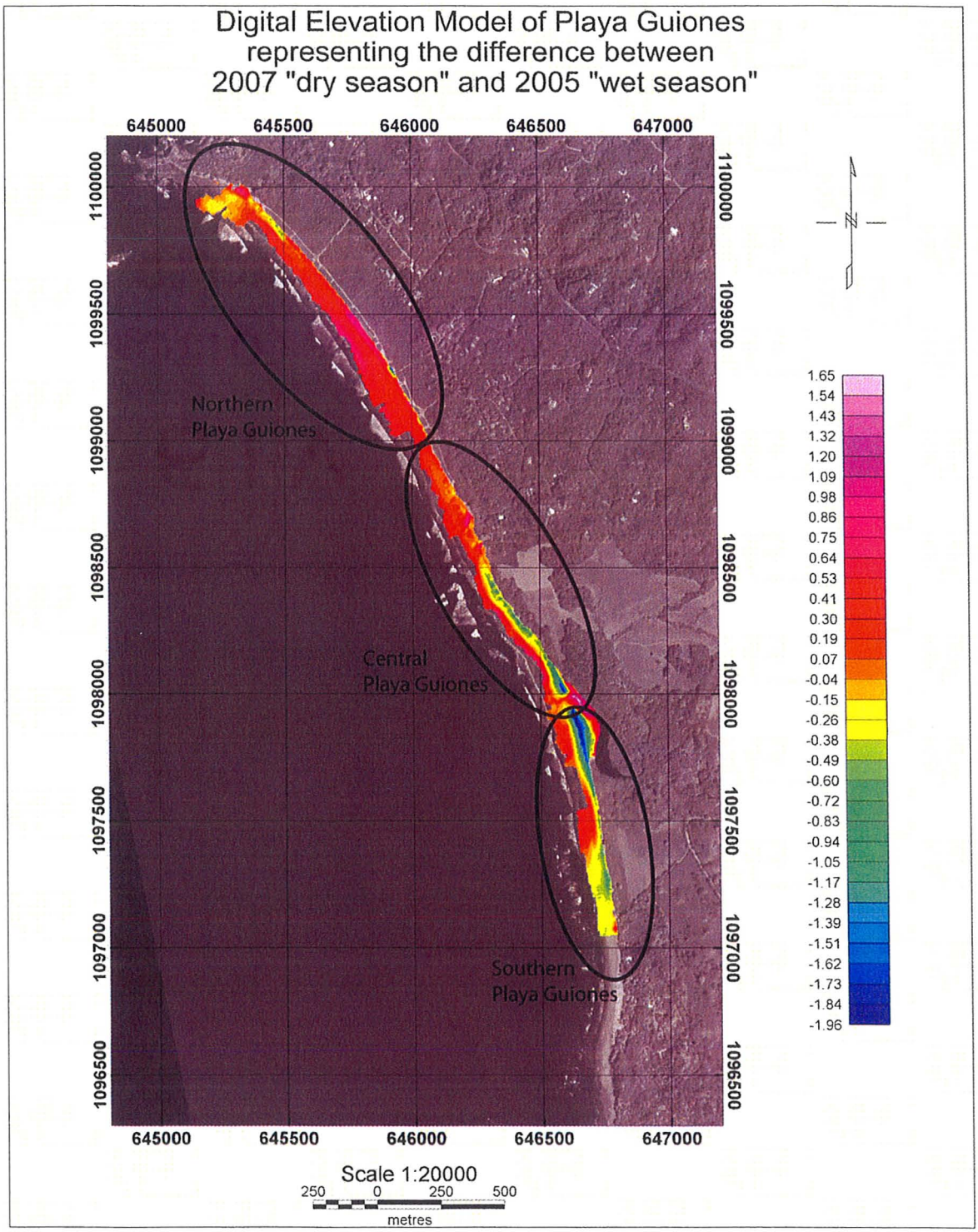

Figure 4.3: Difference in elevation between 2007 and 2005 field season for Playa Guiones. There appeared to be an overall elevation increase in the northern section of the beach, whereas, the southern section appeared to have areas of both accretion and erosion.

A volumetric calculation for the change in elevation between the two years showed that there had been 63, 119 m^3 of accumulation and 40, 451 m^3 of erosion that resulted in a net increase of 22, 668 m^3 of sediment on the beach during this two year period. The DEM area used for the volumetric calculation was 291, 088 m^2. The addition of 22, 668 m^3 of sediment spread evenly over the area would result in an increase of 0.08 m in elevation.

Northern Playa Guiones Enlarged with Profiles 1 - 5

An enlarged DEM of Northern Playa Guiones illustrates that for the majority of this region there was an accumulation of sediment, with the greatest increases at location A and B (Figure 4.4). At location A, there was an accumulation of sediment greater than 1 meter. Location B had the greatest accumulation for this section. The accumulation occurred on both the beachface and the surf zone.

Three locations (C, D and E) were identified as locations in which there was a net sediment loss. At location C, there was an extensive area in the surf zone that experienced a small sediment loss of 0.2 m. It was located further seaward from location A. Location D and E were the two locations that had experienced the greatest amount of sediment loss. The loss was most heavily concentrated along the vegetation line. The magnitude of loss ranged from 0.2 m to 1.5 m.

Profiles 1 – 5 (Figure 4.5) were extracted along Northern Playa Guiones beginning at location A and spaced evenly along the shoreline. The comparison between the two seasons for Profile 1 showed that during the dry season there was an

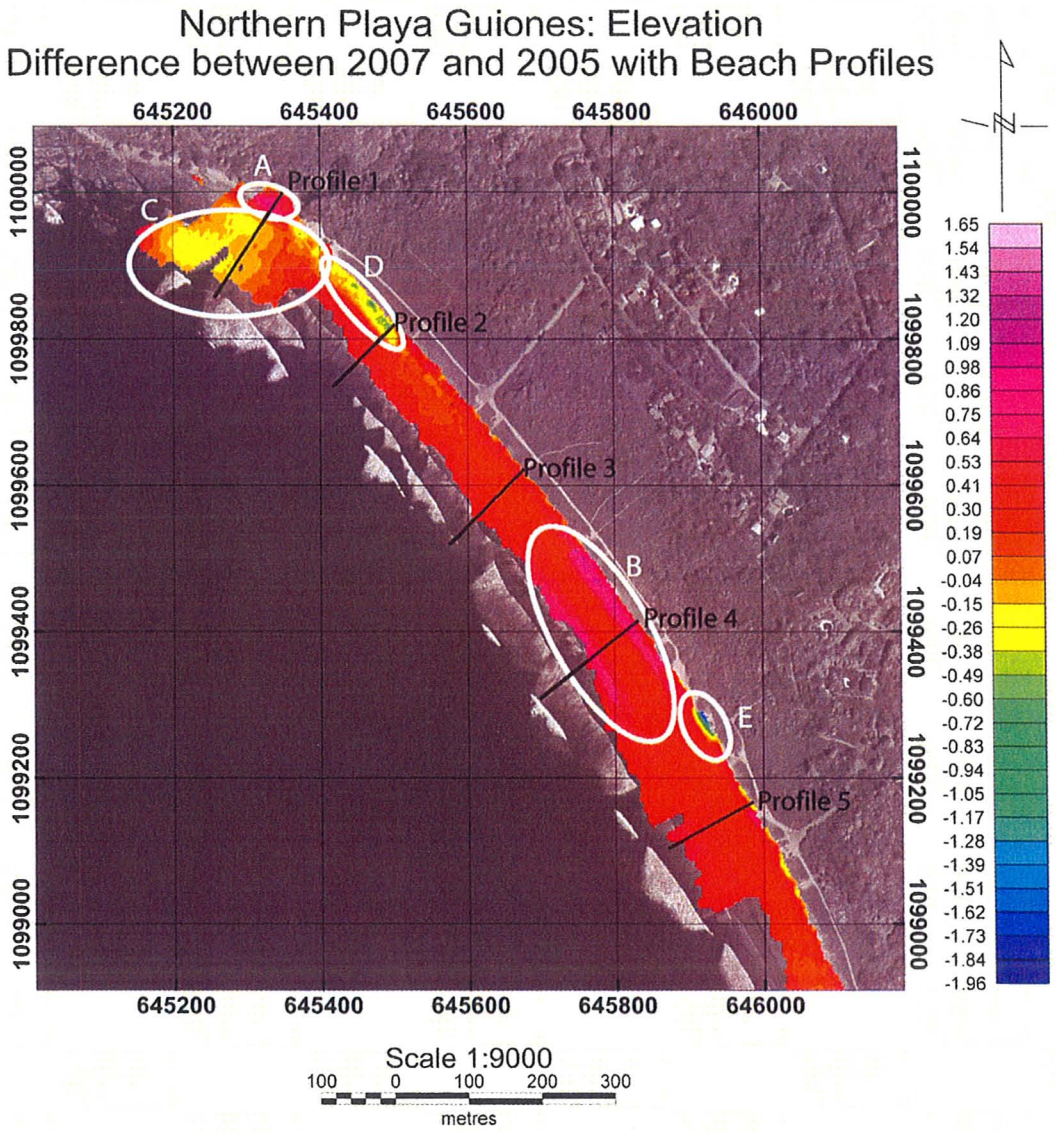

Figure 4.4: Enlarged DEM representing the elevation difference between 2007 and 2005 for Northern Playa Guiones with Profiles 1 – 5.

accumulation of sediment resulting in a steeper beachface when compared to the wet season. Profiles 2-5 were similar to each other. They show an accumulation of sediment on both the beachface and the surf zone, with the exception of profile 2 that experienced a decrease on the beachface.

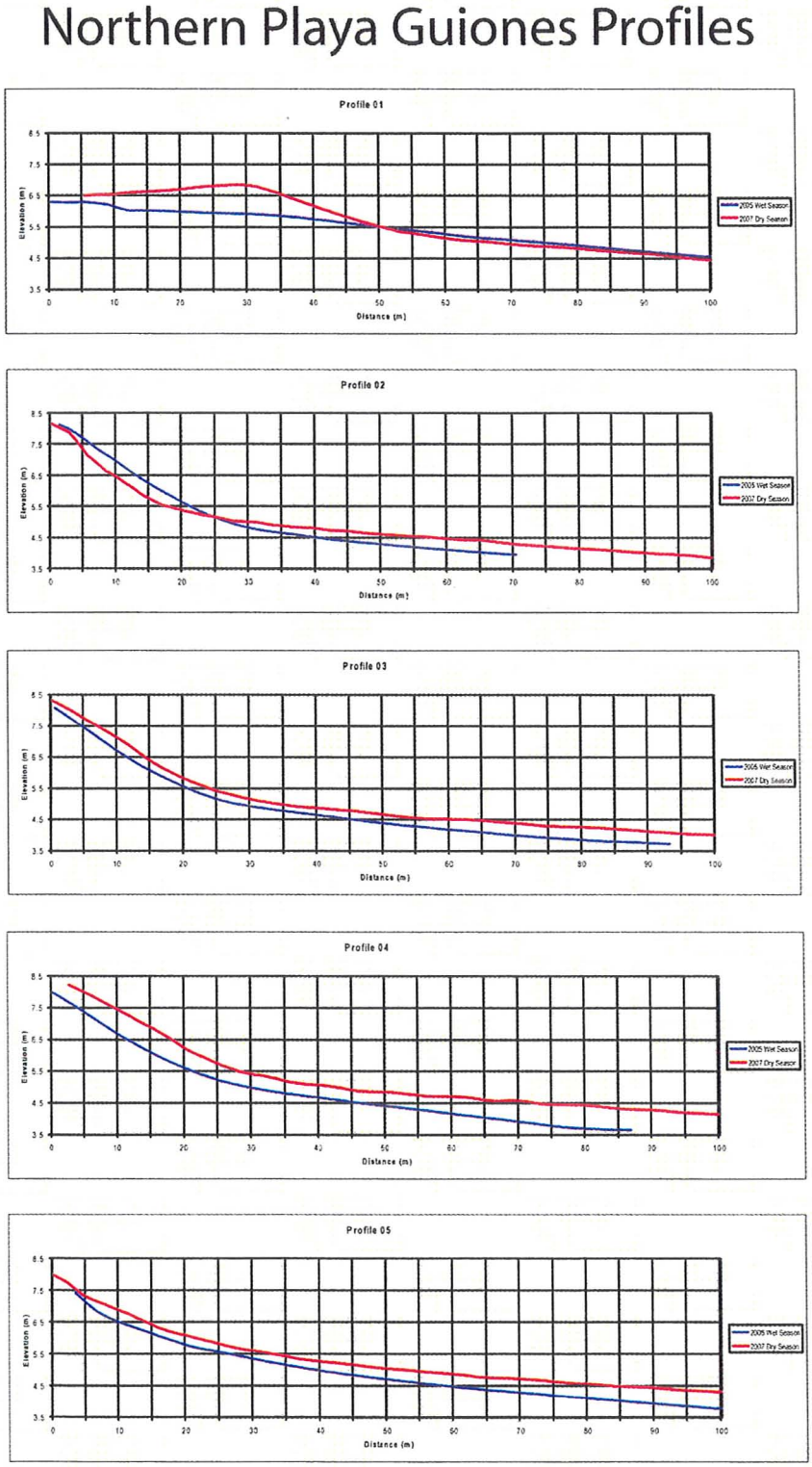

Figure 4.5: Profiles 1-5 as depicted in Figure 4.4 for Northern Playa Guiones.

Central Playa Guiones Enlarged with Profiles 6 -10

The enlarged DEM of Central Playa Guiones (Figure 4.6) shows multiple locations of net sediment loss and net sediment gain both on the beachface and surf zone. For the northern portion of central Playa Guiones, there was a net sediment accumulation along the beachface and surf zone that was comparable in magnitude to northern Playa Guiones. The southern portion, experienced sediment accumulation along the surf zone and sediment loss along the beachface, with the exception at location J where there was an increase along the beachface/backshore. Overall, three locations experienced the greatest sediment accumulation (location F, G and J) and two locations experienced greatest sediment loss (location H and I).

Locations F, G and J, were identified on the 2005 wet season DEM as elongated depressions not parallel to the shore, however, only location J was identified on the 2007 dry season DEM. Location F and G experienced sediment accumulation up to 1 m between the two seasons. At location J, the beachface and backshore experienced a sediment accumulation up to 1.65 m during this time period. Location I experienced a sediment loss up to 1.6 m. Location H, showed a pattern of sediment loss of up to 0.8 m in a region along the beachface that contained elevated crescent shaped features that were identified in the 2005 DEM, however, in the 2007 DEM these features were no longer present.

Profiles 6 – 10 (Figure 4.7) were extracted for central Playa Guiones. Profile 6 and 7 showed little change on the beachface with a small amount of sediment accumulation within the surfzone for the dry season. Profile 8, 9 and 10 were similar to

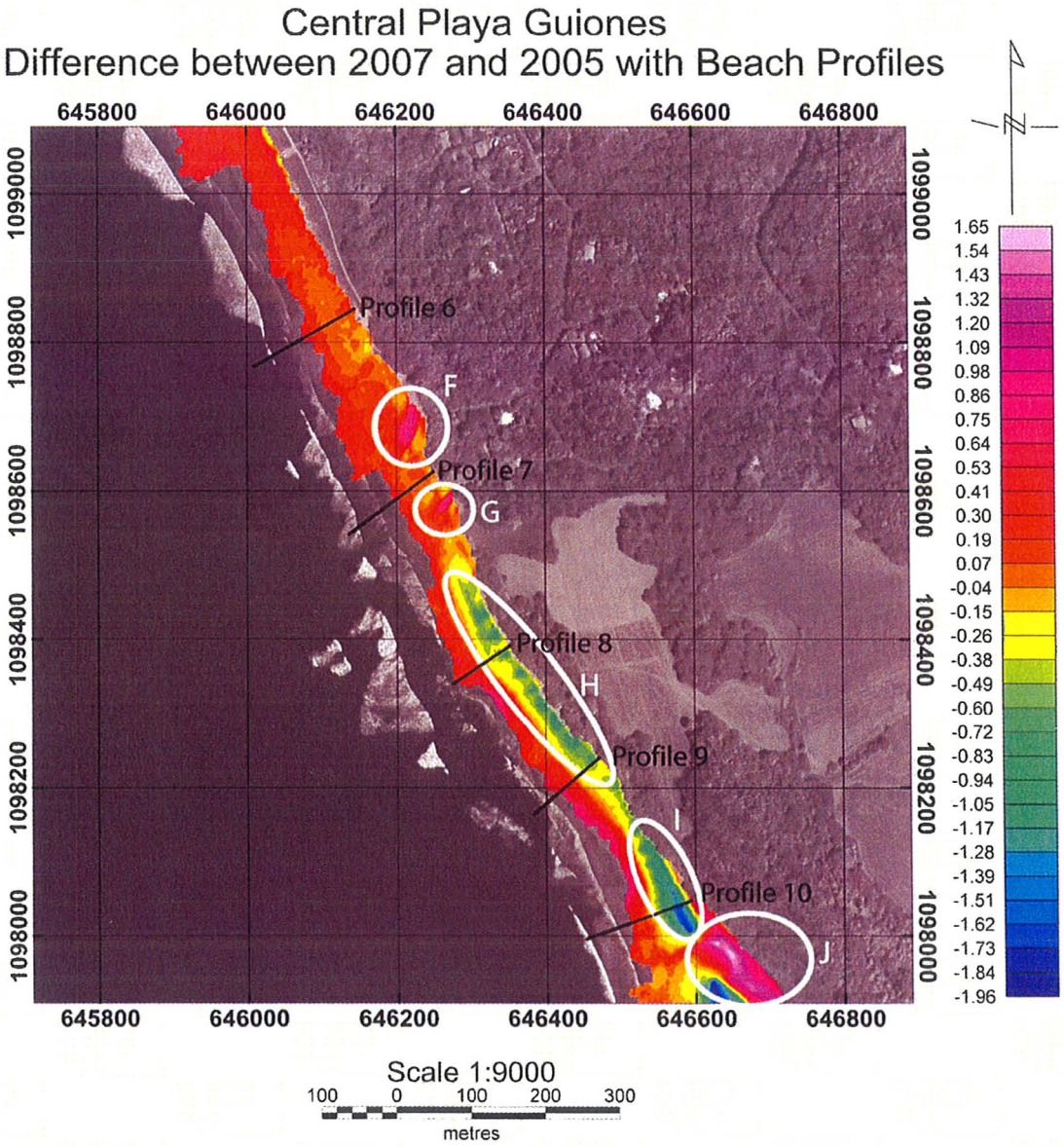

Figure 4.6: Enlarged DEM representing the elevation difference between 2007 and 2005 for Central Playa Guiones with Profiles 6 – 10.

each other, in that from the wet to dry season there was a decrease in sediment on the beachface and an increase in sediment in the surf zone. Profile 10, had the greatest decrease in sediment of these profiles between the two seasons.

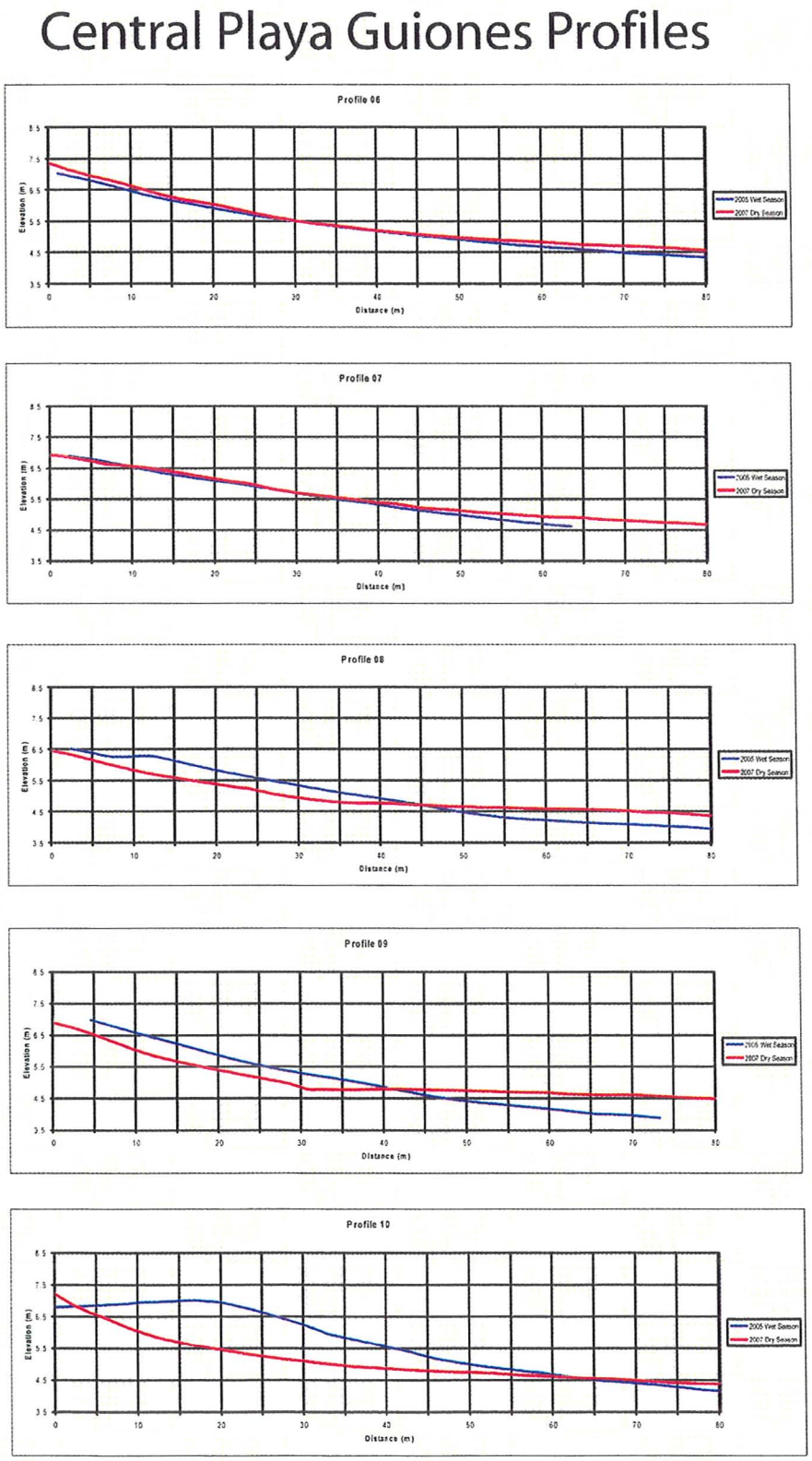

Figure 4.7: Profiles 1-5 as depicted in Figure 4.6 for Central Playa Guiones

Southern Playa Guiones Enlarged with Profiles 11 – 15

Southern Playa Guiones's enlarged DEM (Figure 4.8) has a similar distribution of sediment accumulation and loss as the southern portion of central Playa Guiones, where there was an overall loss of sediment along the beachface and an accumulation of sediment within the surf zone, until the most southern portion of this section is examined. In the most southern portion there is net sediment loss in both the beachface and the surf zone. There were two locations (K and L) that experienced the greatest sediment loss for this area. Location K experienced a decrease in elevation similar to location I, with the exception that there was a greater area that experienced net erosion of up to 1.95 m. Location L, is a region at the southern extent that experienced net sediment loss up to 1 m throughout the beachface and extending up to the vegetation line. There was less net sediment loss at location L in the surf zone.

Profiles 11 – 15 (Figure 4.9) were extracted for southern Playa Guiones. In all 5 profiles, there was a net sediment loss throughout the beachface. The magnitude of sediment loss between the two seasons was greatest for the northern most profile (Profile 11), and the magnitude decreased as the profiles were extracted further south. This resulted in with steeper slopes for 2005 for Profile 11 and 12 when compared to the gradual slopes in 2007. Profile 14 and 15 were nearly identical with similar slopes for each season, and showed that this portion of the beach experienced net erosion on both the beachface and surf zone.

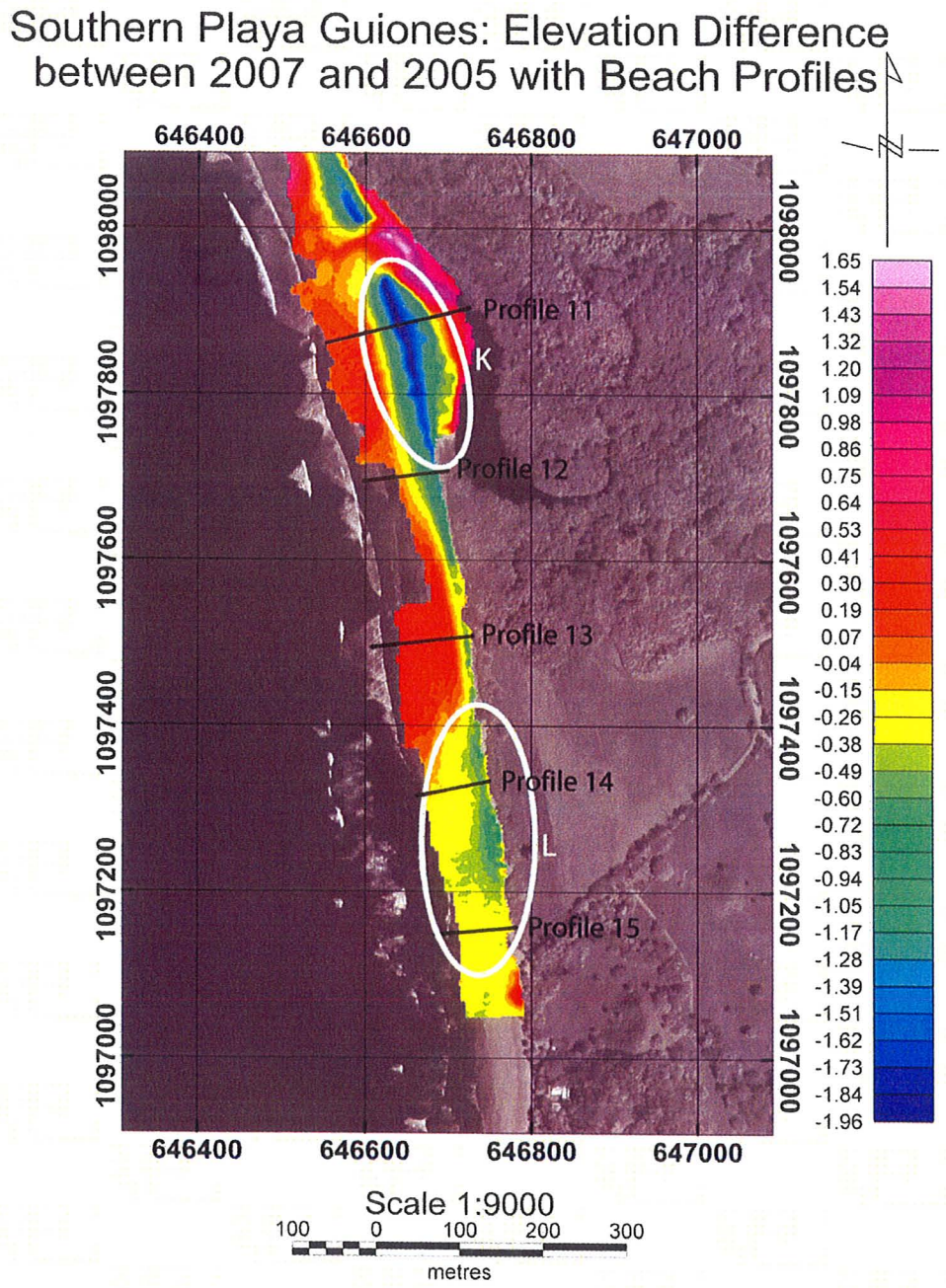

Figure 4.8: Enlarged DEM representing elevation change between 2007 and 2005 for Southern Playa Guiones with Profiles 11 – 15.

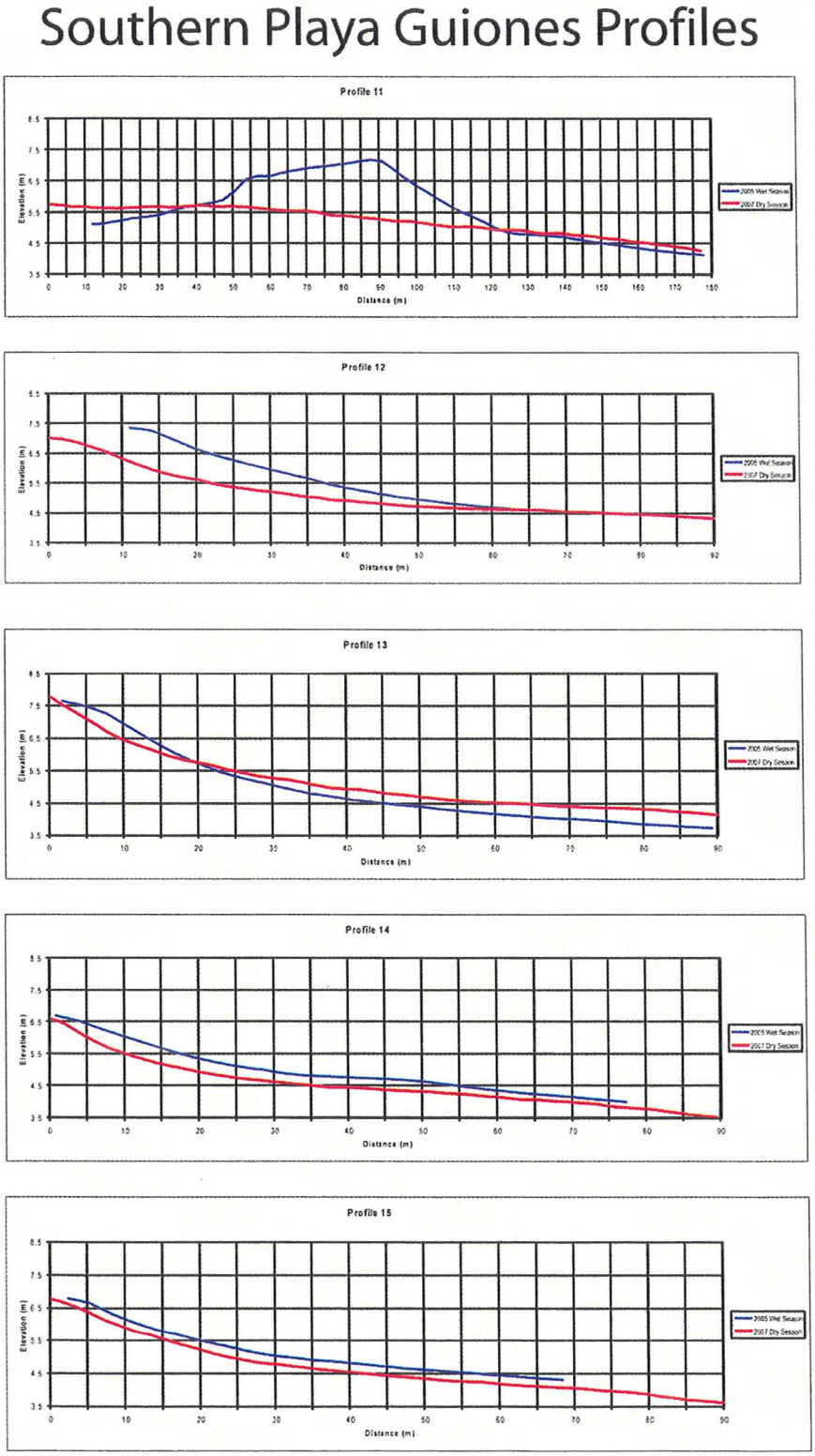

Figure 4.9: Profiles 11-15 as depicted in Figure 4.8 for Southern Playa Guiones.

4.1.2 Sediment Distribution

The locations of the representative grab samples that were collected for both years (i.e., 2005 and 2007) are indicated on Figure 4.10 along with the results of the sediment analysis. There were a total of four sediment samples collected for the 2005 wet season and six samples collected for the 2007 dry season. Although, it is impossible to define the exact location for the change in sediment size, approximate boundaries were created that defined the distribution of sediment. These were based on visual observation from walking the beach daily for several consecutive weeks. The sediment distribution showed, that for both years, fine sediment was located at both the southern and northern extents. The fine sediment in the south gradually became coarser towards Rio Rempujo. The difference between the two seasons was identified in the area north and south adjoining Rio Rempujo. During the wet season, this area consisted on coarse sediment, however, in the 2007 dry season, the sediment was fine grained. For both years, the sediment was calcareous with other minerals such as quartz, olivine, obsidian and k-feldspar present (Bertram, 2006).

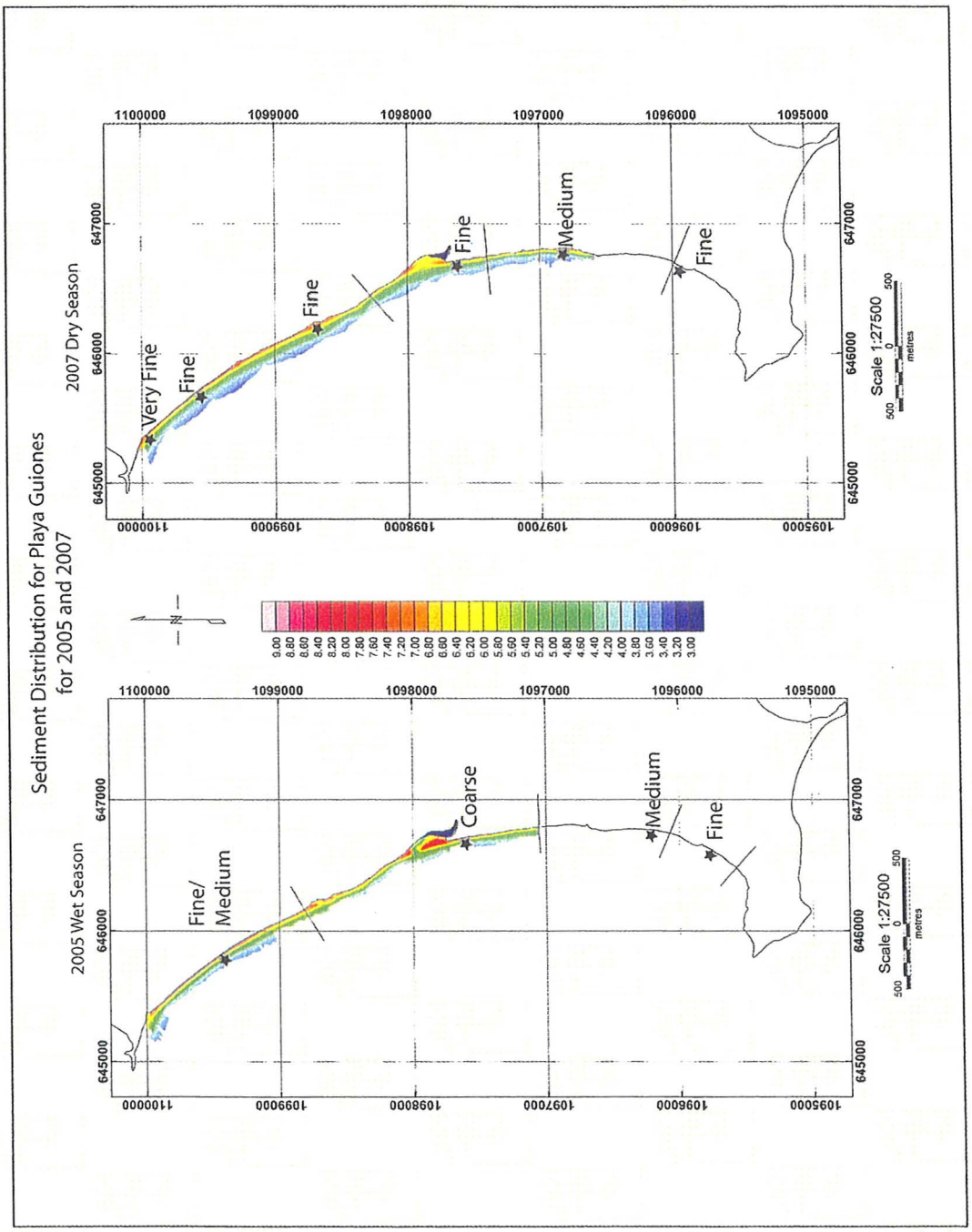

Figure 4.10: Sediment distribution collected for 2005 wet and 2007 dry season along Playa Guiones.

4.1.3 Discussion

The digital elevation models created and profiles extracted for each season provided an excellent way to assess the beach morphology both in two and three dimensions. With this analysis four river channels and a group of cusps were identified in DEM of the wet season (Figure 4.1). When compared to the 2007 DEM (Figure 4.2), only one identifiable river channel remained and the previously evident group of cusps was absent, however, a new group of cusps were present further south. The DEM representing the difference in elevation between the 2007 dry and 2005 wet season (Figure 4.3) provided evidence of changes that occurred during these seasons.

The DEMs showed that during the dry season when the rivers were not discharging into the ocean, the fluvial channels were filled in along the beachface and backshore with sediment deposited through a combination of wave and aeolian processes. The three northern most rivers, which were also the smallest (Location A1, A2 and A3, Figure 4.1) were simply filled in likely the result of primarily deposition of marine sediments from wave action however, for the largest river, Rio Rempujo (Feature A4, Figure 4.1), there was a large amount of seasonality between the erosion and depositional characteristics of the area. For example the 2005 DEM illustrated 1.95 m of net sediment erosion in the area of the riverbanks and up to 1.65 m of net sediment deposition in the former river channel. Upon review of the profiles extracted along the river banks, it showed that the beach face was steeper during the wet season which would be characteristic of a more reflective beach. The significance of the change in elevation at and around these river channels may be important in the overall dynamics of beach

morphology, especially concerning Rio Rempujo due to its size with the potentially large amount of water and sediment discharged into the surf zone during the wet season.

Identification was possible for two sets of cusps, one set for each season at different locations. The northern set was present during the 2005 and identified at location B Figure 4.1, however, they could not be recognized in the 2007 DEM. This feature was confirmed on the difference DEM, as there were a group of circular patterns of elevation loss, indicating that the cusps had been eroded during this period. A southern set of cusps were identified in Figure 4.2 at location B along the vegetation line and they were not present on the 2005 DEM. However, the difference DEM only showed some minor evidence of cusp creation adjacent to the vegetation line with the majority of the area experiencing net sediment loss which does not support the observation of the second set of cusps. Due to uncertainty surrounding the evolution and removal of cusps as described in Chapter 2.2.6, it is unclear if the presence and disappearance of the cusps are the result of seasonal variation, storm activity or the evolution of a dynamic beach feature.

In addition to identifying beach features through the DEMs and extracted profiles, the analysis allowed an assessment of the sediment change and beach slope gradient changes that occurred between the two seasons. The difference DEM showed that the overall change in elevation for the upper half of Playa Guiones was a net gain in sediment along the beachface and surf zone, whereas, the lower half experienced net erosion along the beachface with a net gain only across the surf zone. The extracted profiles confirmed that the overall change in elevation trends and allowed the actual amount of change to be

graphed for ease of assessing. The majority of the profiles confirmed what was visually assessed on the DEM, and that the overall slope for the beach did not change that drastically between the seasons with the exception of the area around Rio Rempujo. Based upon the analysis of the profiles, the majority of the beach can be classified as having characteristics of an intermediate beach as described by Short (1999). The beach area around Rio Rempujo, as the profiles indicate, may change from a more reflective slope in the wet season to more intermediate in the dry season.

The analysis of the sediment grab samples taken along the beach showed little difference for the sediment type and size between the two seasons. The only difference was again near Rio Rempujo. At this location the sediment was finer during the 2007 dry season. The overall majority of the sediment was calcareous based, of various sizes, with small amount of other minerals present (e.g., quartz, olivine, obsidian and k-feldspar (Bertram, 2006)). The small amount of other minerals found in the sediment can likely be attributed to fluvial deposition during the wet season. The source of the calcareous material would be from off shore sources (e.g., reef material). A possible explanation for the difference between the two seasons could be the amount of storm activity in the region. During the wet season, severe storm activity could release calcareous material that was deposited on the beach. By the time of the dry season, the calcareous material has been reworked within the surf and swash zone breaking down the sediment from coarse to fine grain.

Longshore drift was discussed with local fishermen who are familiar with the area, and it was determined that there was not a defined trend of longshore drift present

along Playa Guiones. This is supported by the aerial photos and visual observations by the researcher on several field seasons. For both seasons, the longshore drift could be in either direction at different times.

Playa Guiones is a mixed wave-tide beach, and a conclusion from the observations is that the beach is an intermediate beach, possibly with a longshore bar and trough. This conclusion was reached based on a number of observations that support the literature's definition of an intermediate beach (Short, 1999). The types of waves present for both seasons were spilling/plunging breakers with three waves per set arriving in the surf zone. The slope of the profiles were moderate in both seasons, except for the region of Rio Rempujo during the wet season which makes this section of beach more reflective during the wet season. The sediment distributed along the shore was fine grained which is indicative of an intermediate beach, with coarser sediment present near Rio Rempujo which reaffirms that this section is more reflective. In addition, the researcher observed the presence of a bar that ran parallel to the shore providing support that this beach could be classified as a longshore bar-trough beach.

4.2 Playa Pelada

4.2.1 DEMs and Profiles

2005 Wet Season DEM

Figure 4.12 is the digital elevation model (DEM) of Playa Pelada with the data collected during the 2005 wet season. It is overlain on the satellite image (2004) of the area. This DEM was gridded with a cell size of 3 meters, with a blanking distance of 7.5

meters and extended by 1 cell past the data. As seen in the figure, the DEM coverage of Playa Pelada is approximately 800 meters in length from them the northern extent to the south. The remaining 300 meters of the beach was not represented in the DEM for the same difficulties associated with data collection for Playa Guiones (i.e., a large area of exposed rock and vegetated southern headland that blocked satellite signals).

The 2005 DEM has smooth contours of the beach that run parallel to the shoreline that has formed three individual crescents bounded by two headlands (Feature H1 and H2) created by the presence of eroded headlands that are currently rocky outcrops (Feature R1, R2, R3). The three crescents have similar shape to each other with each end of the crescent anchored either by a headland or a rocky outcrop. Along the shore of the northern crescent, Feature A, is an elongated depression that runs perpendicular to the shore. Feature A, was identified as an ephemeral river that was discharging water into the ocean during the survey. Feature B, is a portion of the southern crescent in which small cusps were identified in which a greater circular pattern of elevation extended from the vegetation line and decreased towards the ocean. Elevation at the vegetation line is greatest in the northern and central crescent as indicated by the color of the contour. The beach slope for the northern and central crescents have a modest slope due to the color contour, and the southern crescent has the least slope of all three crescents.

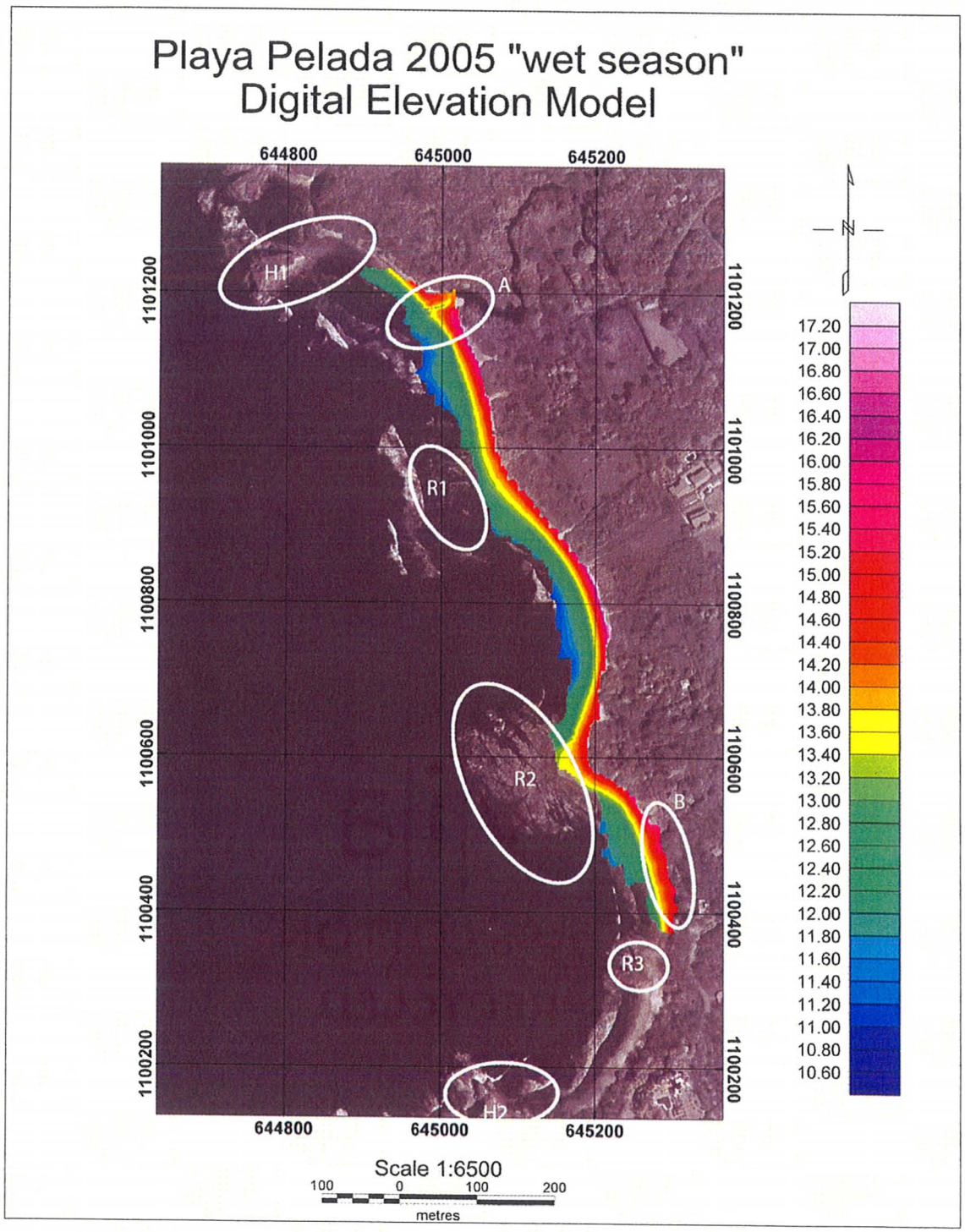

Figure 4.12: Digital Elevation Model of Playa Pelada 2005. Feature A, was identified as an ephemeral river. Feature B, is a group of features identified as cusps.

2007 Dry Season DEM

Figure 4.13 is the digital elevation model that represents Playa Pelada during 2007 dry season. The 2007 DEM was gridded with a cell size of 2 meters, blanking distance of 5 meters and extended 1 cell past the data. A greater area of the southern portion of Playa Pelada is included in the DEM but similar to the difficulties experienced during the 2005 collection period, a small portion of exposed rock was not surveyed.

The 2007 DEM is similar to that of the 2005 DEM in that three individual beach crescents have been identified along the shoreline, each anchored by a headland or rocky outcrop. The 2007 DEM does not include feature A that was previously identified in the 2005 DEM. Feature B was identified in both DEMs, however, the shape of these features has changed over this period of time. For 2007, these features were elevated, elongated crescent shape features, which were narrow closest to the ocean and gradually widened in a circular form to join one another near the vegetation line. Overall, the northern and central crescents had a greater elevation then the southern crescent at the vegetation line as indicated by the color of the DEM at these locations. It appears that the northern crescent and central crescent have the greatest slope at the beachface, whereas, the southern crescent had a more gradual slope. The northern crescent had the greatest slope in the surf zone with the southern crescent having the least. The slope for the central crescent was separated into two halves, with the southern portion being steeper and the northern portion being gradual.

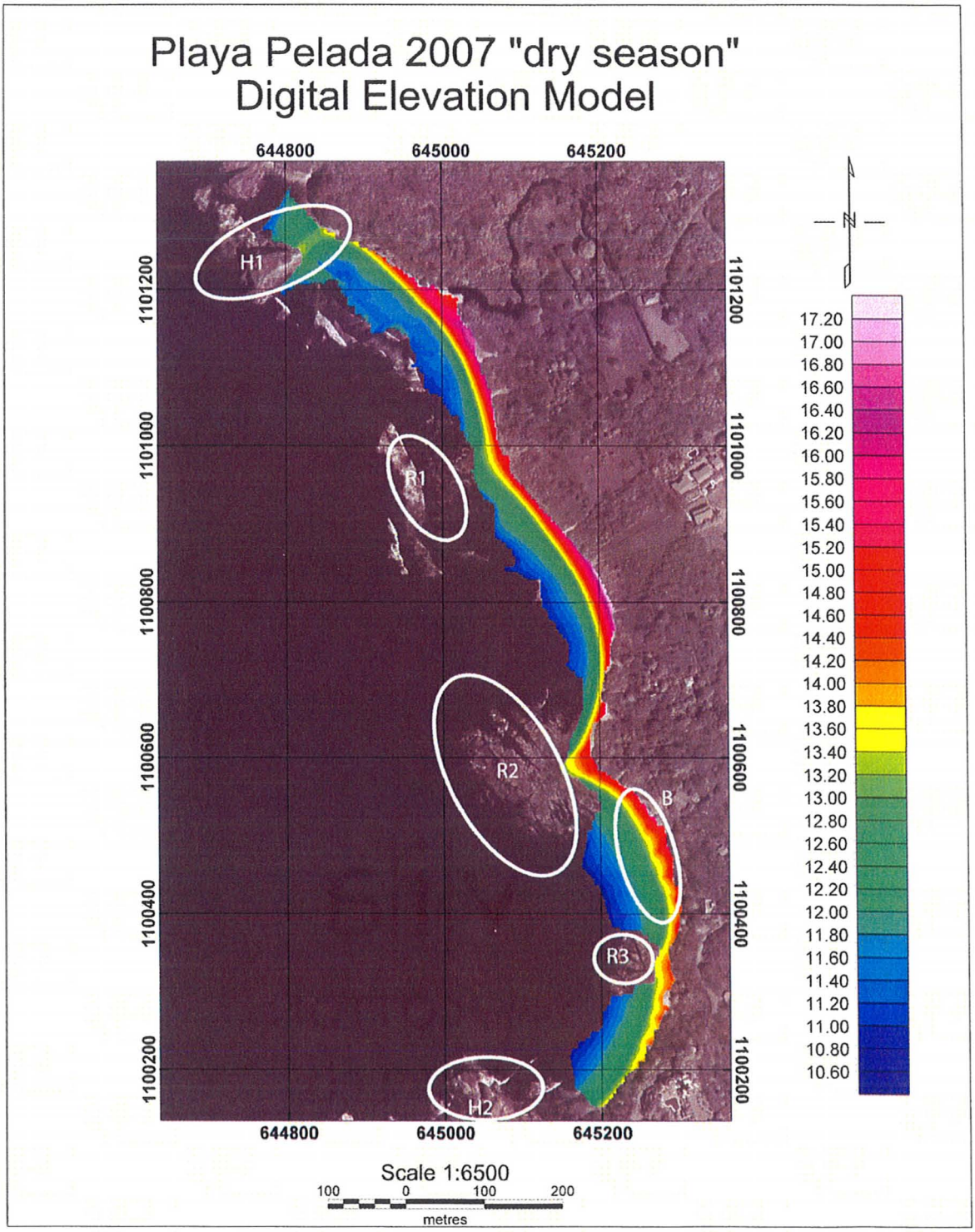

Figure 4.13: The 2007 dry season DEM of Playa Pelada. Feature A, that was present in the 2005 is not featured on the 2007 DEM. Feature B was identified as a group of cusps that extended from the vegetation line.

2007 Wet Season – 2005 Dry Season DEM

Figure 4.14 is a DEM that represents the change in elevation by subtracting the 2005 DEM from the 2007 DEM. Initial observation appeared that there was only one area (Location1) on Playa Pelada that experience elevation increase during this period with multiple areas of erosion (Location 2, 3, 4 and 5).

Location 1, was the feature previously identified as an ephemeral river that was present in the 2005 DEM as feature A but not present in the 2007 DEM. During this period of time, as observed by the shading on the 2007 – 2005 DEM, this river channel had been in filled with sediment resulting in net sediment accumulation up to 2.3 meters.

Three areas of particular interest because of the large sediment loss they experienced are identified at location 2, 3 and 4 on Figure 4.14. Location 2 and 3 are on opposite sides of a headland, and both experienced sediment losses up to 0.8 m. Location 4, on the northern side of the second headland, experienced the greatest loss of sediment (0.9 m).

Location 5, was an area that had a group of elongated regions of sediment loss perpendicular to the vegetation line. This area is identified on the 2005 DEM as cusps, then in 2007 it is identified as narrow, elongated, elevated crescent shaped, connected features located other along the vegetation line. During this time period, it appears that the original cusps had convex sides. The sediment loss appears to have changed this to a concave shape.

When a volumetric calculation is performed on the difference between the two years it was found that there had been an accumulation of 3, 933.25 m^3 and 9, 810.47 m^3

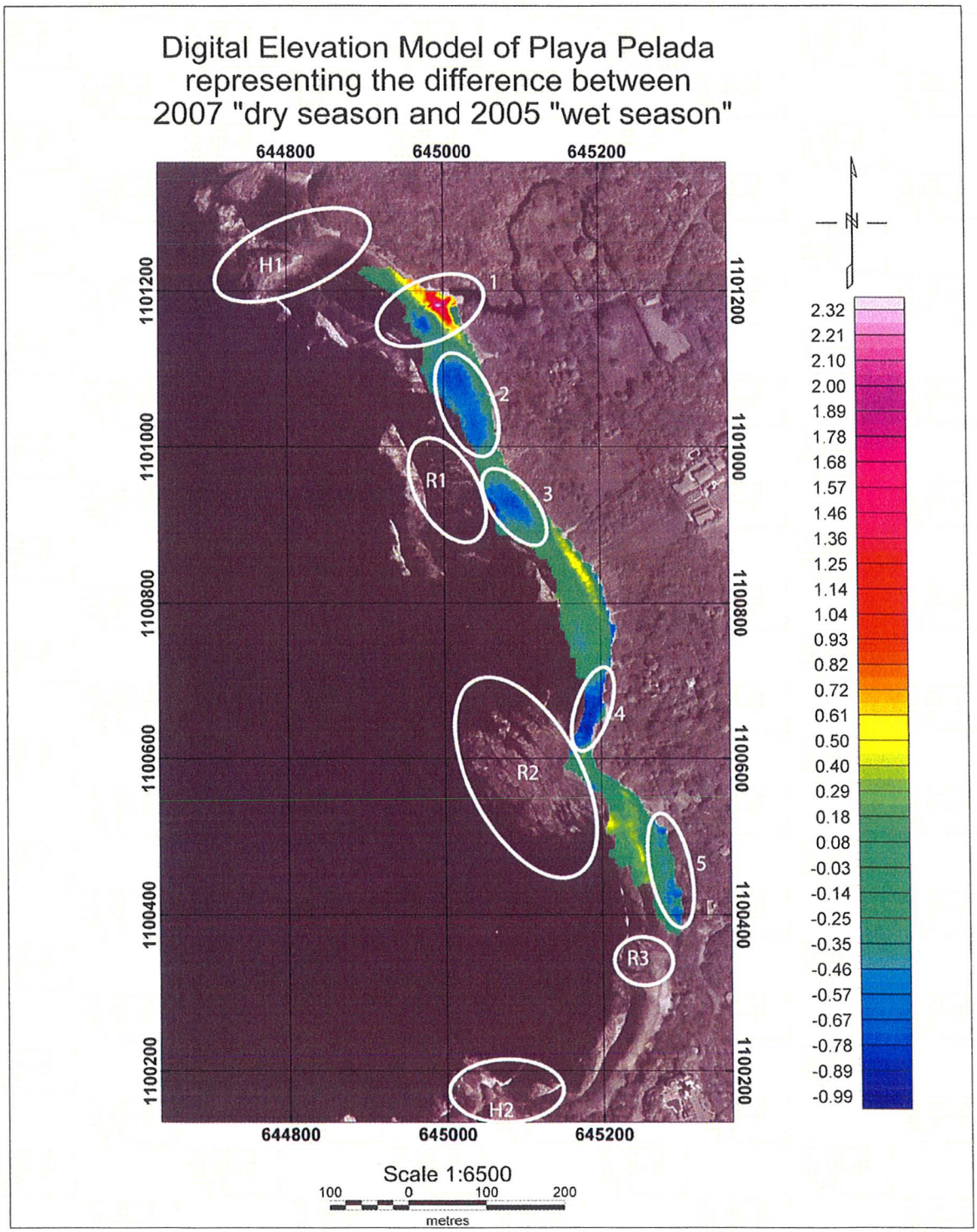

Figure 4.14: Difference in elevation between 2007 and 2005 field seasons for Playa Pelada. Areas of interest were labeled location 1 -5.

were eroded with a net loss of 5, 877 m^3 of sediment. The DEM used for the volumetric calculation was 42, 820 m^2 so with the amount of sediment that increased, if spread over the whole area evenly would result in a 0.14 m loss of sediment across the entire beach.

Profiles Comparing 2007 and 2005 DEMs

The change in elevation DEM that was produced for Playa Pelada highlighted one large area of deposition and three large areas of erosion along the shore. Profiles were extracted in the attempt to explain the changes in elevation observed. These profiles were extracted at the rocky outcrop, to the sides of the outcrops and in the center of each crescent. They were then plotted to permit comparisons (Figure 4.15).

The first sets of profiles compared were Profile 3 and 7 that were extracted along both rocky outcrops, extending from the vegetation line perpendicular to the shore (Figure 4.16). These two profiles were compared to each other since these rocky outcrops divide Playa Pelada into separate beach crescents. Profile 3, extracted along rocky outcrop 1, that had the same elevation at the vegetation line for both years, however, as the profile extends there was a net loss of sediment between the 2007 and 2005 season. This is in contrast to profile 7, extracted on rocky outcrop 2, which had variation throughout the profile (some areas of accumulation and some areas of loss, but overall little variation). The differences between these two sets of profiles are interesting, however, rocky outcrop 1 was submerged underwater for most of the tide cycle, whereas, rocky outcrop 2 was above the water for a greater period of time during the tide cycle.

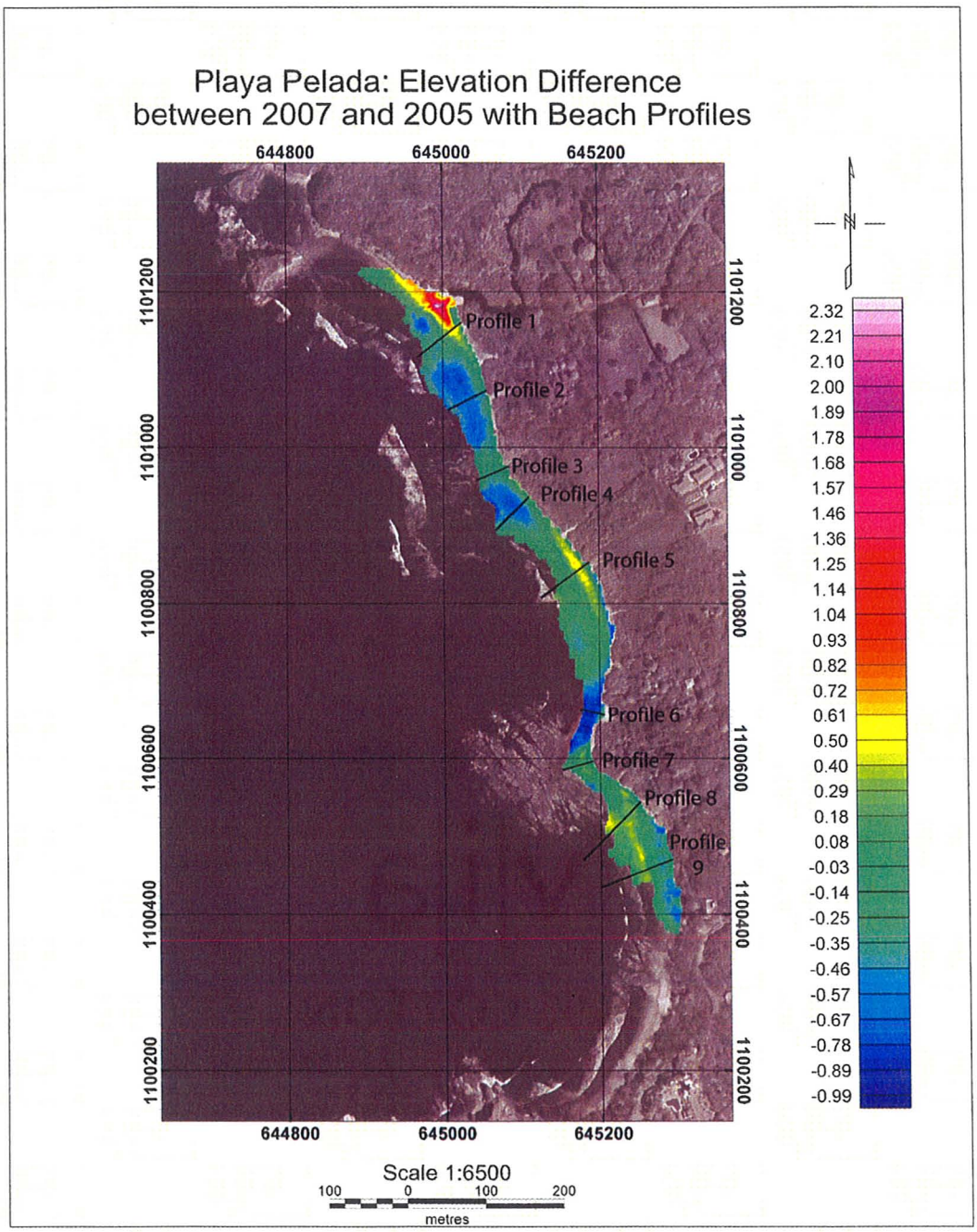

Figure 4.15: Resultant DEM when 2007 DEM was subtracted from 2005 DEM. Nine profiles were extracted from the DEM to observe changes between the two field seasons.

Profiles Comparing Elevation Changes of
Playa Pelada at Rocky Outcrop 1 and 2

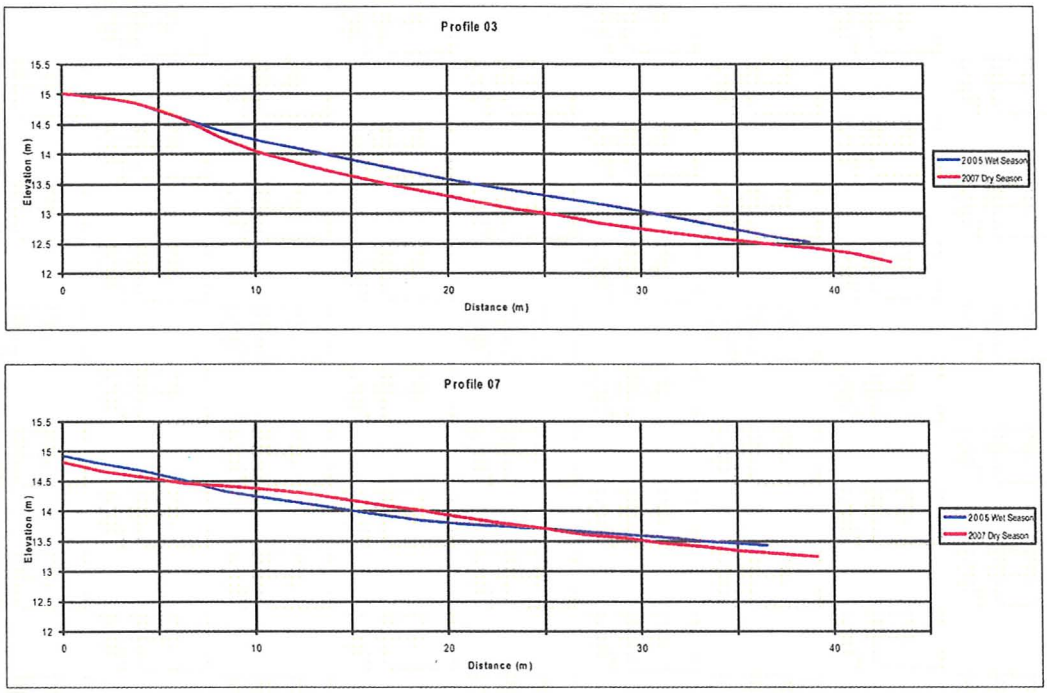

Figure 4.16: Profiles extracted along center of rocky outcrop 1 and 2, perpendicular to the shore.

Profiles were then extracted from either side of the rocky outcrops, Profile 2, 4, 6 and 8, and the differences were compared (Figure 4.17). Profile 2, 4 and 6 all had similar profiles that showed similar elevation between the seasons at the vegetation line and then a loss of sediment throughout the beachface and surf zone between 2007 and 2005. Profile 6 had the greatest amount of erosion, up to 0.85 m, between the compared profiles. Profile 8 was different from the previous profiles in that there was an accumulation of sediment between 2007 and 2005.

The profiles of the sides of the headlands correspond to the previously examined profiles of the rocky outcrops such that rocky outcrop 1 experienced a decrease in

elevation and this was observed in the profiles for both sides. Rocky outcrop 2 had both minimal increases and decreases in elevation along the profile and experienced a net loss of sediment on the northern side, whereas, the southern side had a net accumulation of sediment.

Profiles to examine the beachface and surf zone at the center of each crescent were extracted in profiles 1, 5, 9 (Figure 4.18). Profile 1 and 5 both showed net sediment accumulation along the beachface with a minimal amount of erosion along the surf zone. This is in contrast to profile 9 that showed a net sediment loss at the vegetation line and on the beachface a small net sediment gain in the surf zone. Overall, these profiles show that 2005, the beach profile was gradual in the northern crescent and became steeper in the 2007, while the southern crescent maintained a gradual profile and the central crescent maintained a moderate profile for both seasons.

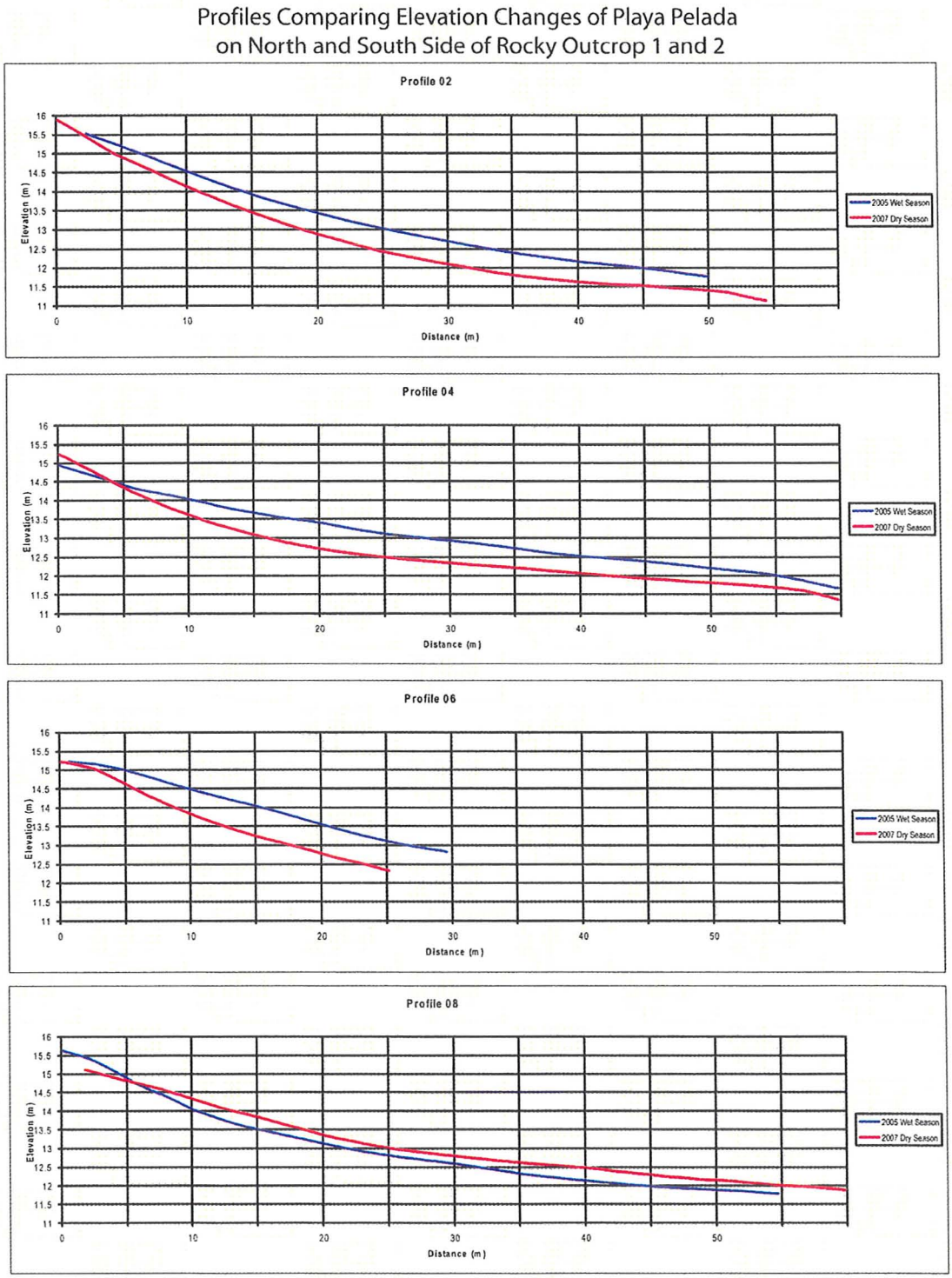

Figure 4.17: Profiles extracted on opposite side of rocky outcrop 1 and 2.

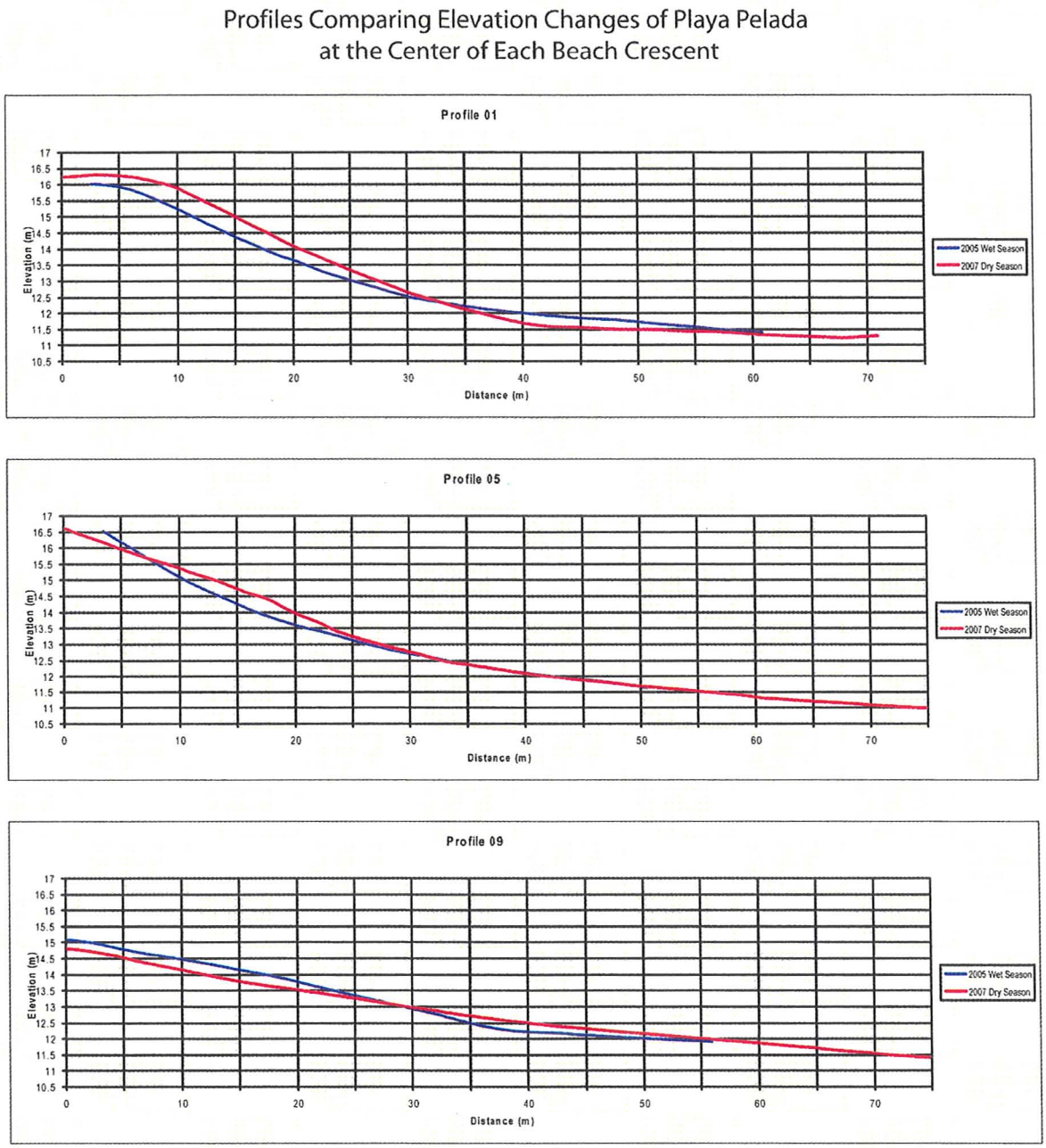

Figure 4.18: Profiles extracted at the center of all three beach crescents that form Playa Pelada

4.2.2 Sediment Distribution

Representative grab samples and field notes were collected for both seasons and were used to create a sediment distribution map for Playa Pelada (Figure 4.19). Similarities exist between the two seasons with fine/medium grain sediment located along the southern crescent and medium/coarse grain sediment on the central crescent. Differences between the two seasons were found along the northern crescent. During the wet season fine/medium grain sediment was present, whereas, during the dry season medium/coarse grain sediment was identified. The finer sediment may have been eroded by aeolian processes. Another difference between the two seasons was the finer grain sediment identified at the rocky outcrops during the dry season when compared to the medium grain sediment in the wet season. This finer grained sediment that was observed at the rocky outcrops maybe the material that was eroded by aeolian processes. The rocky outcrops may have acted to trap the sediment. Overall, it appeared the difference in sediment distribution between the seasons was an increased grain size at the northern and central crescent, while remaining the same for the southern crescent.

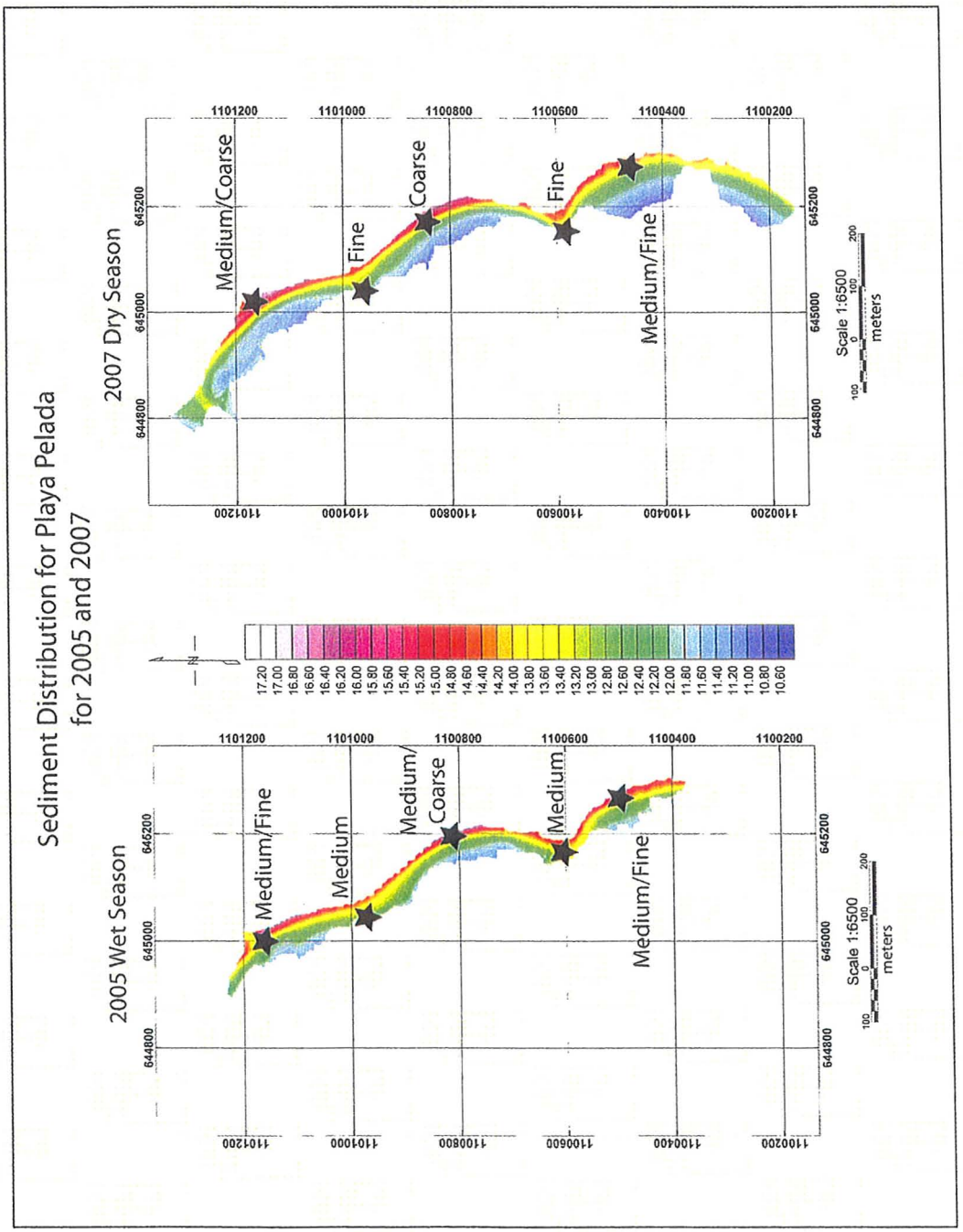

Figure 4.19: Sediment distribution along Playa Pelada for 2005 and 2007.

4.2.3 Discussion

Through the comparison of the digital elevation models, profiles and the sediment distribution completed in this analysis it is possible to identify differences in the beach morphology between the wet and dry season for Playa Pelada. Similar to the Playa Guiones analysis, an ephemeral river outlet and cusps were identified on the 2005 wet season DEM (Figure 4.12). The river outlet could not be clearly identified in the 2007 dry season DEM and the cusps were still present, however, these features had changed shape and height. The difference in elevation of these two beach features was observed on the comparison DEM, which provide evidence of the change between the two seasons. During the dry seasons, the river water stops flowing into the ocean and sediment is accumulated on the beachface to fill in the existing river channel. The cusps during this time period also changed in shape and elevation.

The difference in elevation DEM also identified areas of sediment accumulation and areas of sediment erosion. The area of increased accumulation correspond to the location of the filled in river channel. The profile for the wet season supported characteristics of a dissipative beachface that became more reflective during the dry season as described by Short (1999). There were three areas of erosion that occurred on the side of the rocky outcrops and when compared to the profiles extracted at these locations, the beachface had characteristics of a reflective beach for each season (Short, 1999).

For the wet season, it was observed that the northern and southern crescents had characteristics of a dissipative beach, whereas, the characteristics of the central crescent

were reflective. This is supported by the literature (Short, 1999). Between these two seasons, the beach slope changed at the northern crescent to more reflective similar to the central crescent, and the southern crescent appeared to remain dissipative. These changes in slope correspond to the changes in sediment size, such that when the beach crescent was more reflective, the grain size was larger (i.e., either medium or coarse grained) and when the beach slope was dissipative the grain size was finer (i.e., fine to fine/medium).

The change in slope, elevation and sediment grain size along Playa Pelada is the result of seasonal differences in addition to the geologic control. Playa Pelada is a very short beach, consisting of rocky outcrops and bounded by two headlands. These geologic features control the changes observed such that, the southern crescent has greatest amount of protection from surrounding rock features which resulted in a dissipative beach with fine sediment. The central crescent has the least amount of protection from the headlands, thus, there is more wave activity resulting in a reflective beach with the typical medium to coarse grain sediment (Shortt, 1999). The northern crescent has greater protection from rock features then the central crescent resulting in being less reflective, however, not as much protection as the southern crescent that had a dissipative beach.

Seasonal differences combined with the geologic control cause the northern crescent, during the wet season to form a dissipative slope due to the volume and velocity of the water discharging from the ephemeral river.

4.3 Limitations

One of the objectives of this study was to complete a survey of the beach that consisted of the beachface and as much of the surfzone as possible. The electronic equipment housed within the backpack unit could not get wet, so the survey was limited in the surfzone. To reduce the risk of waves submerging the equipment, the surveyor only went to a maximum depth of the water of 'knee high' to allow sufficient height for incoming waves to break without getting the equipment wet. To maximize the width of the surfzone that could be surveyed using the previous constraint, the surveys were preformed three hours on either side of low-tide, thus, limiting the number of hours each day to collect the survey data. During data collection for the wet season, there were daily thunderstorms that would move rapidly into the area and the equipment needed to be taken down to reduce the chance of a lightning strike and ensure the equipment would not get wet. This further reduced the number of productive data collecting hours each day. Fortunately this concern only pertained to the wet season.

The equipment used to perform the survey utilizes geospatial data provided by multiple satellites that traverse the sky. The number of satellites and their position above the earth are continuously changing creating multiple challenges. The equipment required a minimum number of satellites (4) to initialize, however, at times there were an insufficient number of satellites for this to be accomplished. Other times the equipment for no apparent reason would not initialize even with the required number of satellites present, thus, further limiting the amount of productive survey time. With the equipment working, there were limitations with the amount of beach coverage at the southern extent of both beaches caused

by the presence of rocky headlands and dense vegetation that obstructed the equipment from consistently receiving the signal.

Since benchmarks were not available as a reference points for data collection the data was leveled between successive days based on the overlap between surveys. The elevation and location of the exposed rock at the Playa Guiones's northern headland and Playa Pelada's second headland was assumed to have remained constant between the two surveys and was used as an inter-seasonal reference point. The distance that the radio antenna could communicate between the two GPS receivers was less than a 500 m radius prevented surveying the entire extent of the beach at one time as to tie the data together. The geospatial data collected by the GPS survey was set so that it could have a maximum error of +/- 5 cm both horizontal and vertical. Since each data set is leveled to the previous data set starting at the northern headland, this error could have been compounded over the course of surveying the entire beach. There is uncertainty as to the amount of error that is associated to each beach since the whole beach could not be corrected to one reference point, however, the potential error would be greatest at the furthest extents.

With the survey was completed on loosely consolidated sediment, the minimum curvature interpolation method was used as this is the best method to fit a sheet over an area of sample points. The limitation to using this interpolation method, as discussed in section 2.4.3, is that the sample points are not honored meaning that if a grid and sample point were at the same location, the height could be different since minimum curvature attempts to most effectively fit a sheet over the whole area. Berms and beach steps are two features that would have a rapid change in elevation over a short distance that would be minimized through this interpolation method.

4.4 Aerial Photography and Satellite Imagery

All five sets of aerial images dating from 1945 to 1997 were used to produce five georectified images of Playa Guiones and five of Playa Pelada. Although a large number of ground control points were collected it proved more effective to use the 2004 Quickbird satellite image as the reference for the ground control points. The resolution and condition of the original images differed throughout years resulting in quality differences of the final images (Table 4.1). A time series of all 6 sets of images for both Playa Guiones (Figure 4.20 and 4.21) and Playa Pelada (Figure 4.22) were used for comparison. Enlarged versions of these images are included in Appendix A (Playa Guiones) and Appendix B (Playa Pelada).

Table 4.1: Five sets of aerial photographs and one satellite image dating from 1945 to 2004 were used to analyze the shoreline and land use of Playa Guiones and Playa Pelada.

Type of Imagery	Date of Capture	Wet/Dry Season	Scale/Resolution
Aerial	December 29, 1945	Dry	1:40,000
Aerial	September 22, 1971	Wet	1:20,000
Aerial	January 16, 1975	Dry	1:10,000
Aerial	September 6, 1991	Wet	1:20,000
Aerial	December 4, 1997	Dry	1:40,000
Satellite	February 3, 2004	Dry	60 cm Panchromatic

4.4.1 Vegetation and Land-Use for Playa Guiones & Playa Pelada

On initial inspection of the imagery it is apparent that there have been a number of changes in both land-use and coastal vegetation during the 1945-2004 time period. The position of the vegetation line appears to be relatively stable during the period of observation, however, changes in the density and the type of vegetation could be

Playa Guiones – Time Series of Geo-Rectified Aerial and Satellite Imagery

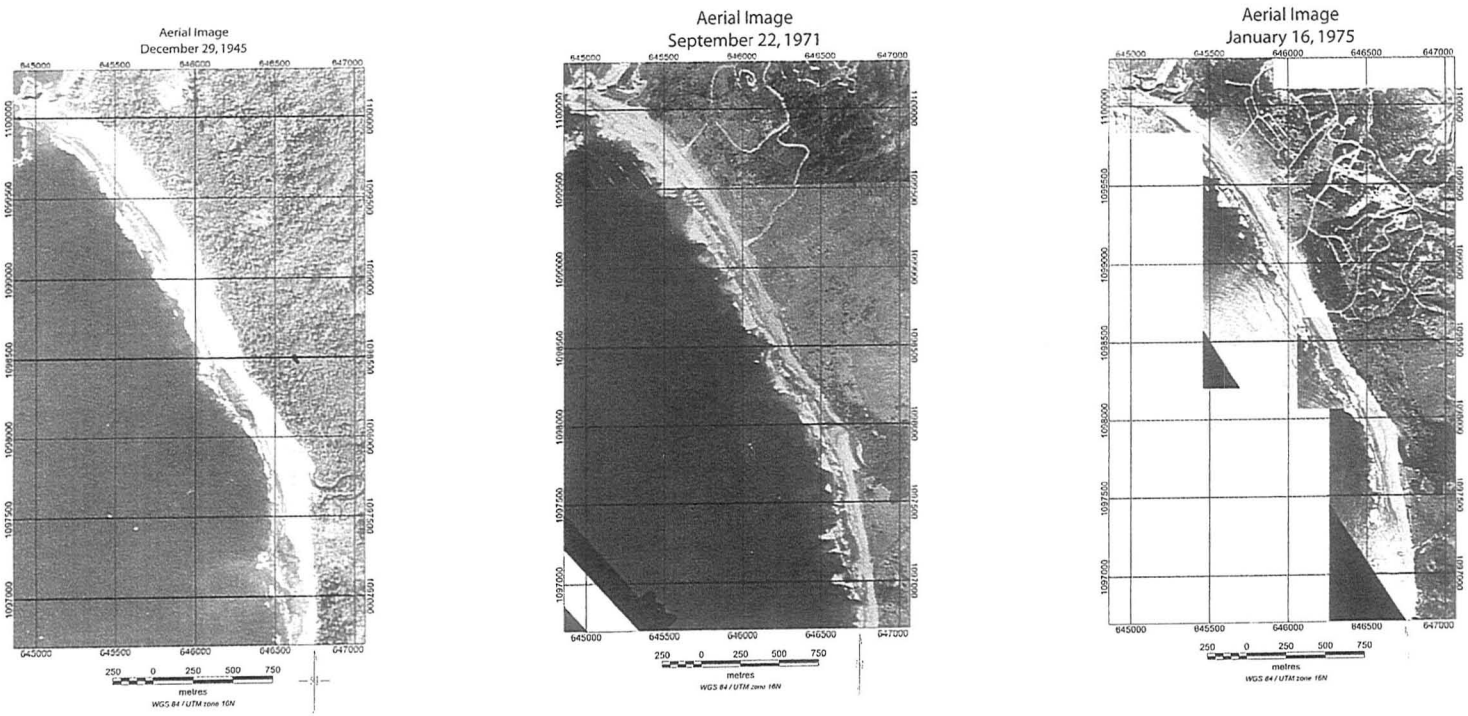

Figure 4.21: A time series of Playa Guiones from 1997 to 1991 using geo-rectified aerial images and a satellite image.

Playa Guiones – Time Series of Geo-Rectified Aerial and Satellite Imagery

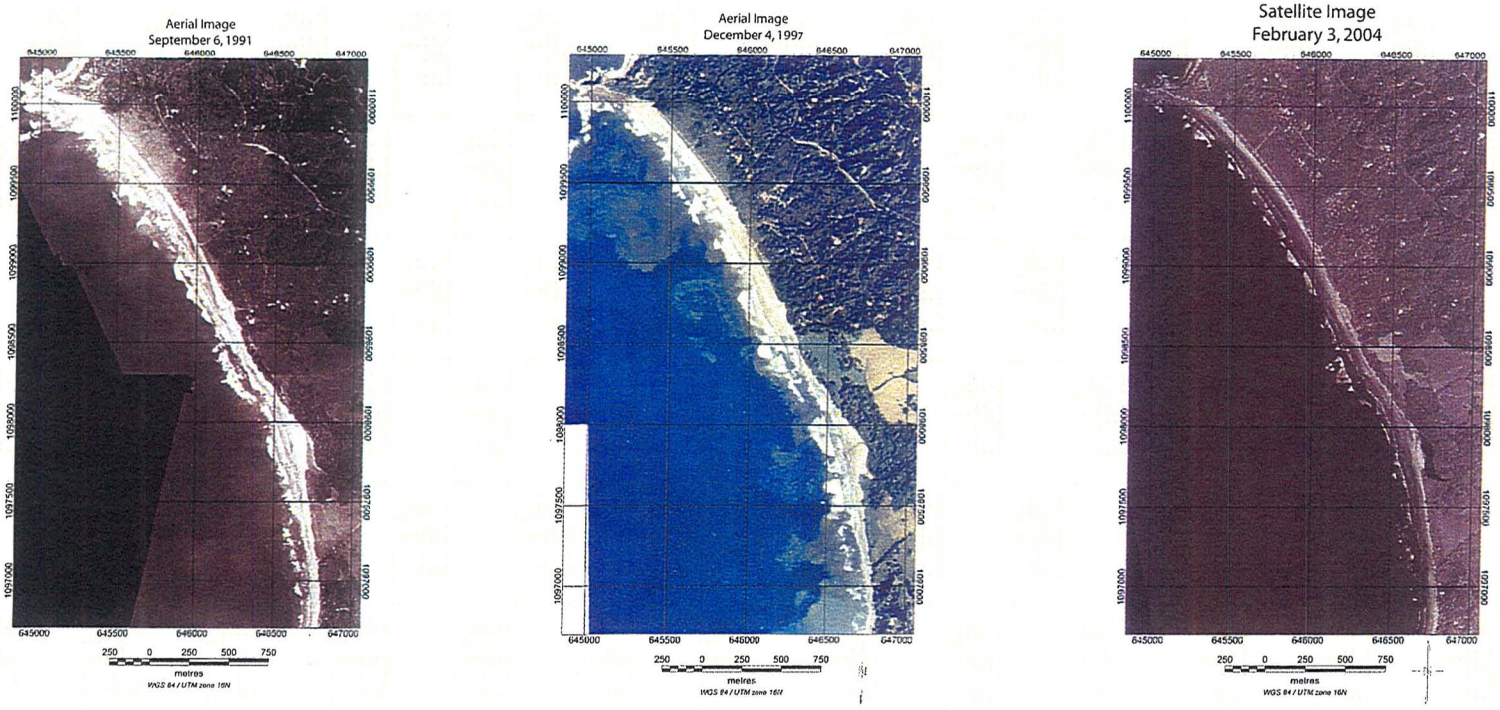

Figure 4.22: A time series of Playa Guiones from 1997 to 2004 using geo-rectified aerial images and a satellite image.

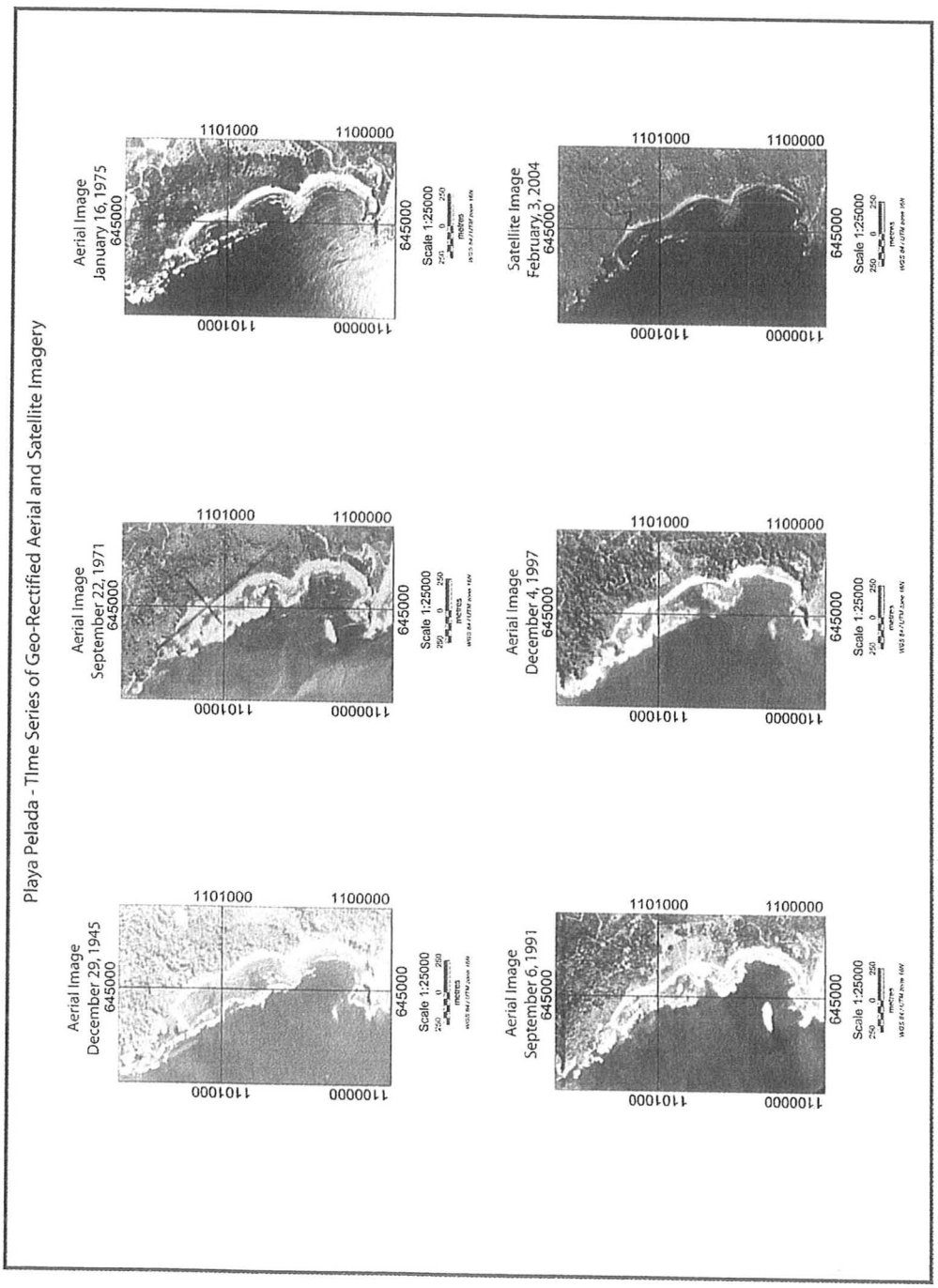

Figure 4.22: A time series of Playa Pelada from 1945 to 2004 using georectified aerial images and a satellite image.

observed throughout the years. In 1945 the dominant type of vegetation along the shoreline and further inland of Playa Guiones (Figure A.1) and Playa Pelada (Figure B.2) was dense tropical vegetation consisting of trees and shrubs with a full canopy. At this time there does not appear to be any human development or inhabitants in the region.

By 1971 much of the dense vegetation inland and along the coast of Playa Guiones has been cleared resulting in grasslands with the exception of some small patches of tropical vegetation including trees and shrubs remaining (Figure A.2). The patches of tropical vegetation along the coast were concentrated around Punta Pelada, Rio Rempujo and a small section between these two points. By 1971 several roads lead to the beach and there is evidence of the onset of development near northern Guiones. This development coincides with the land purchased by Alan Hutchinson in 1969 and 1972. Playa Pelada experiences a similar change in land use inland from the coast; however, the dense tropical vegetation remains intact along the coastline with only minimal clearing inland, two beach entrances and a compound of buildings at the southern extent (Figure B.2).

In the following four years (i.e., 1971-1975), there is substantial clearing of vegetation inland of Playa Guiones, a large network of gravel and mud roads have been constructed and major development of vacation properties can be observed (Figure A.3). The number of beach entrances has increased from four to six during this timeframe. Playa Pelada during the same time period does not experience the same development pressure as Playa Guiones, however, the number of beach entrances does increase from 2 to 3 (Figure B.3).

By the 1990s, it appears that the vegetation that was once cleared for grazing land and development is starting to re-grow inland and along the coast of Playa Guiones (Figure A.4 and A.5). The vegetation adjacent to Rio Rempujo and further north along the coast has increased, as well there is greater canopy cover inland. This is in contrast to Playa Pelada, which showed an increase in cleared land, the introduction of two additional beach entrances and more development of roads and buildings during this time period (Figure B.4 and B.5). The recovery of vegetation at Playa Guiones can be attributed to the foundation of the Nosara Civic Association in 1975 that was established to monitor development in the area while "maintaining intact the natural beauty of our area" (Nosara Civic Association, 2008). The primary difference between the recovery and development between Playa Guiones and Playa Pelada would be the earlier initial commencement date for development at Playa Guiones.

The 2004 images for Playa Guiones illustrate that the number of beach access points and the extent of the road network was maintained; however, there was an increase in the number of buildings located in the region (Figure A.6). Playa Pelada experienced similar changes during this period. By 2004 there were a total of nine access points to the beach and continued development inland (Figure B.6).

4.4.2 Historical Shoreline Position

Playa Guiones - A comparison of historical shoreline positions are presented in Figure 4.23. The historical shoreline was identified as the seaward extent of vegetation. The shoreline position from 1945 to 2004 for northern half of Playa Guiones remained relatively constant, with small indentations of change along the coast. These small changes may represent differences between wet and dry season, they may represent human impact in the region or be the result of some vegetation being lost during storm activity or during harsh dry periods. The historical shoreline positions at Rio Rempujo and further south are very different from one another. As seen in Figure 4.24, before the meandering river channel of Rio Rempujo reaches the coastline, there is a point bar and cut bank that influences the direction of the river. It appears that the cut bank has remained in the same location, whereas, the point bar has migrated to the south-west. The historical shorelines north of Rio Rempujo in this enlarged image appear to be show little variation in location. This minimal movement is supported by ground observations of extensive exposed rock in this region that would not be susceptible to rapid movement.

The historical shoreline representing 1945 (purple) appears to be to have had the greatest change when compared to the other years. This is repeated on the southern half of Figure 4.23 in which the 1945 shoreline appears to be located further west then the other shorelines. This difference is likely an error and can be explained by overlaying the 1945 image on the 2004 image. This overlay identifies weaknesses in the geo-rectifying of the 1945 image. The 1945 image was particularly difficult to correct because there were a lack of human structures in the region and the dense vegetation made it difficult to

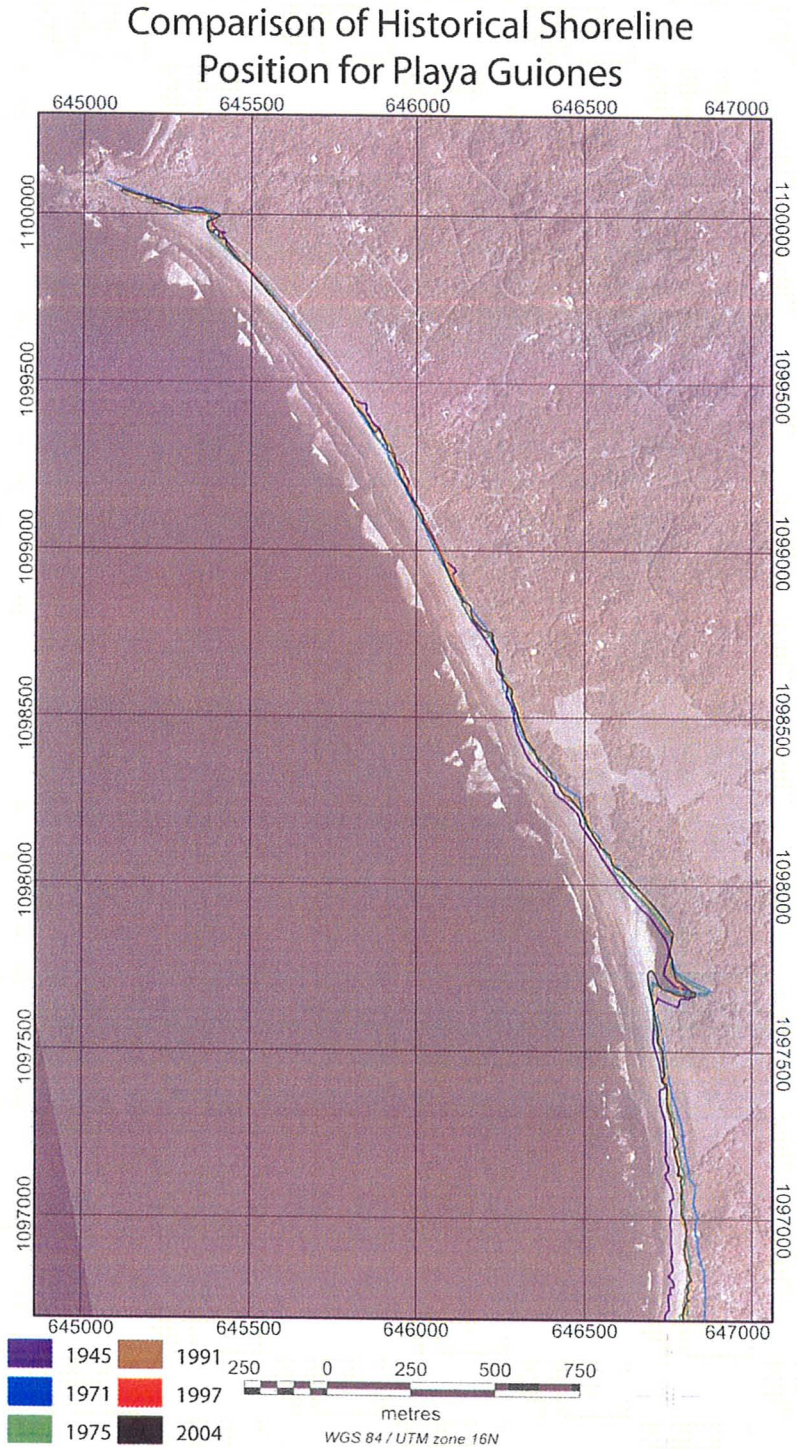

Figure 4.23: Comparison of historical shoreline position using the seaward extent of the vegetation line from aerial and satellite imagery.

identify geomorphic features as well. This lack of features to geo-rectify with makes the final image suspect. The 1971 (blue) historic shoreline can also be observed in the southern extent of Playa Guiones to be located further east then the other shorelines. Again due to the resolution of the image and the extent of the vegetation adequate geo-rectification was not possible.

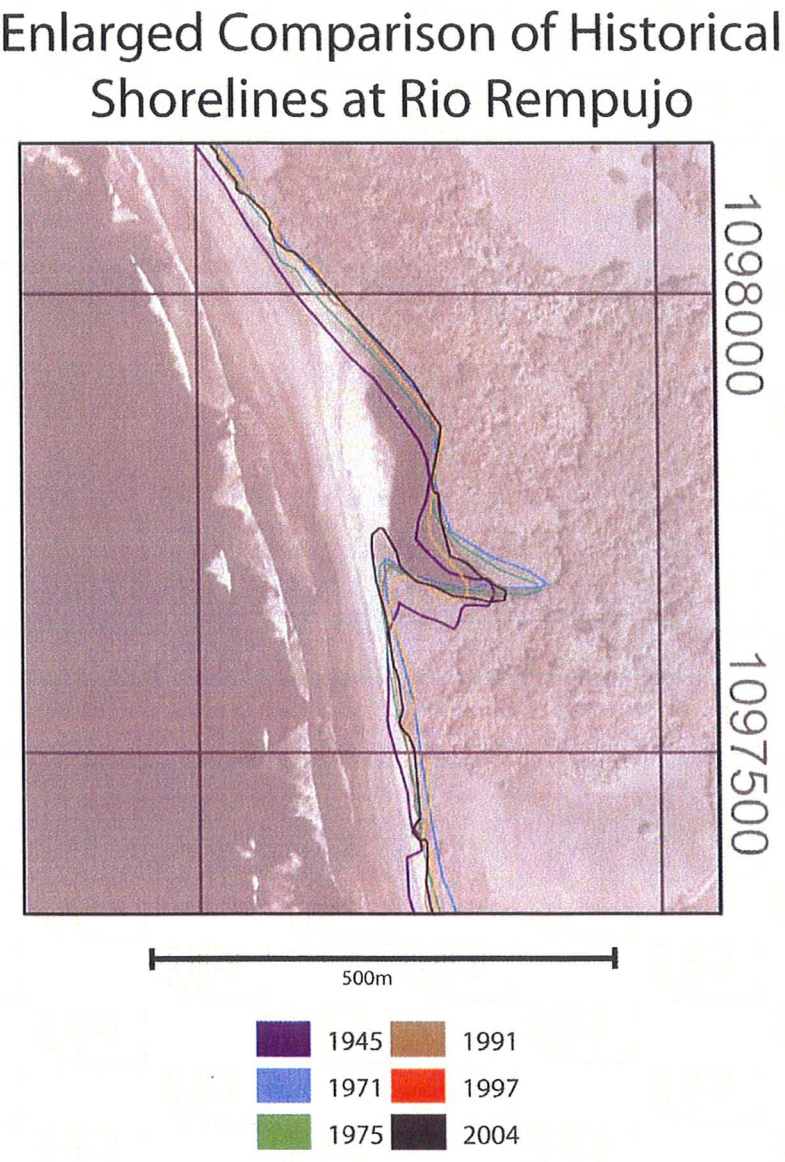

Figure 4.24: Comparison of historical shorelines on an enlarged image of Rio Rempujo.

Playa Pelada - The historical shoreline position for all six sets of images were delineated using the seaward extent of vegetation (Figure 4.24). The majority of historical shorelines were similar to one another as they followed the most recent shoreline (2004), however, the lines did cross back and forth showing small advances and retreats along the shore but at a minimal distance as depicted on the satellite image (black line). These small variations may represent differences from dry to wet season (i.e., periods of sediment accumulation and sediment erosion. The 1971 and 1975 shorelines were very similar to one another, with both extending further seaward then the other years at the second rocky outcrop. None of the other images showed this seaward advance of the coastline.

A set of three enlarged images of this area was created in Figure 4.25 to illustrate this difference. The first image is the 1975 aerial photo with both the 1975 and 2004 shoreline highlighted. The second image is a blend of the 1975 and 2004 aerial images that attempts to highlight the difference in the extent of vegetation at the rocky outcrop. The third image is the 2004 aerial image with both shorelines overlain. There were no other locations along the shoreline between these sets of images that provide any evidence of shoreline change.

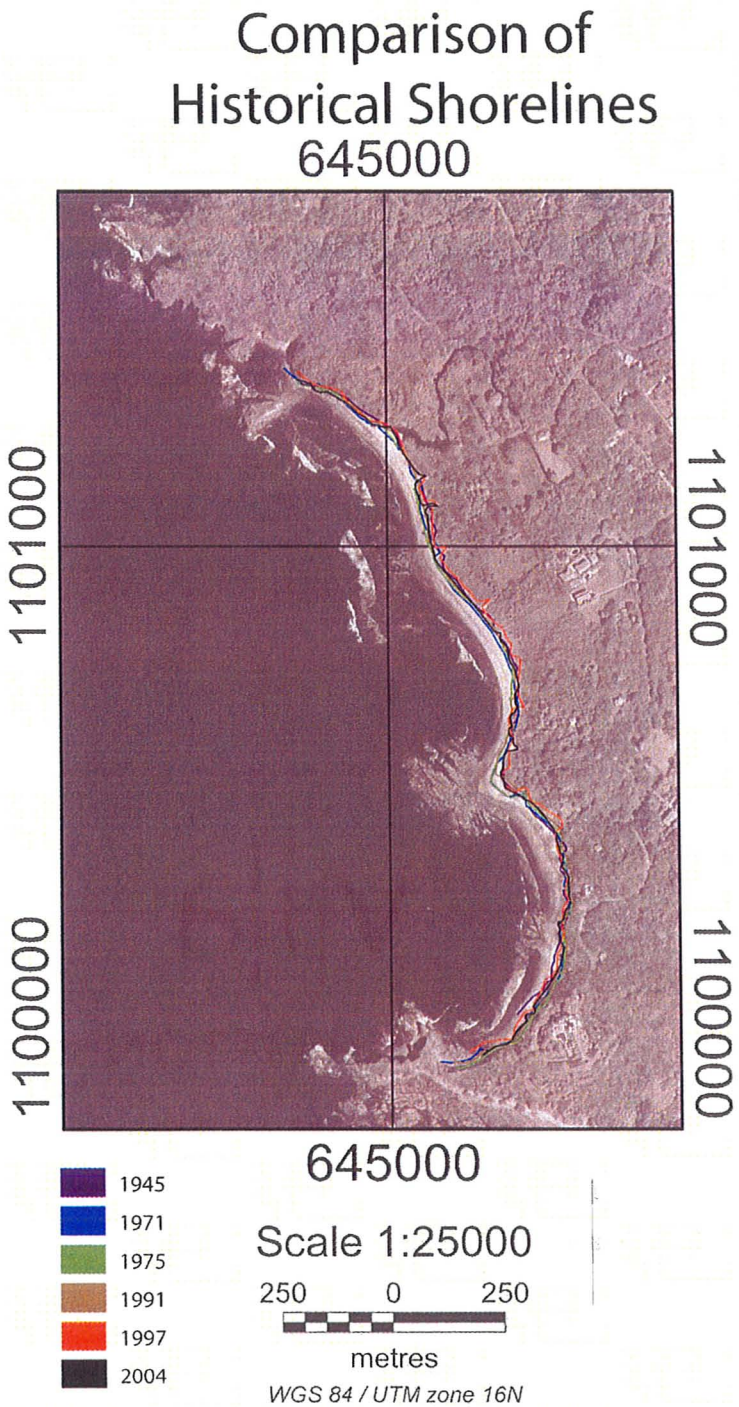

Figure 4.25: Comparison of historical shorelines of Playa Pelada using the seaward vegetation line as a geo-indicator for shoreline position.

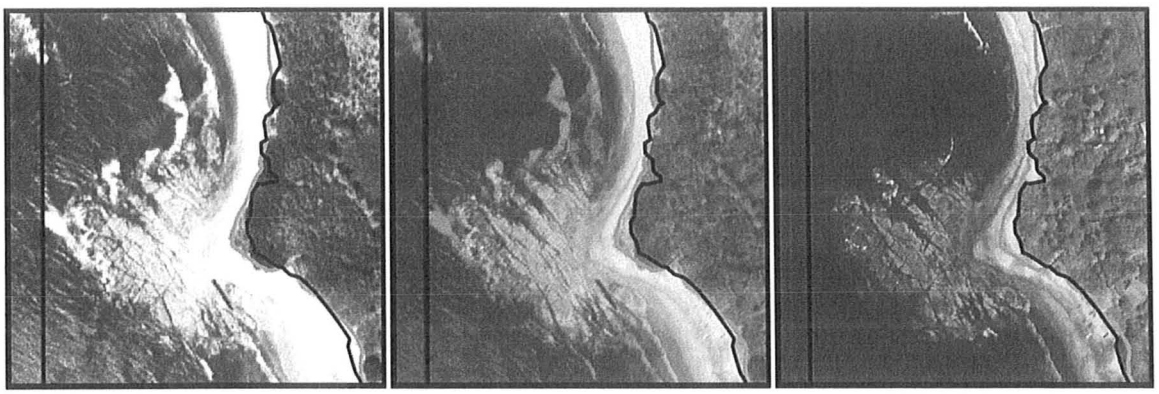

Figure 4.26: Evolution of the vegetation line observed on the second rocky outcrop on Playa Pelada. The left image is a 1975 aerial photograph, the far right image is a 2004 satellite image with the center image is a blend of the two images. The green line is the historical shoreline for 1975 and the black line is the 2004 shoreline.

4.4.3 Discussion

In order to attempt to quantify the historical shoreline change that occurred for Playa Guiones and Playa Pelada over a greater time period, the seaward extent of the vegetation line was used as the geo-indicator for all the remotely sensed imagery. The decision to use the vegetation line as the indicator was determined by the quality and resolution of the aerial images and since the images were taken at various times of the tide cycle. Many geo-indicators presented by Boak and Tuner (2005) are based on the water level, or the ability to recognize where the high tide water mark was located. Since these sets were taken at different times of the tide cycle, if a watermark was recognizable on the beachface there would be uncertainty if it was in fact the high water mark or just the furthest landward watermark after evaporation and infiltration. The other difficulty of using a water based mark on the beachface to determine the shoreline is that many sets of the images that were used were of low resolution that proved impossible to gain sufficient visual clarity to locate a comparable water mark on successive images. The quality of

images also added to this difficulty since some sets were blurred and faded over time. The vegetation line was the only indicator present on all sets of images that was recognizable, however, since these images were captured during both the wet and dry season interpretations of change must be made with caution. During the dry season much of the vegetation loses its leaves in order to stem evapotranspiration and there would be a tendency to locate the vegetation line landward.

The comparison of historical shorelines produced a final image that provided evidence that the over time there has been relatively little change in position of the coastline along the beach except in one position at the second rocky headland. At this location, the shoreline had been further seaward then what was seen in the 2004 image. The 1975 and 2004 images of this area were enlarged and overlain to reveal there had been a noticeable landward movement of the vegetation through time. The images revealed that a portion of the vegetation which could be a several shrubs were no longer present and the remaining vegetation was still intact. A comparison of the 1945 image could not be included in determining where the shoreline was prior to 1975 due to the poor resolution of the image. The remaining shoreline line was examined between these two years without revealing any large changes in shoreline position to aid in understanding how the shoreline position was changing over this period of time.

Aside from the small retreat of the shoreline at one specific location over the 59 years, the remainder of the beach illustrated a dynamically stable shoreline. Between the various years and seasons there were minimal retreats and advances but an overall relatively constant position. The explanation behind the limited change over time is the

beach morphology and the amount of accommodation space for the sediment of Playa Pelada. The beach is bounded by two headlands approximately 1.5 km apart from each other with three rocky outcrops that separate the beach into separate sections. These rock features minimize the longshore transport of sediment from current and wave process to a confined area.

4.4.4 Limitations

There were some limitations to the remotely sensed imagery component of this study. The limitations can be best understood if they are divided into two sections, imagery and data processing. Limitations relating to the imagery involved the availability of image sets, the resolution of the images and the time of collection. Limitations associated with data processing involved the selection of quality ground control points and the ability to geo-rectify the images.

The availability of data was a limitation. There are substantial costs associated with capturing aerial photographs and this is a developing country with modest assets. Historically it was government agencies who captured these images. The data collected was used to map their country. To reduce costs, flights in rural regions are not completed as often and can be biased as to be flown following a natural disaster. Additionally they may have a lower resolution as to achieve a greater coverage area (Boak and Tuner, 2005). This study was limited to the only five sets of aerial photographs of the region available from the Instituto Geographico Nacional of Costa Rica. One satellite image was purchased to augment the coverage.

The resolution of the images was the second limitation of the imagery. Of the five sets of photographs, only one had the scale of 1:10,000 that allowed quality selection of ground control points for geo-rectifying the images to the high resolution satellite image. Two of the sets were 1:20,000 which were reasonable to select points but still uncertainty in the accuracy and the remaining two sets of 1:40,000 did not have the level of resolution required. The overall quality for most images was good with the exception of a few where the original had writing on it or had faded over time.

The year of the photograph combined with the resolution of the image created the third limitation. One of the components of this study was to analyze if there was a long term change in shoreline position. The oldest aerial photograph 1945, would have allowed a 59 year comparison of the shoreline, however, since the scale of this set was 1:40,000 it did not have the resolution required to make a particularly good comparison. This was unfortunate because conversations with locals indicated that there had been substantial change in the beach during the 1950s and 1960s following the 1950 7.7 mw earthquake (Marshall and Anderson, 1995).

The lack of information provided with the aerial photographs was a limitation when processing the photographs into geo-rectified images. These images contained some of the necessary information such as tilt, row and altitude, however, the make and model of the camera and lens could not be obtained from the owners of the photographs. Numerous attempts to track down the information from the company that had been sub-contracted to collect the data were unsuccessful in locating this information. If this information was provided, the software program could automatically geo-rectify the

images. Because of the lack of information additional ground control points were collected but these had the unfortunate condition of introducing more error into the image processing.

The limitation of selecting quality ground control points in the data processing aspect proved to be more difficult for photographs that were older, of lower resolution or were in areas with little or no development. In order to properly geo-rectify a photograph using ground control points, landmarks must be identifiable in both the photo and satellite image that would not have moved such as buildings, telephone poles, etc (Camfield and Morang, 1996). Many parts of this region are heavily vegetated and is the older images had extremely dense vegetation with little or no human structures. It was possible in some cases to work backwards identifying points in younger photographs that had already been identified on the satellite image, however, this was not always possible. The best possible location was always selected, but due to this limitation some parts of the geo-rectified images could be inaccurate. Quality ground control points tended to be clustered in areas of the photograph (e.g., around human structures) and there were extensive portions of the images with no quality ground control points.

Another limitation was due to the region being located along a convergent coastal setting that has topographic extremes. When selecting points for the geo-rectification process they should all be at the same elevation since a difference in elevation will create differences in the distance calculated within the image and will result in a distorted rectified image.

CHAPTER FIVE: CONCLUSIONS AND RECOMMENDATIONS FOR FURTHER STUDY

5.1 Summary

From this research additional geospatial data in the form of a detailed survey have been acquired for Playa Guiones and Playa Pelada during the dry season. This compliments the data collected by Bertram (2006) and Lewis (2006) for the wet season. The processed data were analyzed and used to create both digital elevation models and beach profiles. Differences were observed between the two data sets. It was hypothesized for this work that the differences were the result of seasonal differences in sedimentation patterns between the different season. The differences that were observed including the destruction and movement of beach cusps, changes in beach slope and the net accumulation of sediment in some regions and the net loss of sediment from other regions.

During the wet season, ephemeral rivers discharge water into the ocean creating distinct river channels and embankments. During subsequent dry seasons, these features were either filled in with sediment making it indistinguishable from the surrounding beach area or had been altered (e.g., river mouth migration). During the dry season, the lack of precipitation resulted in little to no discharge through a number of these river channels. The impact of aeolian processes would increase during the dry season and combined with the lack of river discharge often resulted in sediment being deposited at the river mouth.

Playa Guiones experienced both sediment accumulation and loss along the beach. Sediment accumulation occurred along the beachface at the northern extent until right before reaching Rio Rempujo. A loss of sediment along the beachface was observed from this point towards the south. Accumulation of sediment at the surf zone was similar to the beachface, however, it extended further south of Rio Rempujo before a sediment loss occurred. Evidence of these changes were observed in the beach profiles extracted from the DEM. The type of sediment was consistent between the two seasons with the exception of the region adjacent to Rio Rempujo. In this region coarse sediment was present in the wet season and was replaced by fine sediment in the dry season. These observations lead to an overall beach classification for Playa Guiones as an intermediate beach dominated by a mix of wave and tide processes.

The majority of Playa Pelada experienced a minimal amount of net sediment accumulation or loss along the beachface and surf zone with two exceptions. The first exception was the area adjacent to an ephemeral river which experienced a net accumulation of sediment following the wet season. The second exception was adjacent to the rocky outcrops. These areas all experienced net sediment loss except for the southern side of the second outcrop. In this region the rocky outcrop appeared to trap sediment that was being moved by aeolian processes during the dry season. It was determined that seasonality and geology control the type of beach classification for each crescent. The southern crescent is protected by rocky outcrops, limiting the amount of wave energy experienced in the wet season and as a result is dissipative for both seasons. The northern crescent has less protection from rocky outcrops and is influenced by the

ephemeral river changing the classification from dissipative in the wet season to more reflective in the dry season. The central crescent, which remained constant for both seasons had the characteristics of a reflective beach with a steep slope and coarse sediment.

Observations of remotely sensed imagery of the region (1945 -2004) provided evidence of land-use change: first from an uninhabited region of dense tropical vegetation; to cleared regions of grassland with pockets of vegetation; and, finally to the development of vacation properties with some recovery of dense vegetation.

The ability to quantify the historical shoreline position throughout the years was severely limited due the quality and resolution of the aerial photographs. It appeared that the shoreline has remained relatively constant during this time period. This is particularly significant and contradicts some of the primary experiences reported by locals. The 1 m vertical uplift of the Nicoya region caused by the 1950 7.7 Mw earthquake as documented by Marshall and Anderson (1995) could not be observed in differences between the 1945 to 1971 images due to resolution.

5.2 Recommendations for Further Study

This research measured the variation between a single dry and wet season. The collection of additional data sets for subsequent wet and dry seasons would allow more precise conclusions to be drawn about the impact of seasons on the beach morphology. Further geo-indicator work on both beaches could be valuable. Data collection for the creation of a DEM using real-time kinetic GPS is very time consuming. It is unclear still

for the resolution needed for this type of study if this level of data collection is actually necessary. There is a subsequent project that could be conducted in this region that assessed the feasibility of different methodologies for the collection of data used to classify the shoreline morphology.

Ideally additional aerial imagery would be collected for detailed temporal study of shoreline change. An exhaustive search for additional imagery was conducted as part of this research. It is highly unlikely that there are additional data sets that are publicly available. The highest quality image for the region is the satellite image. Subsequent to any future significant tectonic activity in this region additional satellite imagery should be obtained in order to conduct a comparison. The search to attain additional sets of aerial imagery was exhausted during the last data collection period of this research. Without additional historic images that consist of greater resolution for the area, the level of detail for this section of the analysis has been reached.

Little is known about the offshore bathymetry in this region. As part of this project a widely spaced (250 m) bathymetric survey was attempted. It was not successful in obtaining data in the swash zone because of safety concerns. The resolution of the data was suspect and the bottom was not always clearly defined. In order to further understand beach processes a detailed bathymetric study should be undertaken.

Land-use pressures from tourism appear to have increased during the three years of this study. It is anticipated that these pressures will only intensify in the coming years. It is unclear if the Nosara Civic Association will be successful in ensuring a balance between growth and environmental impact. Additionally, the availability of fresh water,

particularly in the dry-season and the management of waste water particularly in the wet season will likely become a larger issue in the future. Land-use pressures and water management (i.e., potable and waste water) issues will impact the beach more in subsequent years. Maintaining monitoring on this beach in order to quantify the impact would be ideal.

References

Andrews, B.D., Gares, P.A. and Colby, J.D., 2002. Techniques for GIS modeling of coastal dunes. Geomorphology, 48, 289-308.

Enavente, J., Del Rio, L., Anfuso, G., Gracia, F.J. and Reyes, J.L., 2002. Utility of Morphodynamic Characterisation in the Prediction of each Damage by Storms. Journal of Coastal Research, SI 36, 56-64.

Bertram, A.M., 2006. Coastal Geomorphology. Playa Guiones, Guanacaste Province, Costa Rica. McMaster University.

Bird, Eric. (2000). *Coastal Geomorphology: An Introduction.* West Sussex : John Willy & Sons Ltd

Boak, E.H. and Turner, I.L., 2005. Shoreline Definition and Detection: A Review. Journal of Coastal Research, 21(4), 688-703.

Briggs, I., 1974. Machine Contouring Using Minimum Curvature. Geophysics, 39(1), 39-48.

Camfield, F.E., and Morang, A., 1996. Defining and interpreting shoreline change. Ocean & Coastal Management, 32(3), 129-151.

Campbell, L.M., 1998. Use them or lose them? Conservation and the consumptive use of marine turtle eggs at Ostional, Costa Rica. Environmental Conservation, 25(4), 305-319.

Dali, H.J., Merrifield, M.A. and Bevis, M., 2000. Steep beach morphology changes due to energetic wave forcing, Marine Geology, 162, 443-458.

DeShon, H.R., Schwartz, S.Y., Newman, A.V., Gonzalez, V., Protti, M., Dorman, L.M., Dixon, T.H., Sampson, D.E. and Flueh, E.R., 2006. Seismogenic zone structure beneath the Nicoya Peninsula, Costa Rica, from three-dimensional local earthquake P-and S-wave tomography. Geophyics Journal International. 164, 109-124.

Digital Globe Incorporated, Satellite Imagery, February 3, 2004. Image 04FEB03160650-M2AS-005519468010_01_P001. Digital Globe Incorporated, 2005.

Escalante, G., 1990. The geology of southern Central America and western Columbia. In; Dengo, G. and Case, J. eds., The Caribbean Region: Boulder, CO, Geological Society of America, The Geology of North America. Vol. H.

Gaba, E., 2009. From:
http://images.google.ca/imgres?imgurl=http://upload.wikimedia.org/wikipedia/commons/d/de/Costa_Rica_relief_location_map.jpg&imgrefurl=http://commons.wikimedia.org/wiki/File:Costa_Rica_relief_location_map.jpg&usg=__tzeZBdmA2leAdfZ01HGuHrPqlYY=&h=1034&w=1148&sz=491&hl=en&start=3&sig2=ahkRNPiRrlRaXrl6ThhbRA&tbnid=Je6qhgP5GkKX0M:&tbnh=135&tbnw=150&prev=/images%3Fq%3Dwiki%2Bgaba%2Bcosta%2Brica%2Bmap%26gbv%3D2%26hl%3Den%26sa%3DG&ei=XBPCStacIJO6lAeG8rDaBA Accessed: January 15, 2008/

Gardner, T.W., Back, W., Bullard, T.F., Hare, P.W., Kesel, R.H., Lowe, D.R., Menges, C.M., Mora, S.C., Pazzagalia, F.J., Sasowsky, I.D., Troestrer, J.W. and Wells, S.G., 1987. Central America and the Caribbean, *in* Graf, W.L., ed., Geomorphic systems of North America: Boulder, Colorado, Geological Society of America, Centennial Special Volume 2.

Geosoft, Unknown, Topics in Gridding.
http://www.geosoft.com/resources/papers/pdfs/topicsingriddingworkshop.pdf, August 10, 2008.

Haxel, J.H. and Holman, R.A., 2004. The sediment response of a dissipative beach to variations in wave climate. Marine Geology, 206, 73-99.

Hare, P.W. and Gardner, T.W., 1985. Geomorphic indicators of vertical tectonism along converging plate margins, Nicoya Peninsula, Costa Rica in Hack, J., and Morisawa, M., eds., *Tectonic Geomorphology:* Proceedings of the 15th Geomorphology Symposium Series, Binghamton, p. 76-104.

Inman, C., 2002. Tourism in Costa Rica, The Challenge of Competitiveness. http://www.incae.ac.cr/EN/clacds/investigacion/pdf/cen653.pdf. October 25, 2005.

Instituto Geográfico Nacional Costa Rica, Aerial Photography, June 9, 1997. Photos R272 - R275. 1:40,000. Instituto Geográfico Nacional Costa Rica, 1997.

Instituto Geográfico Nacional Costa Rica, Aerial Photography, June 9, 1991. Photos R272 - R275. 1:10,000. Instituto Geográfico Nacional Costa Rica, 1991.

Instituto Geográfico Nacional Costa Rica, Topographic Map, 1981. Garza. Edition 2. 1:50,000. Costa Rica 3045 I. San Jose: Costa Rica.

Instituto Geográfico Nacional Costa Rica, Aerial Photography, 1977. Photos 1624 - 1627. 1:10,000. Instituto Geográfico Nacional Costa Rica, 1977.

Instituto Geográfico Nacional Costa Rica, Aerial Photography, 1944. Photos CAW11 – 13 to 15. 1:10,000. Instituto Geográfico Nacional Costa Rica, 1944.

Instituto Meteorológico Nacional, 2008. http://www.imn.ac.cr/IMN/MainAdmin.aspx?__EVENTTARGET=ClimaCiudad&CIUCAC=6 Accessed November, 17, 2008.

Isaaks, E.H. and Srivastava, R.M., 1989. An Introduction to Applied Geostatistics. New York, Oxford University Press, pp561.

Jones, N.L. and Nelson, J., 1992. Mapping Contouring, Geoscientific Modeling With TINs. Geobyte, 44-49.

Krause, G. and Soares, C., 2004. Analysis of beach morphodynamics on the Bragantinian mangrove peninsula as prerequisite for coastal zone management recommendations. Geomorphology, 60, 225-239.

Lillesand, T., Kiefer, R. and Chipman, J., 2004. Remote Sensing and Image Interpretation. Fifth Edition. United States, John Wiley & Sons, Inc,

Marshall, J.S. and Anderson, R.S. 1995. Quaternary uplift and seismic cycle deformation, Peninsula de Nicoya, Costa Rica. GSA Bulletin, 107(4), 463-473.

Mercer, B., Thornton, S. and Tennant, K., 1998. Operational DEM Production from Airborne Interferometry and from RADARSAT Stereo Technologies. In: *Proceedings of ASPRS-RTI Annual Conference,* Tampa, Florida, U.S.A, March 31 – April 3

Mercer, B., 2001. Comparing Lidar and IFSAR: What can you expect? In: *Proceedings of Photogrammetric* Week 2001, Stuttgart, Fritsch/Spiller (Eds.)

Morton, R.A., 2002. Coastal geoindicators of environmental change in the humid tropics. Environmental Geology, 42, 711-724.

Morton, R.A., Leach, M.P., Paine, J.G. and Cardoza, M.A., 1993. Monitoring Beach Changes Using GPS Surveying Techniques. Journal of Costal Research, 9(3), 702-720.

Muzuka, A.N.N. and Shaghude, Y.W., 2000. Grain Size distribution along the Msasani Beach, north of Dar es Salaam Harbour. Journal of African Earth Sciences, 30(2), 417-426.

NOAA, 2008. http://www.hpc.ncep.noaa.gov/international/scs/Costa_Rica1.html Accessed November 17, 2008.

Nosara Civic Association, 2008. http://nosaracivicassociation.com/project_history.htm Accessed November 17, 2008.

Open University Course Team. (2005). *Waves, Tides and Shallow-Water Processes.* (2 ed.). Oxford : Butterworth-Heinemann

Sambridge, M., Braun, J. and McQueen, H., 1995. Geophysical parametrization and interpolation of irregular data using natural neighbours. Journal of International Geophysics, 122, 837-857.

Short, A., 1999. (Ed.) Handbook of Beach and Shoreface Morphodynamics. Toronto. John Wiley & Sons, Ltd, pp. 379.

Woodroffe, Colin. (2003). *Coasts. Form, process and evolution.* Cambridge : Cambridge University Press

Wright, D. and Short, A.D., 1984. Morphodynamic Variability of Surf Zones and Beaches: A Synthesis. Marine Geology, 56, 93-118

Windevoxhel, N.J., Rodriguez, J.J. and Lahmann, E.J., 1999. Situation of integrated coastal zone management in Central America: Experiences of the IUCN wetlands and coastal zone conservation program. Ocean & Coastal Management, 42, 257-282

Yang, C., Kao, S., Lee, F. and Hung, P., Twelve Different Interpolation Methods: A Case Study of Surfer 8.0. In: *Proceedings of ISPRS Congress XXth,* 2004. Istanbul, Turkey.

APPENDIX A

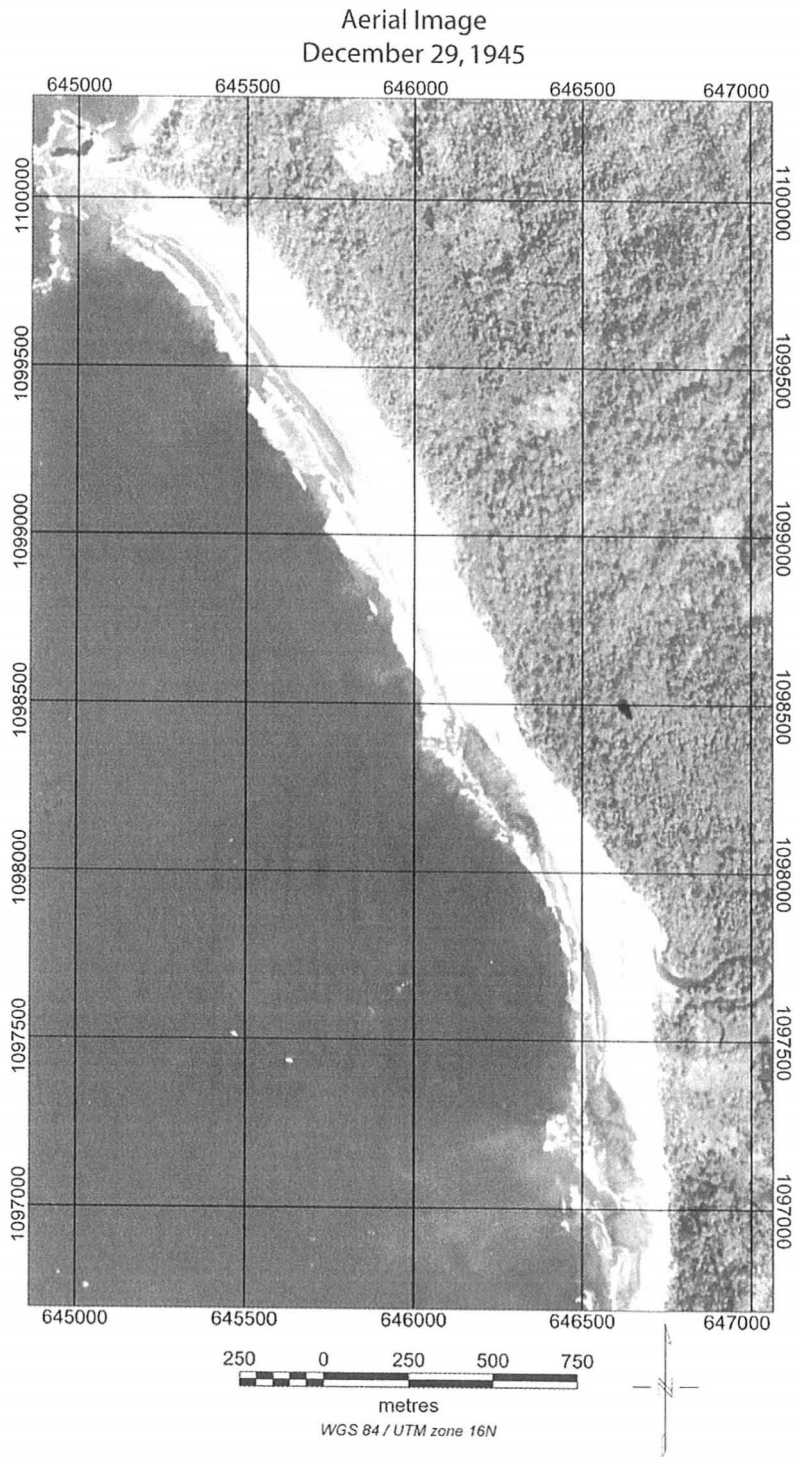
Aerial Image
December 29, 1945
645000
645500
646000
646500
647000
1100000
1099500
1099000
1098500
1098000
1097500
1097000
250 0 250 500 750
metres
WGS 84 / UTM zone 16N

Figure A.1

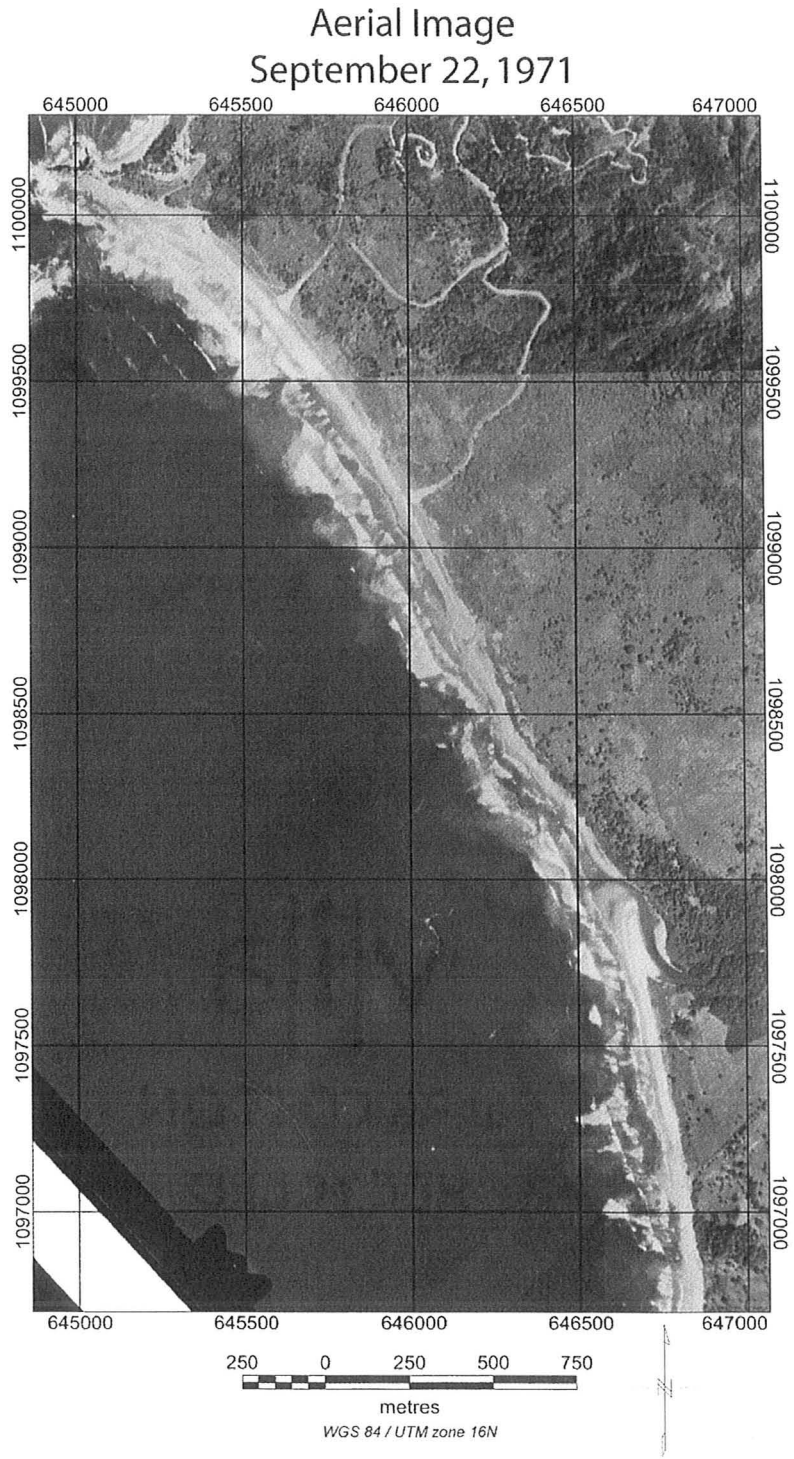
Aerial Image
September 22, 1971
645000
645500
646000
646500
647000
1100000
1099500
1099000
1098500
1098000
1097500
1097000
250 0 250 500 750
metres
WGS 84 / UTM zone 16N

Figure A.2

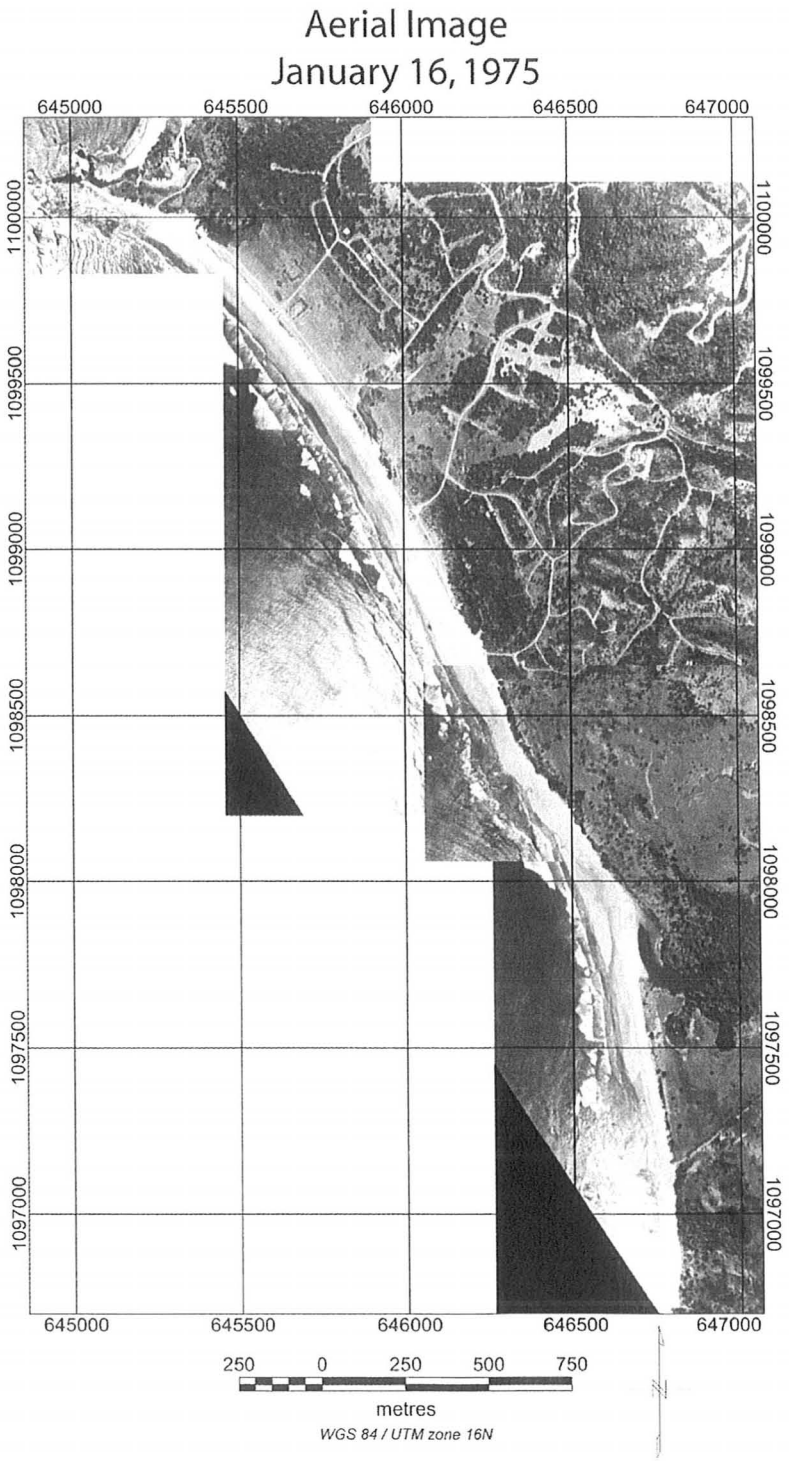
Aerial Image
January 16, 1975
645000
645500
646000
646500
647000
1100000
1099500
1099000
1098500
1098000
1097500
1097000
250 0 250 500 750
metres
WGS 84 / UTM zone 16N

Figure A.3

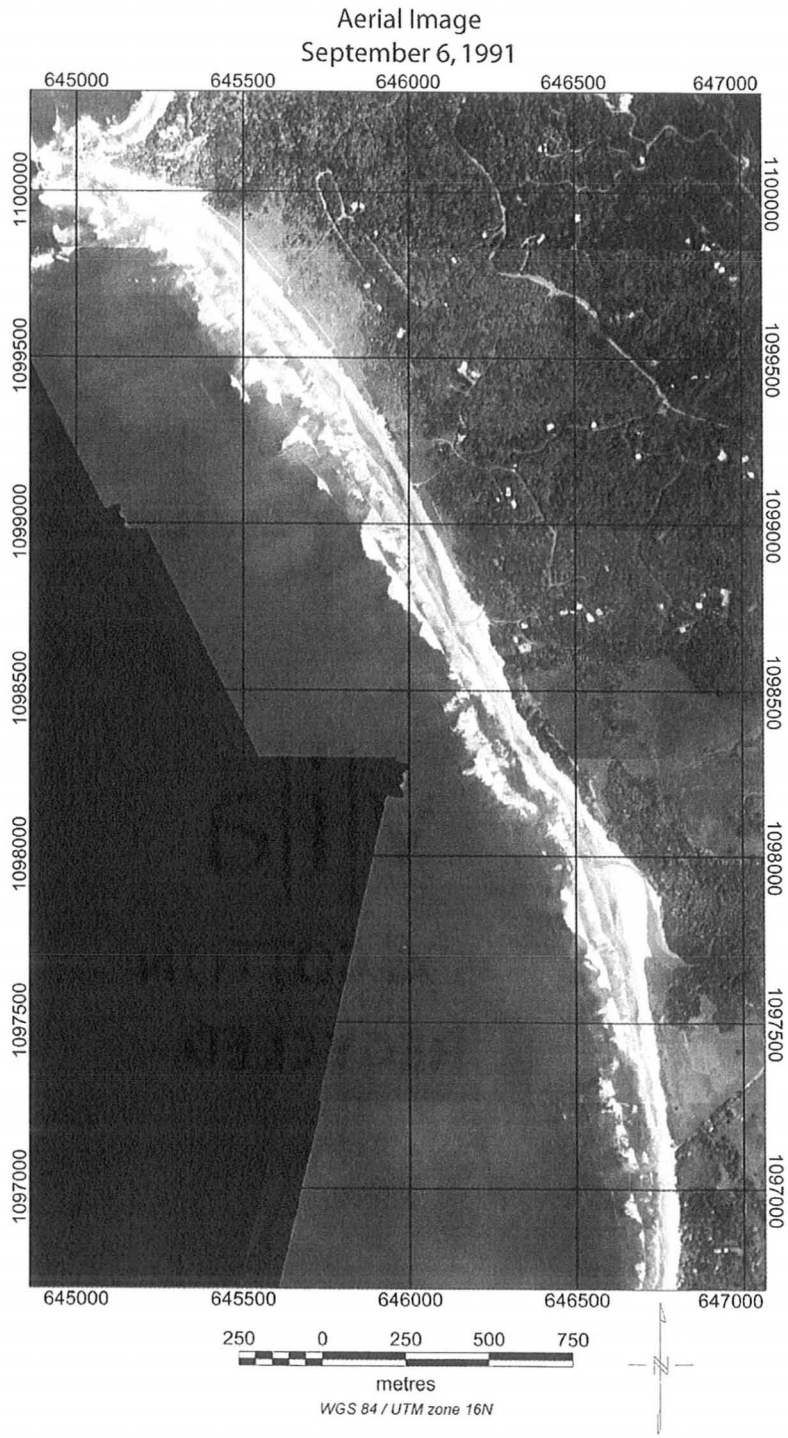
Aerial Image
September 6, 1991
645000
645500
646000
646500
647000
1100000
1099500
1099000
1098500
1098000
1097500
1097000
250 0 250 500 750
metres
WGS 84 / UTM zone 16N

Figure A.4

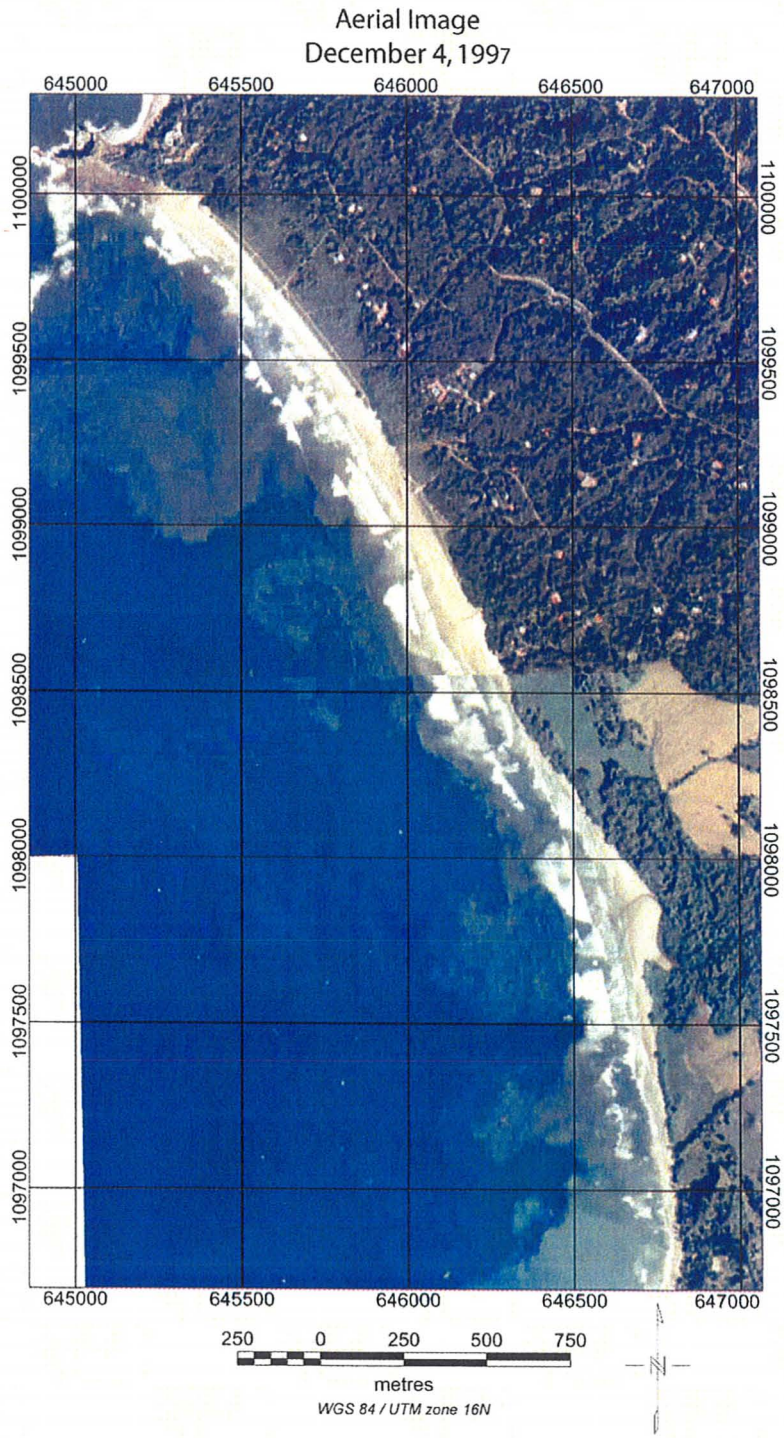
Aerial Image
December 4, 1997
645000
645500
646000
646500
647000
1100000
1099500
1099000
1098500
1098000
1097500
1097000
250 0 250 500 750
metres
WGS 84 / UTM zone 16N
N

Figure A.5

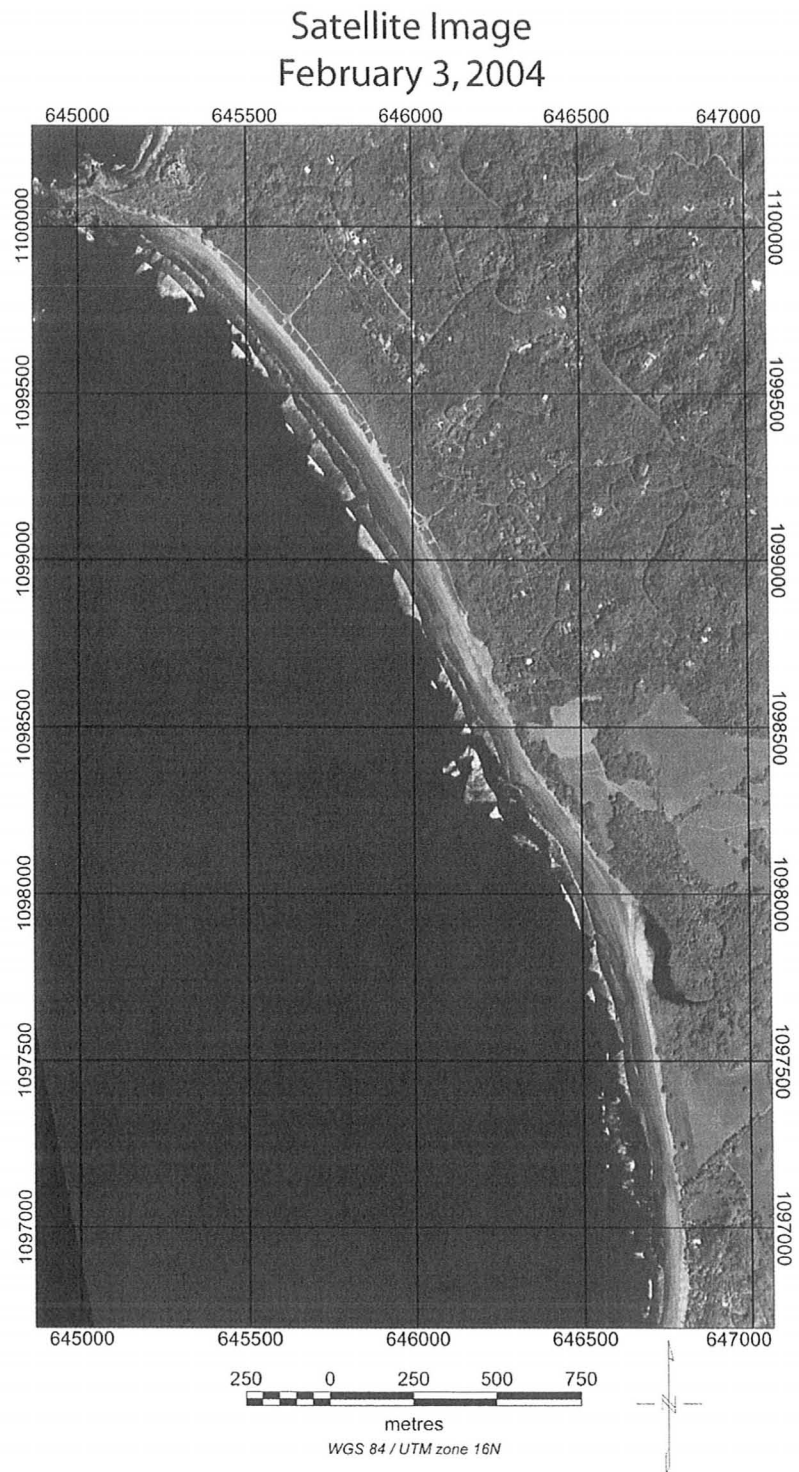
Satellite Image
February 3, 2004
645000
645500
646000
646500
647000
1100000
1099500
1099000
1098500
1098000
1097500
1097000
250 0 250 500 750
metres
WGS 84 / UTM zone 16N

Figure A.6

APPENDIX B

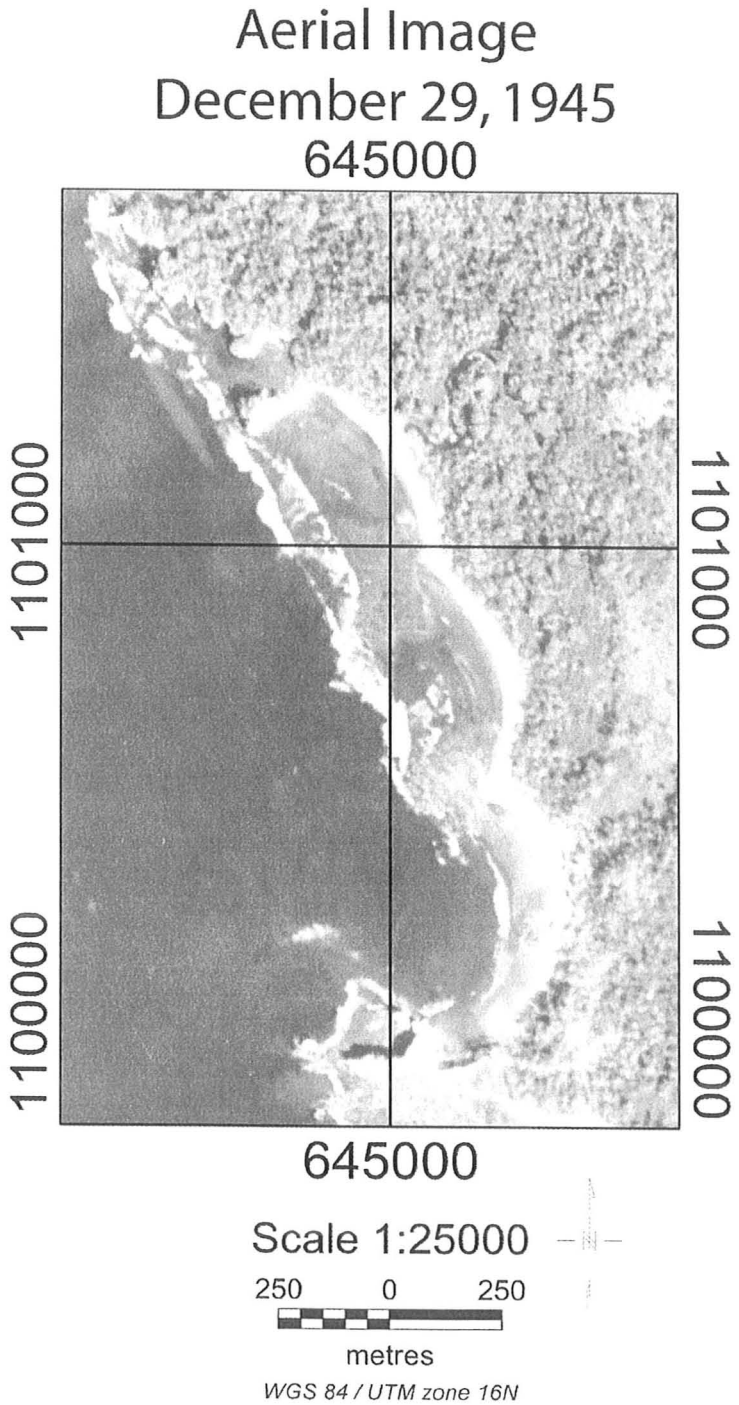
Aerial Image
December 29, 1945
645000
1101000
1101000
1100000
1100000
645000
Scale 1:25000
250 0 250
metres
WGS 84 / UTM zone 16N

Figure B.1

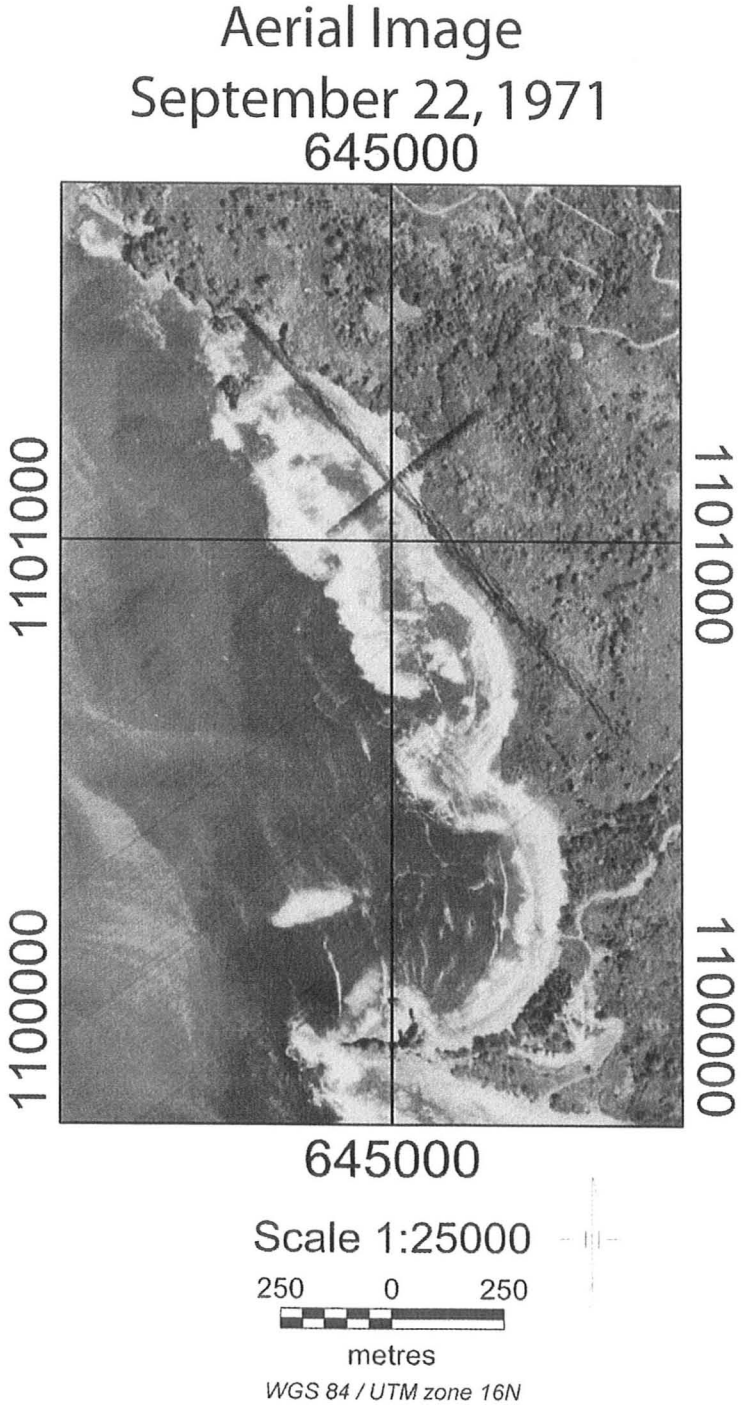
Aerial Image
September 22, 1971
645000
1101000
1101000
1100000
1100000
645000
Scale 1:25000
250 0 250
metres
WGS 84 / UTM zone 16N

Figure B.2

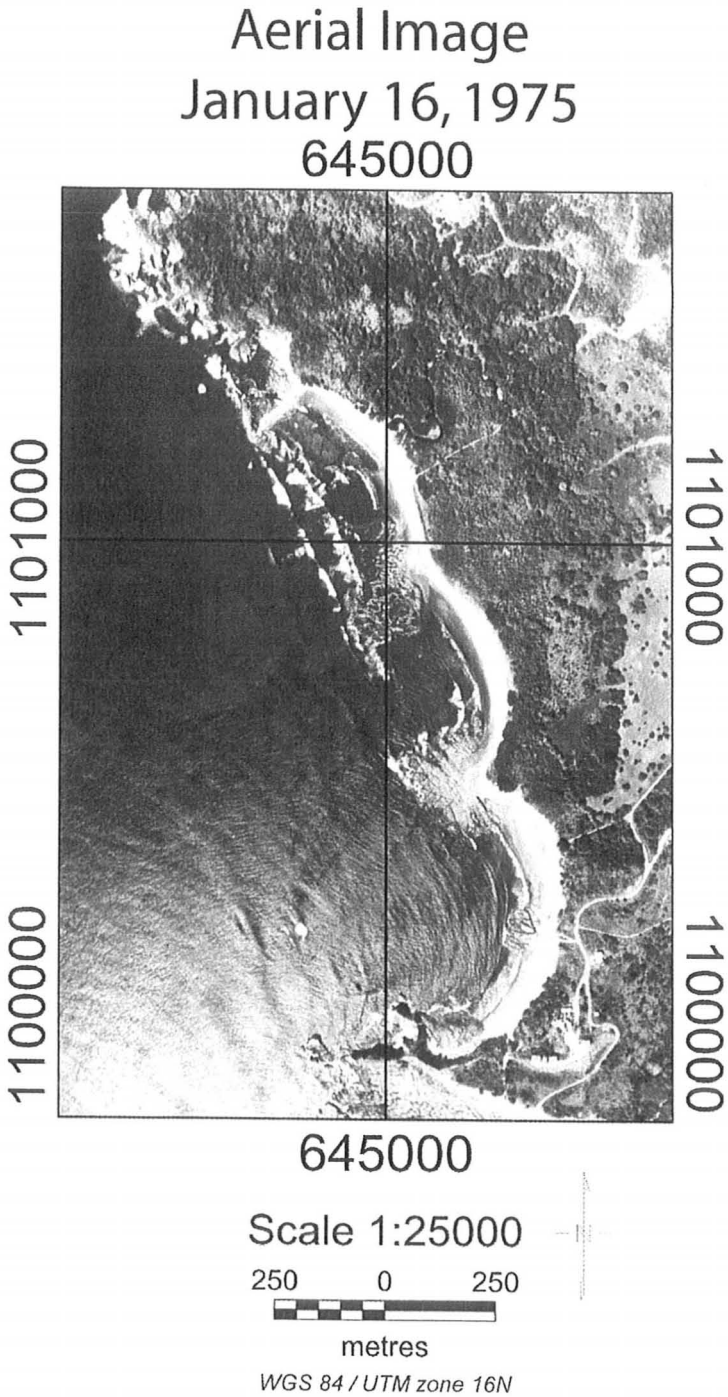
Aerial Image
January 16, 1975
645000
1101000
1101000
1100000
1100000
645000
Scale 1:25000
250 0 250
metres
WGS 84 / UTM zone 16N

Figure B.3

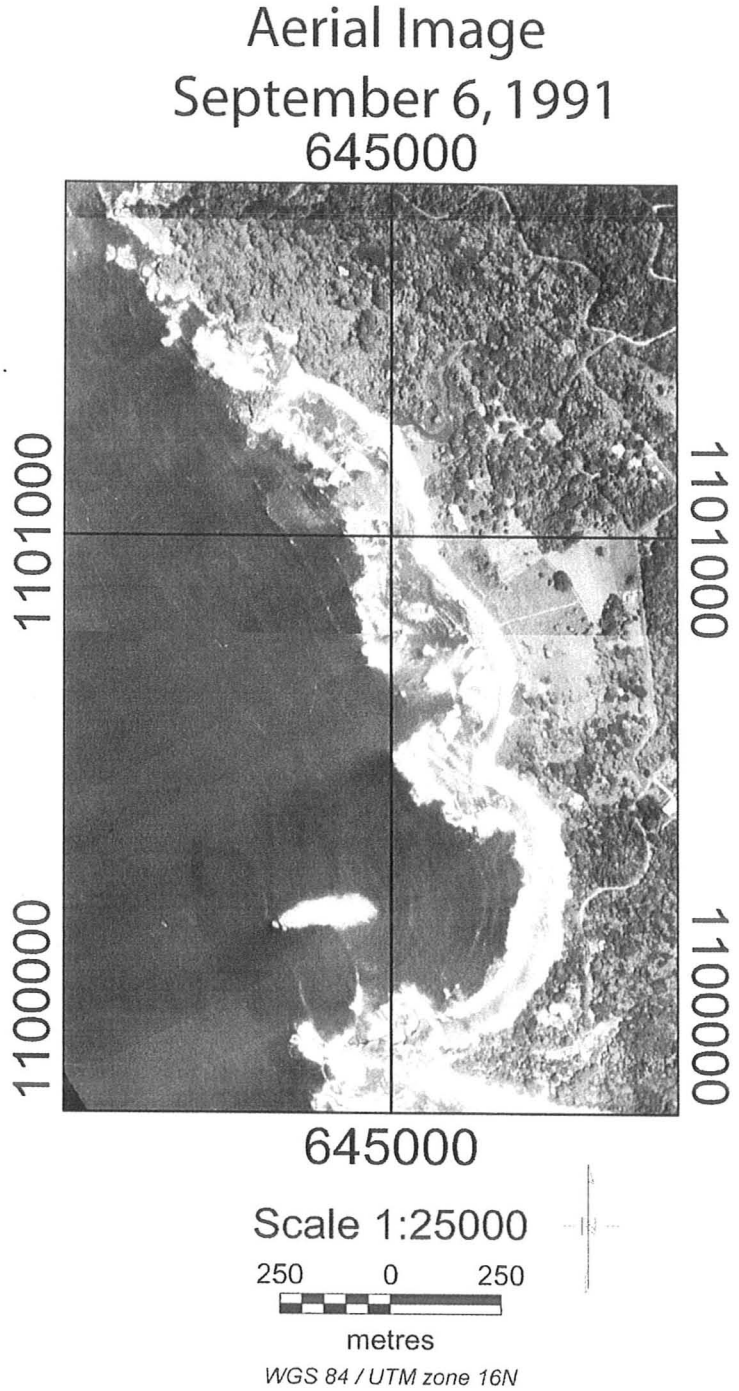
Aerial Image
September 6, 1991
645000
1101000
1101000
1100000
1100000
645000
Scale 1:25000
250 0 250
metres
WGS 84 / UTM zone 16N

Figure B.4

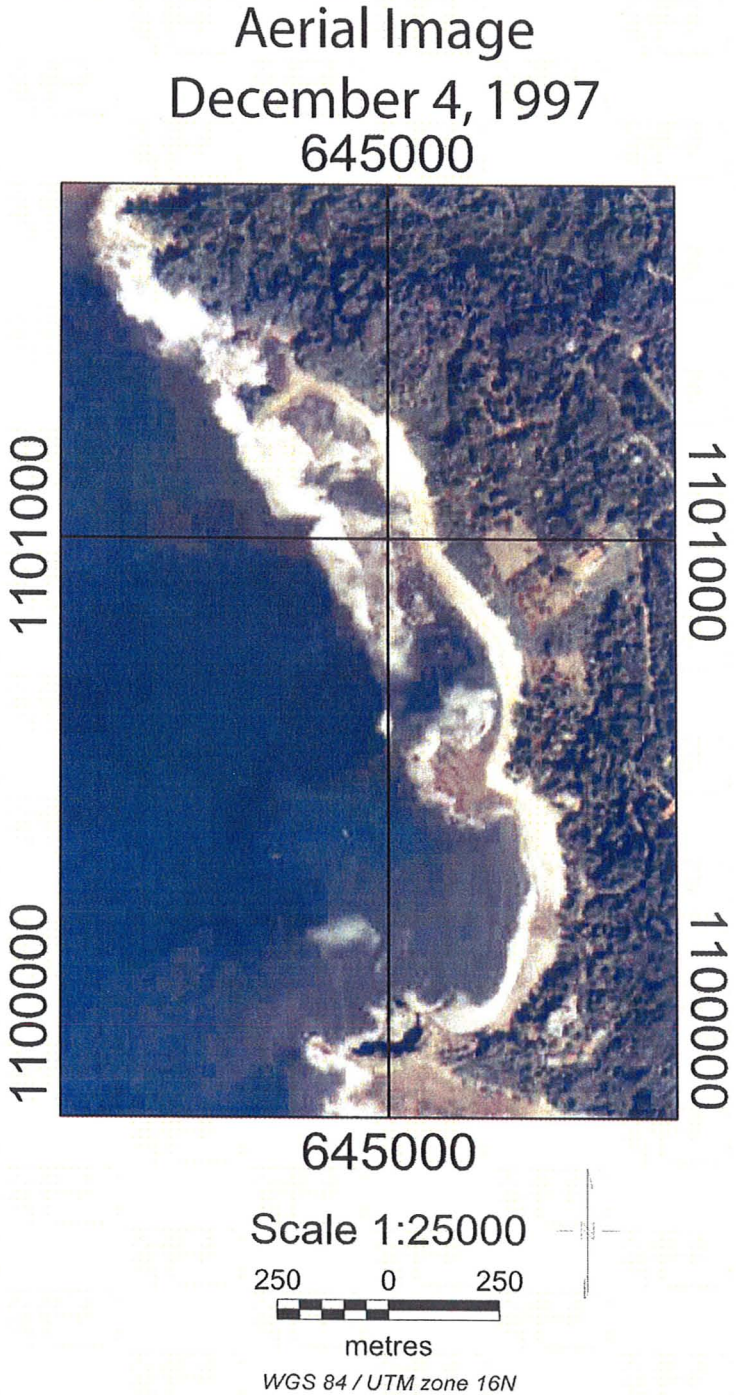
Aerial Image
December 4, 1997
645000
1101000
1101000
1100000
1100000
645000
Scale 1:25000
250 0 250
metres
WGS 84 / UTM zone 16N

Figure B.5

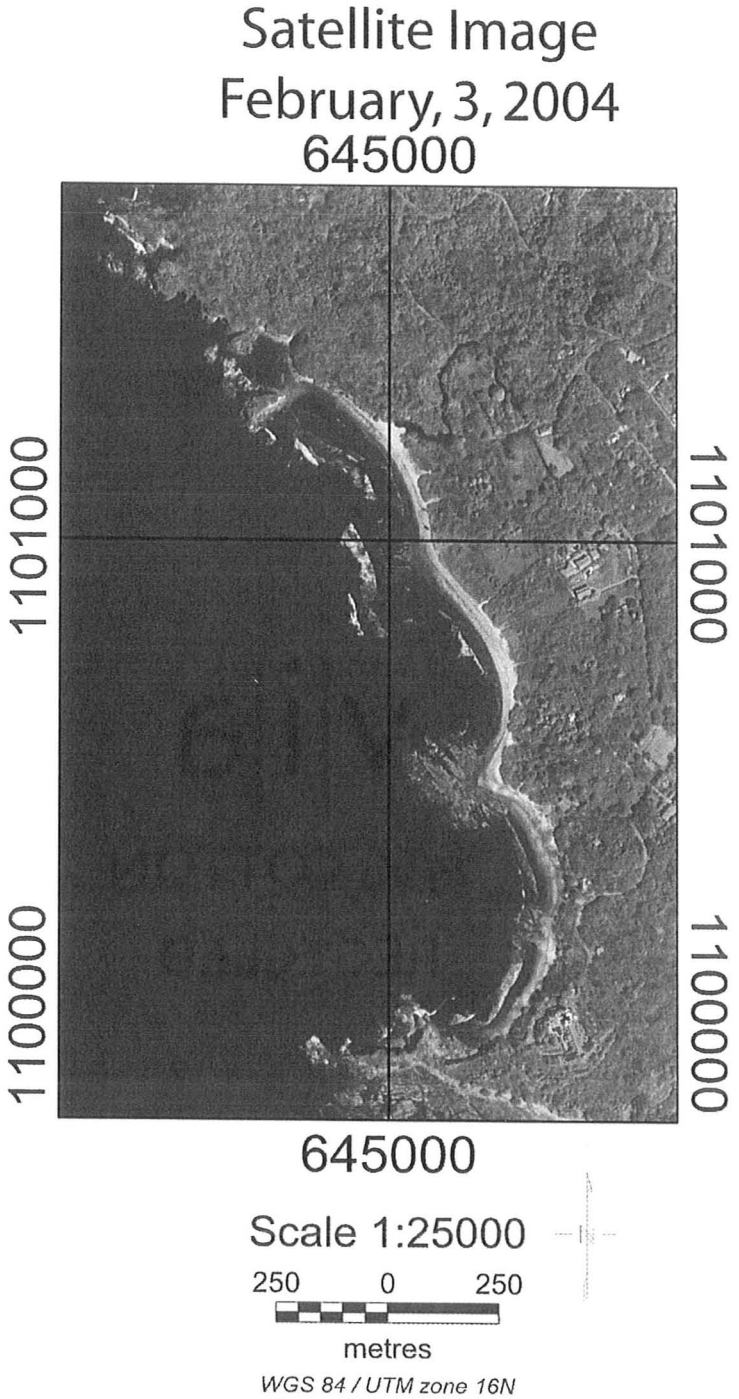
Satellite Image
February, 3, 2004
645000
1101000
1101000
1100000
1100000
645000
Scale 1:25000
250 0 250
metres
WGS 84 / UTM zone 16N

Figure B.6

APPENDIX C